1992

Investigation of hydrometeorological relationships, Pasu Glacier basin, northern Pakistan

Bob Boyce
Wilfrid Laurier University

INVESTIGATION OF HYDROMETEOROLOGICAL RELATIONSHIPS PASU GLACIER BASIN, NORTHERN PAKISTAN

By

Bob Boyce

B.A., Wilfrid Laurier University, 1988

THESIS

Submitted to the Department of Geography
in partial fulfilment of the requirements
for the Master of Arts Degree
Wilfrid Laurier University
1992

ISBN 0-315 78138-6

Acknowledgements

It took a mighty long time to complete this thesis and the patience of everyone who was around until the end are particularity appreciated. A special note of thanks must go to Bev Freeborn from Graduate Studies who made special allowances throughout the period of my absence.

I am eternally indebted to Richard Kelly, Paul Frey, and Chris Bradley, who provided many many hours of intellectual conversation and unbridled entertainment both in the field and at home in the "Ice House". Also to Chris Jarvis, Graham Boyce and Dr. David Collins from the Alpine Glacier Project who endured the lone Canadian for four months in Pakistan and helped him return with most of his mental and physical facilities intact.

Through the many years I was at Laurier Ken Hewitt and especially Houston Saunderson played an integral role in stimulating and nurturing my academic career. I am also eternally grateful to Gordon Young, mentor and employer who exposed me to the realm of snow and ice hydrology and the adventures of Pakistan. Gordon always displayed an incredible amount of stamina with me as his student and research assistant.

Financial support for this project was provided by the Canadian Government, Wilfrid Laurier University and Dr. Gordon Young's research grants. Many thanks must also go employees of the Water And Power Development Authority of the Government of Pakistan, especially Mohammed Ilias, who provided endless hours of companionship, entertainment and nerve wrecking driving during the 1988 and 1989 field seasons.

Thanks to you all!

ABSTRACT

Records of air temperature, global radiation and discharge from the Pasu Glacier basin in the Upper Indus River Basin have been examined with a view to developing a modest understanding of the simple physically based processes in action within this globally extreme mountainous region. Some glaciological data are also reported but in a preliminary manner. Relationships between air temperature characteristics, global radiation and discharge were investigated using correlation techniques. Daily average air temperatures recorded at the highest meteorological station, Patundas (4200m), provide the strongest degree of association with discharge. The data shows that this highly glacierised Karakoram basin exhibits similar relationships between air temperature and runoff as compared to other alpine basins in the mid-latitudes of the northern hemisphere.

Table of Contents

List of Figures

List of Tables and Plates

Tables

Plates

Chapter 1

Introduction

1.1 Foreword

Variations in glacier meltwater runoff are naturally linked to variations in meteorological conditions. The spatial and temporal variation of the generation of meltwater is a function of the spatial variation of snow cover with altitude, the migration of the snowline with altitude and the degree of glacierisation of the catchment. Generally, in the mid-latitudes of the northern hemisphere, over 80 per cent of the total annual discharge, from a glacierised basin, occurs between May and September. Glaciers can act as moderators of river flow in alpine regions, often producing greater amounts of runoff in low snowfall years and lesser amounts in high snowfall years. Glaciers accumulate and transfer water from zones of high precipitation to zones with a lower precipitation regime. The presence of even a small glacier in a catchment area may significantly alter the catchments hydrological balance.

The snow- and ice-fed rivers of the Upper Indus Basin are the principal source of surface water for more than one hundred million people, most living in the dry. subtropical lowlands of Pakistan. An extensive and large scale system of irrigation and hydropower developments regulate the meltwaters essential to agriculture-dependent Pakistan. The Tarbela earth dam development was built in an attempt to regulate the meltwaters originating from the Karakoram mountain system (Figure 1.1). However, characteristically variable river flow and insufficient understanding of the complex hydrometeorological relationships within the major runoff source zones of the Upper Indus Basin has made water management difficult.

The Upper Indus Basin (UIB), 162 000 km^2 above Tarbela Dam, encompasses an area having the largest concentration of perennial snow and ice on the mainland of Asia as well as one of the most rugged mountain environments in the world (Figure 1.2). Numerous peaks rise over 7000 m a.s.l. creating a global extreme of climatic variation between the arid and semi-arid valley bottoms to the permanently snow covered peaks. Over 12 per cent of the UIB is glacierised including several of the largest glaciers outside the polar regions (Table 1.1). It seems probable that 80 per cent of the total flow of the Upper Indus River is generated from almost 25 per cent of the catchment area (S.I.H.P., 1988). This 25 per cent of the catchment area corresponds to the zone containing of the ablation zone of the region's glaciers. On the southern Himalayan ranges, extensive and deep seasonal snowpacks are the main source of meltwater, contributing perhaps half of the total flow.

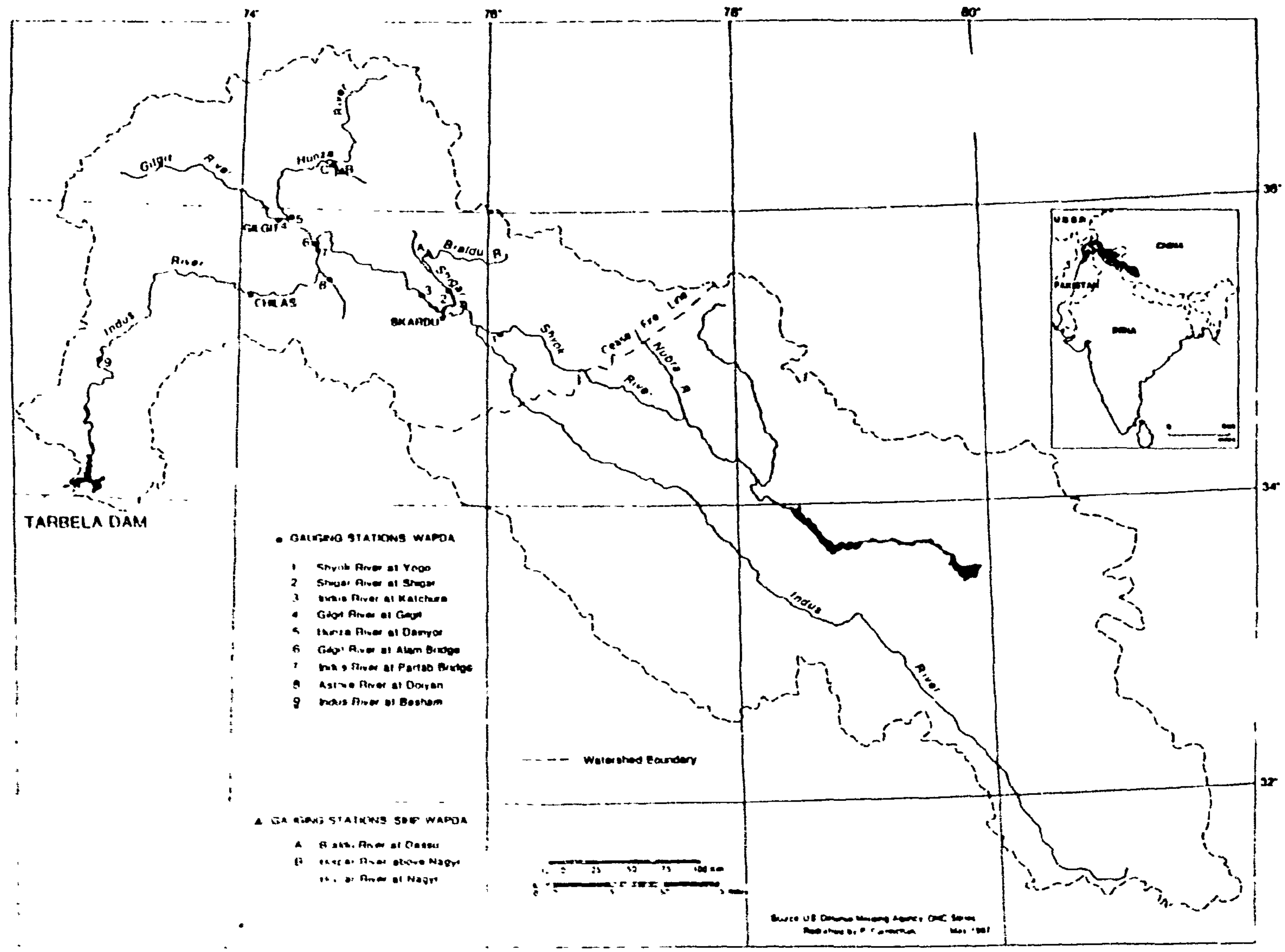

FIG 1.1 Map of Upper Indus Basin above Tarbela Dam.

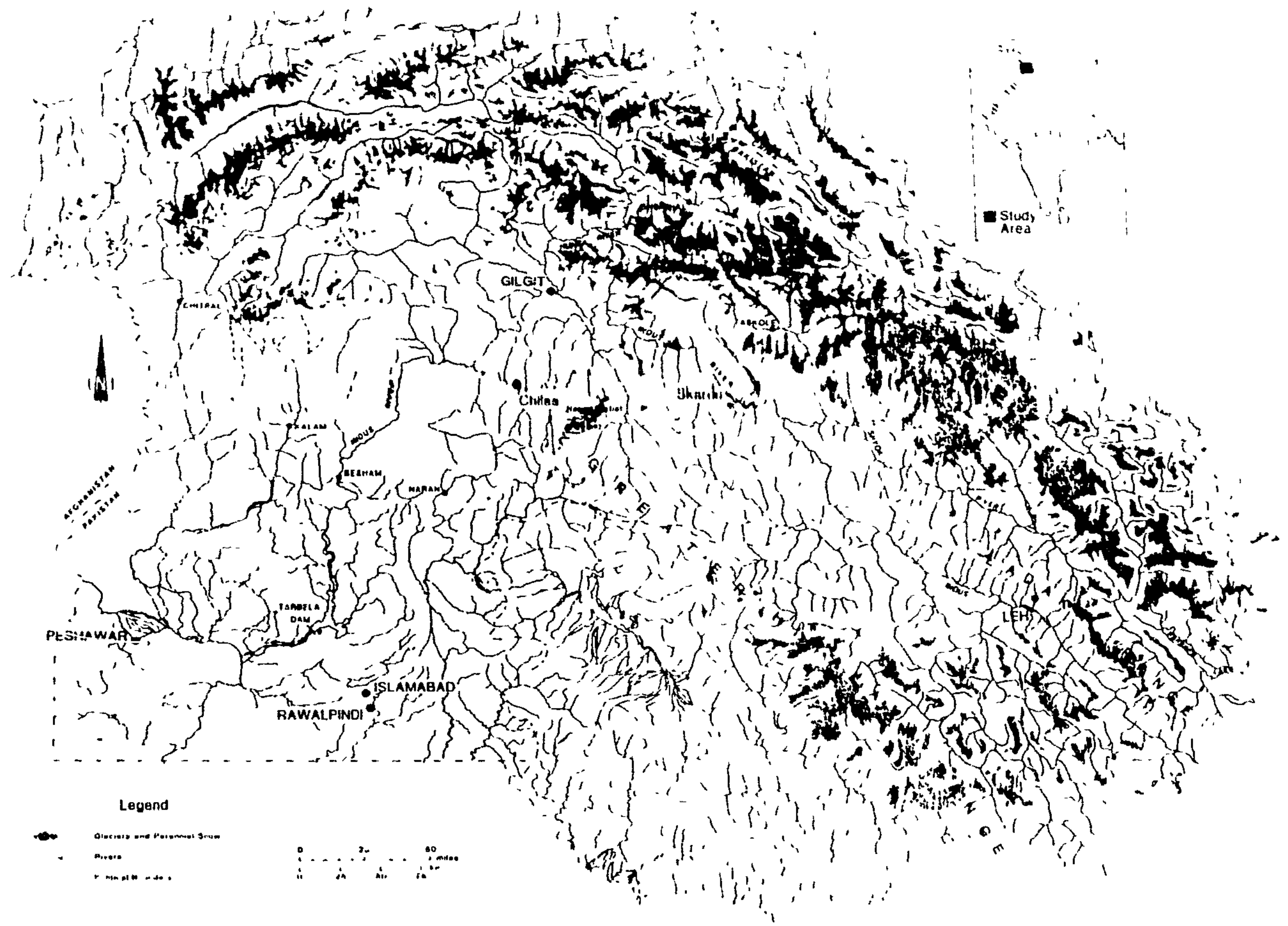

FIG. 1.2 Glaciers and Rivers of the Karakoram Range (Source: Hewitt, 1989).

Most tributary rivers in the UIB display a strong diurnal and seasonal regime with peak flows in summer. Snow covers 60 per cent to 90 per cent of the UIB from January to March. From early-March until July snow melt constitutes the bulk of river flow. As the transient snowline recedes up-slope glacier ablation areas become exposed contributing vast quantities of meltwater that dominate river flow from July to September. On a daily basis river flow varies with the change of available energy, principally incoming solar radiation. These short term, seasonal and year-to-year fluctuations of river flow are distinctly alpine in character. Unfortunately, understanding of the relationships between snow cover, glacier ablation and runoff in the UIB is rather poor.

Table 1.1 Length and Area of Some Karakoram Glaciers.

Glacier	Length(km)	Area(km^2)
Siachen	75	1183
Hispar	53	622
Biafo	68	628
Baltoro	62	757
Batura	60	296
Chogo Lungma	47	332
Miar	28	53
Pasu	22	60
Ghuilkin	18	45
Minapin	16	35

(Source: Hewitt and Young, 1989)

In recent years, improvements in satellite imagery technology and availability have been useful in revealing some important hydrological relationships. However, comparisons of areal snow cover with discharge records of several of the larger rivers in the UIB have produced inaccurate simulations and forecasts (Tarar, 1982). At least a modest sensitivity of the hydrological characteristics of glaciers and the meteorological interrelationships are essential in effectively developing any operational forecasting model of river flow in high mountainous areas.

The Pakistan Water and Power Development Authority (WAPDA) governs the network of irrigation and hydropower developments. One of WAPDA's primary directives is effective management of the natural water reservoirs of the UIB. Several stream gauging and weather stations throughout the UIB are maintained by WAPDA to better facilitate their forecasting requirement. However, all the weather stations are in dry valley floor locations which do not represent the precipitation or thermal regimes of the runoff source zones between 3000 m and 5500 m a.s.l. (Hewitt and Young, 1988; Butz, 1989).

In 1981 the Government of Canada consulted with WAPDA on a programme to apply the Canadian experience of snow and ice hydrology to the UIB. The Snow and Ice Hydrology Project (SIHP) 1985-1988, a collaborative effort funded jointly by the Canadian International Development Research Centre (IDRC), WAPDA and Wilfrid Laurier University (WLU), collected and analyzed relevant glaciological, hydrological and climatic data from the runoff source zones (Figure 1.2). The main aim of the project was to develop a better understanding of the hydrological system with an emphasis on developing an operational forecasting model for the UIB. In many respects the project was a success as represented in the voluminous database, annual research reports (S.I.H.P., 1985, 1986, 1987, 1988, 1989) and associated scientific articles (e.g. Hewitt *et al*, 1989; Butz, 1989; Wake, 1989; Young and Schmok, 1989; DeScally and Gardner, 1989).

1.2 Research Objectives

Radiation is the main energy source for snow and ice melt in high mountainous regions. It is often necessary, however, to find a practical surrogate variable for radiation in order to make estimates about the amount of meltwater from a highly glacierised basin. A study by Lang (1968) demonstrated that daily mean air temperature data measured outside the glacier basin correlated with melt from the Aletsch Glacier Basin in the Swiss Alps better than temperature measured on the glacier or just directly outside the glacier. This has recently been confirmed by other studies such as Braithwaite (1988) and Collins (1989a). Lang and Braun (1988) and Braun and Aellen (1990) discovered that daily temperature range represented global radiation to a much higher degree than mean air temperature as an input into forecasting models. Meteorological stations in the mountains, however, provided a low level of association between daily air temperature range and global radiation.

The main thrust of this study will determine which of the two characteristics of air temperature best represent global radiation and hence meltwater runoff within the highly glacierised Pasu Basin in the Karakoram Himalaya. Experiences of the SIHP reveal that measurement of hydrometeorological variables is very difficult in such a rugged and demanding environment as the Himalaya. Financial limitations and the lack of reliable meteorological instruments also hindered the design of this study. The highly crevassed nature of the Pasu Glacier surface does not allow for the establishment of an "on-ice" meteorological station and hence a complete energy balance approach to the study. The study is therefore employs air temperature and incoming solar radiation from directly outside the glacier to investigate the variations in runoff from the Pasu Glacier basin. Meteorological data from outside the basin may be used if available. Several other objectives will also be met by this study :

a) To develop an understanding of the physical relationships governing the evolution of meltwater generation within a glacierised basin by expanding and extending the meteorological and hydrological database within the major zone of runoff.

b) Describe and analyze the fluctuation and variation of river discharge draining from a highly glacierised basin during the season of significant snow and ice melt.

c) Describe and analyze the variations within and between meteorological variables over a range in elevation corresponding to the major runoff zone during an ablation season

d) Compare and contrast the results with other glacierised basins within the Karakoram with similar hydrological characteristics.

It is essential before proceeding with the study to give a comprehensive discussion on the hydrological and meteorological characteristics of glacierised basins with emphasis on the general area of the study location. The following chapter provides an outline of the general hydrological characteristics of glacierised basins. Examples are taken from around the world as well as within the Karakoram range. Chapter three follows with a discussion about the general physiography and climatology of the Karakoram area. A description of the study site, an outline of the field procedure adapted for this study and a summary of the measurement record is given in Chapter four. Chapter five analyses, interprets and discusses the data obtained during the 1989 field season followed by a general summary, conclusions and future recommendations.

Chapter 2

The Hydrologic Role of Glaciers in High Mountain Areas

2.1 Introduction

The high mountain areas of the world play an extremely important and distinctive role in the regulation of streamflow in the headwaters of many major rivers in most continents. Runoff from glacier basins is a crucial water resource for domestic and commercial development of hydro-electric power, irrigation and agricultural purposes (Meier and Roots, 1982). Most glacier runoff occurs between mid- and late-summer when supply of water from other sources is low and demand is high (Krimmel and Tangborn, 1974). It is in high mountain areas where meteorological, hydrological and glaciological phenomena have their most intimate and complex interactions. There is enormous variability over short and long time scales and short space scales yet the results of these interactions have a profound effect on hydrological regimes over vast areas. This variability of interaction is a reflection of the characteristic irregularities of topography and exceptionally large range in altitude found in high mountain areas.

2.2 Mass and Water Balance in High Mountain Areas

There are two basic approaches in investigating the components responsible for the amount of runoff released from a glacierised basin, either the mass balance approach or the water balance approach. The mass balance approach employees glaciological methods in evaluating the hydrological conditions within a glacierised basin. The water balance approach uses meteorological variables and runoff in the classical hydrological method which must be modified slightly for use within glacierised basins. It is necessary to the study that the fundamentals of each approach are understood and therefore a much more detailed discussion of each of the two methods is given below.

2.2.1 Mass Balance

A significant proportion of precipitation in high mountain areas, is stored from year to year as glacier snow and ice. A glacier is a mass of ice flowing down-slope from an area of snow accumulation and storage, called the *accumulation area*, to the *ablation area*, an area of snow and ice melt (Figure 2.1). In the accumulation area, more snow accumulates than is melted (i.e. a positive balance) over a hydrological year. Most of the snow accumulation is derived from direct precipitation on the surface of the glacier. However, other sources of accumulation, such as sublimation, superimposed ice, blown-in snow and avalanches from the valley walls, can also contribute significant amounts of mass to a glacier. Under the weight of successive snow falls, snow eventually becomes transformed into glacier firn and ice. Glacier

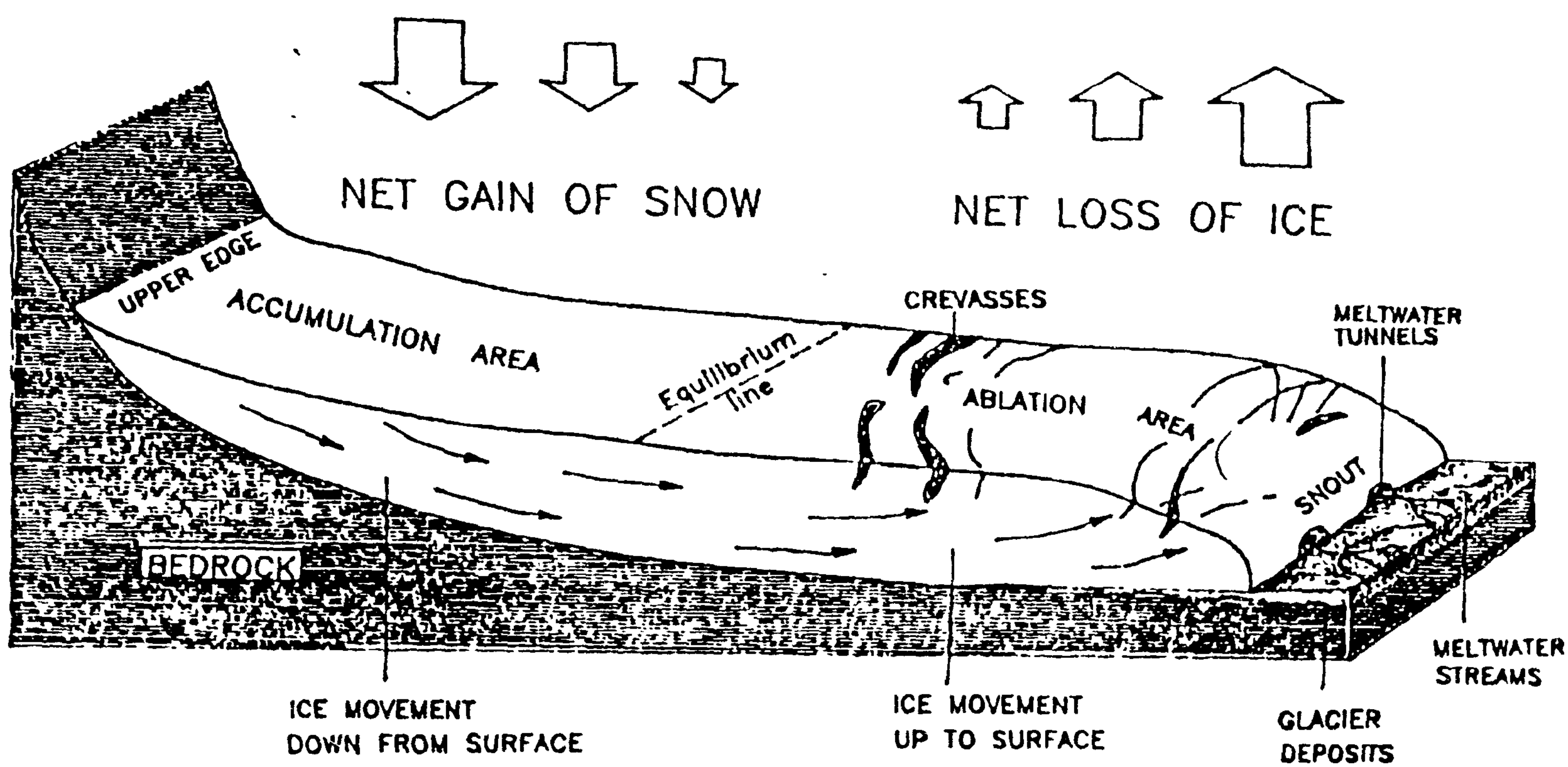

FIG 2.1 Schematic Diagram of a Typical Mountain Glacier.

ice flows down-slope, under the influence of gravity, from the accumulation area to the ablation area by plastic internal deformation of the ice as explained by Nye (1952). In the ablation area more snow and ice is melted and evaporated than replaced by solid precipitation (i.e. a negative balance). Snow and ice from the accumulation area replaces ice that has been melted in the ablation area (Meier, 1973).

The difference between net accumulation (c) and net ablation (a) determines the annual mass balance (b) of a glacier as expressed by a simple storage equation:

$$b = c - a \qquad (2.1)$$

If the amount of ablation equals the amount of accumulation (i.e. $b=0$) then the glacier is said to be balanced. However, the inherent variability of climate dictates that the mass balance of a glacier will normally be either negative or positive.

The depth of the winter snow pack and the progression of summer air temperatures have a profound effect on the net annual mass balance (Hino *et al*, 1987). For example, a thick winter snow pack coupled with low summer temperatures will significantly retard snow and ice ablation well into the summer resulting in a strong positive net balance. Conversely, a strong negative balance is seen in years when a shallow snow pack is coupled with high summer temperatures. The thin winter snow pack quickly disappears exposing the glacier ablation area for a prolonged period resulting in appreciable wasting of glacier ice. Results from mass balance studies on Peyto Glacier (22.8 km^2 and 61 per cent glacierised), in 1974 and 1970 respectively, exhibit quite explicitly this particular phenomenon (Young, 1982).

As a general rule, in the northern hemisphere, the ablation season starts in early-May and ends in mid-September. The length of the ablation season is a function of the prevailing weather conditions. In years with low precipitation and high temperatures the length of the ablation season is considerably longer than a year with abundant precipitation and predominantly low temperatures.

Studies of glacier mass balance are concerned with the interaction between the general environmental conditions and the dynamics of glacier activities. The mass balance of a glacier obtained using the glaciological method, equation 2.1, involves direct measurements of accumulation, by pits or cores, and ablation against stakes throughout the year (Östrem and Stanley, 1969). Measurements of general meteorological variables, such as air temperature, global radiation, wind and precipitation, taken within the basin or detailed energy balance studies of conditions at the glacier surface can be taken to determine relations between mass balance and glacier variations (Östrem, 1973; Young, 1977b; Braithwaite, 1981; Kuhn *et al*, 1985).

2.2.2 Water Balance

Over a hydrological year the storage factor for an unglacierised basin can usually be ignored in water balance studies leaving annual streamflow equal to precipitation minus evaporation (Gregory and Walling, 1979). However, the yearly total runoff from a glacierised basin is very rarely equal to the sum of precipitation minus evaporation because of natural changes in storage of glaciers (Fountain and Tangborn, 1985). In a hydrological context, a mountain glacier can be thought of as a reservoir of water which gains precipitation in both liquid and solid form, stores a large share of this precipitation and then releases it at a later date from several hours to several tens of years. For a highly glacierised basin the change of storage is essentially the annual mass balance (*b*) in water equivalence from equation 2.1. The yearly total runoff (*R*) from a glacierised basin can therefore be expressed as the difference between precipitation inputs in both solid and liquid form (*P*), evaporation and sublimation (*E*) and changes in the storage of the glacier (ΔS) as follows:

$$R=P-E-\Delta S \qquad (2.2)$$

This hydrological method of determining mass balance is concerned with the change in storage of not only the glacier but, change in storage of the whole drainage basin (equation 2.2). Basin water balance is obtained by the continuous measurements of meteorological variables and runoff which is not possible in mass balance studies. The continuous record provides an indication of runoff sources and changes in glacier and basin water storage revealing their relation to the hydrometeorological variables over diurnal, seasonal and annual timescales (Elliston, 1973; Collins, 1989a).

An excellent collection of examples of water and mass balance studies for the European Alps are given by Röthlisberger and Lang (1987).

2.3 Geographical controls of the water balance of an alpine glacier basin

Several geographical factors govern the relation between precipitation inputs, evaporation and changes in storage of snowpacks and glaciers. Latitude, altitude and topography play the major roles in controlling the basic hydrometeorological variables: temperature, global radiation, precipitation, wind, evaporation and sublimation (Sugden and John, 1984). Each of the hydrometeorological variables will be discussed with respect to their geographical controls.

2.3.1 Air temperature

Temperature controls the ability of air to hold water. Warmer air masses may hold significantly greater amounts of moisture than colder air masses (Geiger, 1965). With increases in altitude there is a corresponding decrease in temperature of roughly 6.5 °C km^{-1} on average called the *adiabatic lapse rate* (Henderson-Sellers and Robinson, 1986). The adiabatic lapse rate changes with the degree of saturation of the air mass such that when the air is saturated the adiabatic lapse rate drops to less than 5 °C km^{-1} (SALR) and when the air is dry the adiabatic lapse rate is 9.8 °C km^{-1} (DALR). However, when air temperature is below zero, the ability of the air to hold moisture is so low that the SALR may become equal to the DALR. Therefore, lapse rates vary in relation to different synoptic weather conditions and to season (Harding, 1979; Kang and Xie, 1989).

As air is orographically forced upward, there is a greater amount of precipitation. Also, at the colder temperatures encountered at higher altitudes, liquid water begins to crystallize making snowfall more dominant. As a result, temperature variations with altitude control not only the amount of precipitation, but also the form in which the precipitation falls. Daily mean gradients of maximum temperatures are controlled by altitudinal effects whilst minimum temperature gradients are more likely influenced by the local topography (Harding, 1978).

During the night and the winter, nocturnal radiative cooling at the ground surface, may cause a *temperature inversion*, where the temperature lapse rate becomes reversed and temperatures increase with altitude (Henderson-Sellers and Robinson, 1986). Other factors inducing a temperature inversion, especially in a glacierised basin, are the advection of a warm air mass over a colder surface, föhn winds and katabatic drainage (Barry, 1981).

2.3.2 Solar radiation and heat balance

Solar radiation varies diurnally and seasonally, and with latitude, in accordance to relations in the earth-sun orbit. The slope angle and slope orientation (aspect) of the terrain within a mountain basin, determine the intensity of solar radiation striking the surface (Garnier, 1970; Obled and Harder, 1979). In the northern hemisphere, south facing slopes receive more solar radiation than north facing slopes. The closer to perpendicularity the slope surface is to the incoming rays of the sun, the greater the intensity. The longer the sun shines on a surface, the greater the heating that takes place. The combination of all the above factors control the location of perennial snow patches and glaciers (Graf, 1977) and the spatial and temporal variation of snow and ice melt.

The thermal regime within any mountain basin is a direct result of the balance of available energy components near the surface. Available energy at the snow or ice surface is balanced as follows:

$$Q_{NR}+Q_S+Q_L+Q_C+Q_M=0 \qquad (2.3)$$

where Q_{NR} is the net radiation, Q_S is the sensible heat flux, Q_L is the latent heat flux, Q_C is the conductive heat flux from the snow pack or glacier ice and Q_M is the heat for snow or ice melt. Net radiation (Q_{NR}) is the sum of the net short-wave radiation, Q_{RS}, and the net long-wave radiation, Q_{RL}, and is expressed as:

$$Q_{NR}=Q_{RS}+Q_{RL} = G(1\text{-}A)+Q_{RL}\downarrow+Q_{RL}\uparrow \qquad (2.4)$$

where G is global radiation, A is the albedo of the surface, $Q_{RL}\downarrow$ and $Q_{RL}\uparrow$ are the downward (atmospheric) and upward (terrestrial) long-wave radiation respectively (Röthlisberger and Lang, 1987).

It is possible to observe or calculate the components of the balance equation to determine the amount of snow or ice melt and the relative influence of each component on melt (Hoinkes, 1955; Goodison, 1972a; Zuzel and Cox, 1975; Xie *et al*, 1979; Ambach and Kuhn, 1987; Greuell and Oerlemans, 1987). Although net radiation has been established as the chief agent in the melting of snow and ice, it has long been known that air temperature gives the best results for hydrometeorological studies since air temperature integrates short- and long-wave radiation, and the sensible and latent heat fluxes (Hoinkes, 1955; Braithwaite, 1981; Sloan, 1986).

On a diurnal scale, incoming solar radiation generally shows a midday maximum with a delay in the occurrence of maximum temperature until roughly two hours later (Figure 2.2). The lag time between maximum radiation and maximum temperature is caused by the gradual heating of the air by convective heat transfer from the ground. The decrease in temperature after mid-afternoon is slowed by heat supplied from the ground while radiation inputs diminish much more quickly. Minimum air temperature occurs shortly after sunrise. The cooling of the ground and surface air may continue for a half hour or so after sunrise as outgoing long-wave radiation exceeds incoming radiation. Surface heating may be longer when the ground is moist and available energy is used for evaporation. Furthermore, there is a delay in the transfer of heat from the ground through the air to the temperature recording device. The occurrence of the diurnal minimum and maximum temperature is directly related to the amount of incoming solar radiation and its diurnal regime. However, minimum temperatures are delayed with altitude through the summer months whilst maximum temperatures advance with altitude (Kang and Xie, 1989). The diurnal temperature range decreases with altitude due to a decrease in the radiative and turbulent heat exchanges between the surface air and the free air (Price, 1981).

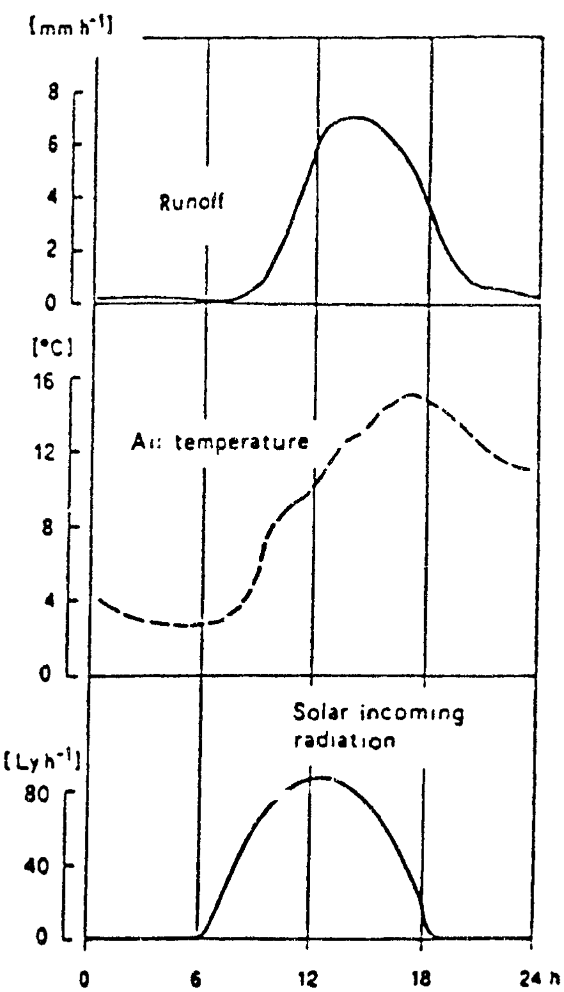

FIG. 2.2 Diurnal Variations of Runoff, Air Temperature and Radiation, Gornergletchser 1959 (Source: Röthlisberger and Lang, 1987).

2.3.4. Cloud cover

Cloud cover, which varies from season to season, according to time of day and prevailing weather systems, alters the amount of solar energy received on a surface, and hence air temperature (Barry, 1981). During cloudy weather, cloud type and amount regulates the amount of solar radiation reaching a surface. For example, convection clouds do not retard incoming radiation as effectively as stratus clouds. A cloud cover traps outgoing long-wave radiation ($Q_{RL}\uparrow$), such that air temperatures are moderated reducing diurnal ranges drastically compared to clear days. Afternoon clouds or haze can cause the maximum daily air temperature to advance by two to three hours (Flohn, 1974)

2.3.5 Wind

Topography, rather than altitude, is usually the major geographic control governing wind velocities (Barry, 1981). However, wind speed does increase with altitude in the middle latitudes, on average, because of the westerly wind belts (Reiter, 1963). It is often the case that high, steep topography diverts wind patterns from their original course. Some of the extremely high peaks where elevations are high enough to penetrate the jet stream, as found in the Himalayas, experience exceptionally high wind speeds. Indeed, the Himalayas split the jet stream in two during the winter months (Barry and Chorley, 1985). Deep, narrow valleys intensify wind speed as well as govern direction. Daytime warming of the lowest part of the atmosphere in mountainous areas creates up-valley winds as the lighter warm air rises. As the temperatures begin to drop towards nightfall there is a draining of cold dense air at higher elevations into depressions and valleys creating a *mountain wind* (Geiger, 1965). Up-valley winds are usually stronger than down-valley winds because of the greater daytime radiative exchanges feeding the wind system (Gleeson, 1953). In a glacierised mountain basin, a persistent down-valley wind occurs. The *glacier wind* is generally strongest in the early afternoon when the difference in temperature between the glacier surface and the surface air is at a maximum.

Wind has a profound effect on the spatial distribution of snow accumulation. Snow is redistributed around a basin causing a differential snow cover depth. This has a profound effect on the timing and duration of snow melt. Exposed slopes are typically swept clean of snow by wind. Wind-blown snow is deposited in areas where the local topography creates a decrease in wind speed.

2.3.6 Precipitation

Precipitation is the most important component of the water balance equation. Precipitation is the source of input to the hydrological system within both nival and glacierised mountain basins. The orographic effect of a mountain system has a profound effect on the precipitation processes (Barry, 1981). A mountain system acts as a barrier forcing air masses upward as they approach. As the air mass rises condensation of water vapour increases and precipitation may eventually occur. The increase of precipitation with altitude is well known (Flohn, 1974; Barry, 1981; Price, 1981; Wake, 1989). In the middle latitudes of the northern hemisphere, where most of the alpine glaciers lie, precipitation increases at least up to the highest levels of direct observations beyond which little is known (Barry, 1981). In the Austrian Alps, Lauscher (1976) found that precipitation increased from about 350 mm near sea level to more than 1500 mm at an altitude of 3000 m. In the Himalayas, snow pit studies by Ageta (1976), BGIG (1979) and Wake (1989), indicate precipitation reached a maximum of 1500 mm or greater between 4900 m and 5400 m a.s.l. and probably decreases at higher altitudes.

2.3.6.1 Snow Accumulation and Spatial Variation

The increase in the amount and proportion of precipitation, in the form of snowfall, with altitude has a profound effect on the hydrologic regime of a high mountain basin. At 3000 m a.s.l., Lauscher (1976) found that 75 per cent of the annual precipitation, and as much as 65 per cent of the summer precipitation, was in solid form whereas near sea level the fraction drops to roughly 40 per cent. Maximum precipitation takes place at or above the upper limit of snow melt. Therefore, most precipitation in a mountain basin provides nourishment for glacier(s) or perennial snow patches rather than direct runoff.

The winter snow pack varies over the whole basin as a consequence of its altitudinal range and orientation (Andrews, 1975). For example, precipitation increases with altitude but snow on slopes exposed to strong winds is blown off and redistributed around the basin and deposited in hollows or depressions (Graf, 1976). Indeed, the existence of some glaciers is a result of redistributed snow accumulating in areas where it is not exposed to conditions sufficient to melt all the snow away. In the northern hemisphere, the glaciation limit is lower on north-facing slopes than on south-facing slopes (Östrem, 1966).

2.3.7 Runoff in a glacier basin

Runoff in a glacier basin varies spatially and temporally yielding hydrological characteristics unique to high mountain areas. The compensating effect of glacier runoff is the most profound characteristic with diurnal variations being the most recognisable. Both of these characteristics are intrinsically linked to the secular variations in climatic variables.

2.3.7.1 The compensating effect

The runoff from a glacierised catchment originates from two different source areas, the glacierised area and the non-glacierised area. The glacierised areas derive runoff from the ablation of glacier snow, ice and firn, rain that falls on the glacier surface, from the internal drainage networks of the glacier and meltwater from ice-cored moraines (Krimmel and Tangborn, 1974; Collins, 1982a). Non-glacierised areas generate runoff from the melting of the seasonal snow pack, groundwater and liquid precipitation events. In warmer, drier summers, a larger proportion of the glacier is exposed releasing greater quantities of water from storage by the melting of glacial ice, compensating for the diminished contributions to runoff from lower precipitation inputs (Young, 1982; Braithwaite and Olesen, 1988). Cooler, wetter summers experience a reduction in the contribution of meltwater released by glacier ablation and runoff is maintained by the higher precipitation inputs (Collins, 1984, 1989a; Braithwaite and Olesen, 1988). For non-glacierised basins, maximum runoff occurs in May. Maximum runoff in a glacierised basin is prolonged later and later in the summer as the degree of glacier cover increases (Fountain and Tangborn, 1985).

There is a significant reduction in runoff in response to summer snowfalls which are normally associated with colder temperatures (Figure 2.3) (Collier, 1958; Lang, 1973; Young, 1982; Collins, 1984). Braithwaite and Olesen (1988) found a negative correlation between snow accumulation and runoff. The correlation becomes stronger with increasing glacier cover (Tarar, 1982; Ferguson, 1985). The timing and volume of runoff, during any particular summer, is a function of the depth and areal extent of the winter snow pack with altitude, basin topography and the regional thermal and precipitation regimes.

2.3.7.2 Snow, Firn and Ice Melt

Most snow, firn and ice melt is generated at the surface of the glacier or snow pack. Melt only occurs when the surface, not the surface air temperature, has absorbed enough energy to raise the surface temperature to 0 °C (Schytt, 1967; Kuhn, 1987). Once the critical threshold is reached, any additional incoming energy is employed for the melting of snow, ice or firn (Oerlemans, 1986). Kuhn (1987) estimates that snow melt may occur at temperatures as low as -10 °C. Some melting occurs within the glacier by heat generated from the internal deformation of

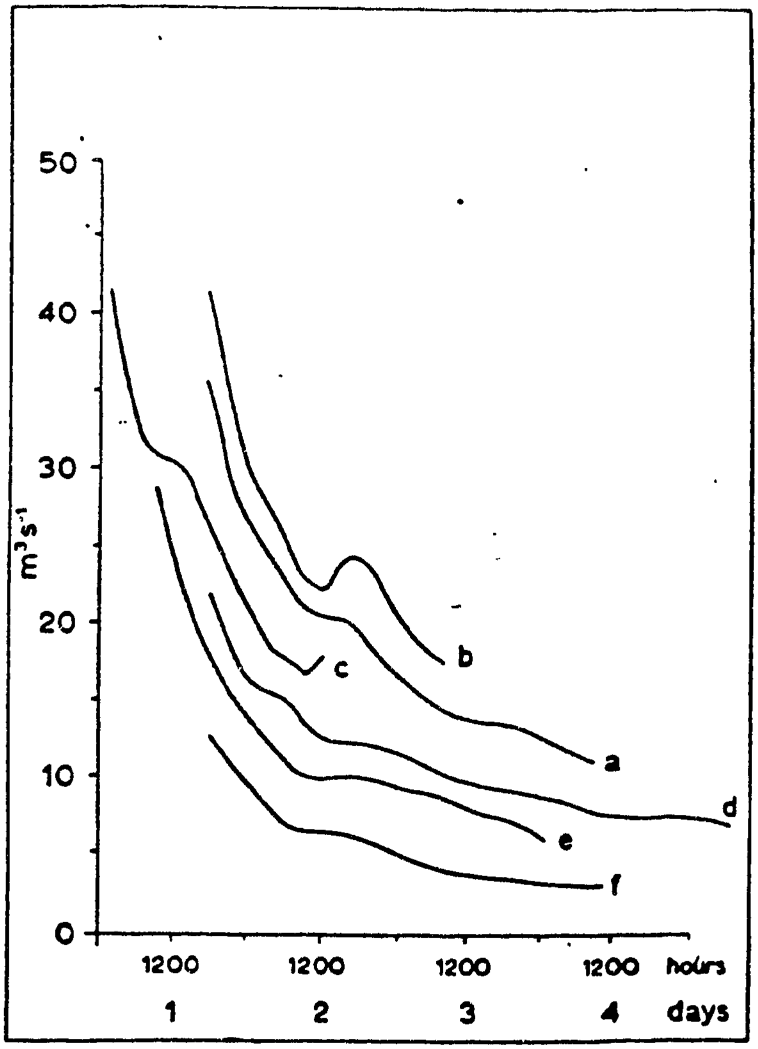

FIG. 2.3 Depletion of Matter-Vispa and Gonera after summer snowfalls. Matter-Vispa: (a) 29 June-2 July 1959; (b) 30 July-1 August 1959; (c) 26-28 June 1960; (d) 4-8 September 1960; (e) 17-19 September 1960. Gonera (f) 29 June-2 July 1959. (Source: Elliston, 1973)

flowing ice and by geothermal heat radiated into the base of the glacier but, these amounts are negligible by comparison to the quantity of surface melt (Meier, 1973). Paterson (1981), Braithwaite (1981) and Röthlisberger and Lang (1987) have shown that energy released by rainfall negligibly contributes to snow or ice melt.

The rate of snow and ice melt varies in accordance with altitudinal and topographical variations of a surface and in response to changing energy inputs. Irregular surface topography promotes the pooling of cool air in hollows, producing variations in surface heat balance and hence melting (Goodison, 1972b). Meier and Tangborn (1965) and Schytt (1967) found that ice ablation decreased with altitude. The amount of ablation at higher altitudes is more sensitive to precipitation than to heat transfer, because of the more uniform albedo of snow cover, and by more frequent snowfalls within the ablation season. The amount of ice lost near the snout is more sensitive to heat transfer because of the lower albedo of glacier ice, greater surface roughness and a longer period when the surrounding terrain is free of snow. Advective transfer of heat from regions surrounding the glacier ablation zone, which varies according to terrain type, is therefore, a very influential factor. Goodison (1972b) determined there was no simple relation between global radiation and the amount of glacier ablation, allowing for aspect, gradient and shadow. However, Röthlisberger and Lang (1987) illustrate that the diurnal pattern in runoff corresponds closely to the diurnal pattern of global radiation (Figure 2.2).

Although solar radiation increases with altitude the relative effectiveness of the energy source is dependent upon slope aspect and the albedo of the receiving surface.

Albedo is the ratio of reflected to total short wave radiation of a surface (Barry, 1981). More energy is absorbed by glacier ice than by snow because ice and firn have lower albedos, between 0.2 and 0.4, while snow has a high albedo, between 0.6 and 0.8, and reflects most incoming radiation (Henderson-Sellers and Robinson, 1986). Therefore, glacier ice melts at a much faster rate than does glacier snow which has profound consequences for glacier mass balances in years of extreme weather conditions. A debris cover on the glacier surface alters the rate of ice melt by changing the albedo of the ice surface (Nakawo and Young, 1982). A debris cover of 10-50 mm actually enhances ablation. Below 10 mm solar energy is not stored within the debris and is available for the melting of glacier ice. A larger debris cover reduces melting because the debris cover acts an insulator by trapping the solar energy within the air between the debris (Mattson and Gardner, 1988).

Within the lower reaches of the accumulation zone areas of firn may also become exposed especially during warm, dry summers, contributing relatively smaller quantities of meltwater to streamflow. Since firn has a lower albedo than ice, it melts relatively faster (Fountain, 1989). Quantities of meltwater from the combined melt of glacier ice and firn offset the rapid decline of snow available for melting on both the glacierised and non-glacierised areas. Little, if any, ablation occurs in the upper accumulation zone as temperatures are normally too low and albedo is high.

2.3.7.3 Spatial and temporal distribution of runoff

Annual variations in climatic conditions generate variations in mass balance which in turn determine the amount of runoff within high mountain areas. Variations in seasonal and annual runoff for nival basins are directly related to irregular precipitation inputs. However, the total annual runoff from such a basin will always be less than the total precipitation (Meier, 1969). The range of variation in runoff from glacierised basins is reduced by comparison to that of nival catchments (Ramussen and Tangborn, 1976). Kasser (1959) and Krimmel and Tangborn (1974) determined a minimum variation in annual runoff is observed in basins with about 30 per cent glacier cover. In basins with greater than 30 per cent glacier cover, year to year variations in annual runoff, which may be at least 20 per cent of the mean (Collins, 1982a; Haserodt, 1984), are not directly related to annual variations in precipitation inputs as are basins below 30 per cent glacier cover. Annual runoff from a highly glacierised basin may be greater than, equal to, or less than total precipitation inputs (Collins, 1984).

Generally, over 90 per cent of the total annual runoff from a glacierised basin is produced between May and September and about 80 per cent of this occurs in June, July and August (Young, 1982; Collins, 1982a). The spatial and temporal distribution of summer runoff depends on both the area/altitude distribution of glaciers and seasonal snow patches as well as the evolution of the transient snowline within the drainage basin. From October, the beginning of the hydrological year, to April, a low runoff regime dominates as temperatures remain low. However, intermittent melt periods can produce a slight, temporary increase in runoff. With the onset of spring, energy inputs, and subsequently air temperatures, begin to increase and the thinner part of the winter snow pack begins to melt, since precipitation, and consequently snow depth, generally increase with elevation (Barry, 1981). Streamflow continues to increase as the thicker areas of the snow pack begin contributing to runoff. Maximum snow melt runoff occurs in June, after which, the contribution of snow melt to runoff declines because of the dwindling winter snow pack (Ferguson, 1985). In nival basins, streamflow now becomes dependent on precipitation inputs and ground water as the primary sources of runoff. However, in a glacierised basin, runoff continues to increase after peak snow melt, because the depleting winter snow pack has uncovered an increasingly larger portion of the glacier surface and intense melting occurs (Östrem, 1973). Maximum runoff occurs in July and August as the transient snowline reaches its maximum altitude exposing the maximum areal extent of the ablation area. Decreasing air temperatures coupled with new winter snowfalls in September, retard snow and ice melt such that runoff quickly diminishes. However, runoff would decrease almost immediately if not for the lag effects of water storage within the glacial drainage system (Stenborg, 1973; Collins 1989b). Although the seasonal patterns of runoff are similar from year to year, the timing and quantity of runoff significantly varies from year to year as shown by Collins (1984) in the Swiss Alps.

The distinctive diurnal and seasonal rhythms in runoff reflect the spatial and seasonal distribution of snow and ice, diurnal and seasonal variations in available energy, primarily in the form of solar radiation, and the changing contributions of snow and ice melt (Hoinkes, 1955; Meier and Tangborn, 1961; Meier, 1969; Tallan, 1972; Elliston, 1973; Lang, 1973; Young, 1980; Braithwaite, 1981). Maximum daily flow occurs roughly six hours after the midday maximum of incoming solar radiation in May or June and decreasing to three hours in late-August (Lang, 1968).

There is a lag of about three hours between maximum daily melt and maximum daily runoff because of the transport time from the maximum source of melt to the flow recorder (Figure 2.2). Minimum daily flow corresponds to minimum temperature in late-summer and mid-morning in May and June. The diurnal range between minimum and maximum runoff is small prior to the disappearance of the seasonal snowcover. As a larger area of the glacier becomes exposed the diurnal range expands by several times by August (Elliston, 1973) (Figure 2.4). The decrease in lag time of maximum flow and the increase in diurnal range is also closely linked to the migration of the transient snowline up-slope and the subsequent increase in contribution of ice melt and the maturing englacial drainage system (Iken *et al*, 1983; Hooke *et al*, 1985). Stenborg (1970) observed a very significant delay of runoff in June to July within the glacier drainage network by as much as 25 per cent to 33 per cent.

2.3.7.4 Analysis of hydrometeorological phenomena

The energy balance within glacierised basins is important in understanding the physically based processes of glacier melt and runoff (Hoinkes, 1955). However, the empirical results obtained from the relations between air temperature and runoff provide a more comprehensive explanation of the hydrometeorological phenomenon within a basin than the energy exchanges at a certain point on the glacier surface (Lang, 1968, 1973; Young, 1982; Braithwaite, 1988; Collins, 1989a).

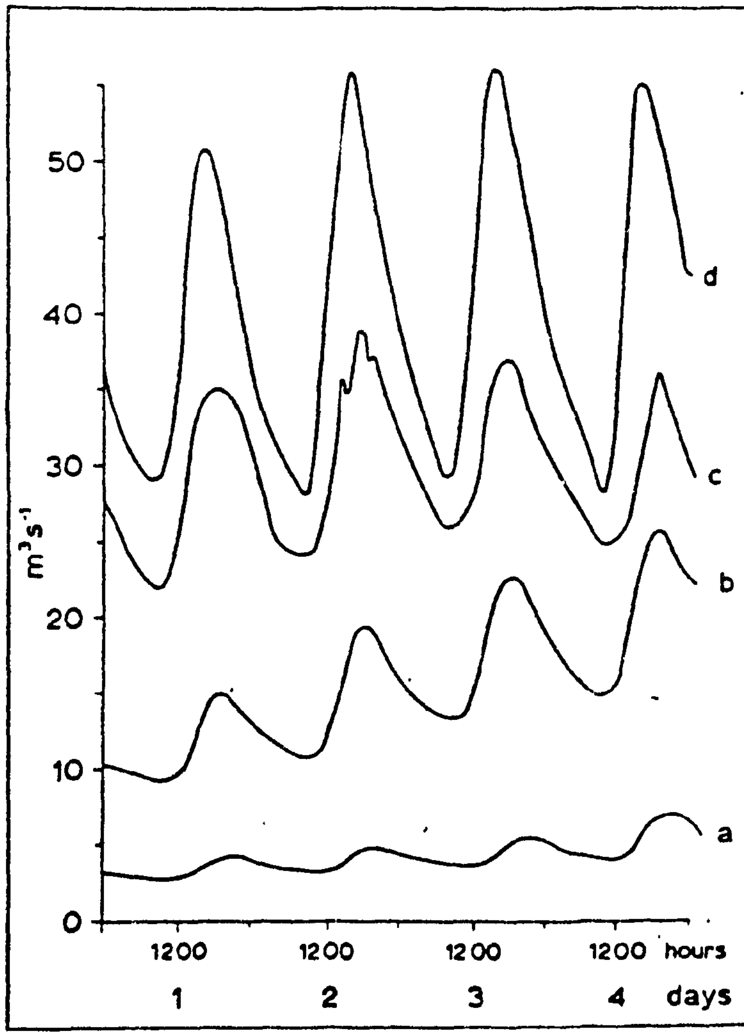

FIG. 2.4 Discharge of the Matter-Vispa Over Selected 4 Day Periods in 1959; (a) 17-20 May; (b) 14-17 June; (c) 23-26 June; (d) 19-22 July. (Source: Elliston, 1973)

Lang (1968) determined, using multiple regression analysis, that on a hourly basis, global radiation had the greatest influence (r=0.921) on meltwater runoff generated in a glacierised basin in the Swiss Alps. However, air temperature observed"out-side" the glacier gave a much better correlation (r=0.733) than temperatures observed on the glacier (r=0.591). Using daily means, air temperatures observed on the glacier showed the best relation to runoff (r=0.861). The influence of wind appears only to affect temperatures outside the glacier. Lang (1968, p.437) suggests '[temperature] contributes a large amount of "information" to glacier ablation, which seems to be valid especially for a drainage basin with a large altitudinal range'.

In another Swiss glacierised basin, Collins (1984), using a data series of several years and multiple regression, determined the relation between the average monthly temperature for the months May - September to be significantly correlated with runoff (r=0.73) over the same period. It should be noted that Collins also found that the precipitation in May was negatively correlated with the total summer runoff (r=-0.63). This is because relatively high precipitation in May, usually in the form of snow in the Alps, retards glacier melt well into the ablation season.

Time dependent spectral analysis did little to improve on the relation between meteorological elements and runoff (Gudmundsson, 1975). Gudmundsson found, in August, 70 per cent of the variance of runoff was due to variations in temperature and part of the remaining variance could be accounted for by wind. Gudmundsson concludes that the addition of non-linear analysis techniques, may provide more explanation of the variation in runoff from glacierised basins. Hu (1989) suggests a combination of a linear and a time series analysis can be used to explain the relation between glacier melt and air temperature. By using this method, Hu was able to simulate runoff from temperature data within ±20 per cent.

Although observations of hydrometeorological variables are not truly independent but are naturally time dependent most researchers have found that linear regression techniques are adequate for the explanation of relationships between meteorological elements and meltwater runoff in high mountain basins. The possible loss of information is generally accepted by researchers using the conceptually simpler linear regression analysis rather than the mathematically intense time series analysis methods because they provide a reliable explanation of the variation in hydrometeorological variables. Unfortunately no studies known to this author have been preformed to quantify this loss of information.

2.4 Water movement within and beneath a glacier

Our knowledge of the movement of surface, englacial and basal meltwater, from its source to the snout of the glacier via the intra- and subglacial drainage network, is still incomplete. Basically there are two methods available for exploring the drainage system within and at the bottom of the glacier: a theoretical approach, using complex mathematics, and field observations of natural and artificial tracers injected into the system. This discussion by no means attempts to thoroughly review or evaluate these contemporary approaches but, rather provides the fundamental principles of the drainage system of glaciers as it pertains to the present study.

Hino *et al* (1987) suggests that a great deal of melting occurs at the equilibrium line and must find its way to the snout of the glacier. Meltwater and meltwater streams attempt to form a supraglacial drainage network surface before entering into the glacier through infiltration, crevasses or moulins. In the upper regions of the glacier meltwater percolates into snow and firn where it may be stored analogously with a thin, unconfined aquifer (Fountain, 1989). Upon entering the moulin or crevasse, water pools in the bottom and overflows for some distance in channels that follow the crevasse in which the moulin was formed (Röthlisberger, 1982). The channels often meander deeper into the glacier and, after about 40 m below the ice surface, virtually all knowledge is based on theoretical and tracer studies. The water is usually not seen again before emerging from beneath the snout of the glacier.

Following the work of Hodge (1974) and Tangborn and others (1975) it is now widely accepted that conduits close and become considerably smaller in size during the winter. Plastic flow of ice during the winter, when water input is small or negligible, provides the mechanism for conduit closure (Nye, 1952). In May, when melting starts, water pours into the glacier faster than it can be transmitted through the shrunken conduits. The water then builds-up in the subglacial drainage system, resulting in high water pressures at the bed. The build-up of water within the englacial and subglacial conduits in early spring may increase flow velocities as the water pressure is sufficient to "lift" the glacier off its bed as observed by Hooke *et al* (1983) and Iken *et al* (1983). Eventually the combination of high water pressure and increasingly greater amounts of water enlarge and develop the internal drainage network. As a result, lag times between daily maximum ice melt and daily maximum runoff decrease and the diurnal range of discharge increases with the progression of the ablation season (Elliston, 1973).

Theoretically, if englacial passages are completely filled with water, they should form an upward dendritic network oriented with the equipotential planes within the ice (Shreve, 1972). The equipotential planes dip up-glacier at an angle several times greater than the slope of the glacier. Dispersivity is higher in englacial and subglacial networks than in proglacial networks because of the three dimensional branching of the internal drainage system (Krimmel *et al*, 1973).

Tracer studies by Stenborg (1969), Krimmel *et al* (1973), Behrens *et al* (1975), Lang *et al* (1979), Collins, 1982b, Burkimsher (1983), Humphrey *et al* (1986) and Burgman (unpublished) reveal that in some cases water is delayed in its passage through the glacier. In some cases, however, they found that there was no delay. In the latter instance some of the authors compared flow velocities and dispersion characteristics in the englacial-subglacial and the supraglacial systems, and concluded that the water flowed in open channels along most of its path after reaching the glacier bed (Krimmel *et al*, 1973; Behrens *et al*, 1975). Water emerging from the snout of the glacier is usually sediment laden indicating contact with the bed of the glacier for at least a short period of time. However, Collins (1982b) suggests alternative interpretations are possible. For example, water maybe in contact with the glacier bed for substantial period of time in the form of a subglacial pool or lake or indeed, open flow channels covering extensive areas on the glacier bed (1982b, 1989b).

The interactions between geographical controls and hydrometeorological variables and production of meltwater are especially complex in high mountain areas. Precipitation and thermal regimes govern the spatial and temporal distribution of runoff within a glacierised basin. The following chapter will focus this general discussion of the hydrological role of glaciers to the Karakoram Mountain Range in order to better acquaint the reader with the general study area and its climatic and hydrologic regime.

Chapter 3

General Physiography of the Karakoram Region

3.1 Overview

The Karakoram Mountain Range stretches in a WNW-ESE direction for nearly 700 km as part of the Himalayan alpine orogenic belt. The maximum width is about 600 km but narrows to a minimum of 150 km at the Hunza Valley in Northern Pakistan. Within the confines of the Hunza Valley numerous peaks over 7000 m tower above the valley floors producing some of the most spectacular and precipitous terrain. Indeed, it is within this region that the greatest vertical relief in the world can be found. Near the Hunza River at Karimabad (1850m) the ground rises for nearly 6000 m over 11 km to the summit of Mt. Rakaposhi (7788m). Such a place of extreme vertical relief enforces considerable influence on regional climate and hydrology. The exceptionally long steep slopes of the Karakoram induce a global extreme in environmental conditions from the permanently snow and ice covered peaks to the arid and semi-arid valley bottoms. During the summer, snow and ice capped peaks provide a spectacular contrast to the barren rock landscape and the intense greens of cultivated land on the lower slopes and valley bottoms. Nearly all available water is generated from the meltwaters of the large and dynamic mountain glaciers resulting in highly variable and definitely seasonal river discharge. This chapter examines the primary physiographic elements essential to establishing a modest appreciation of the hydrological regime within the Karakoram region.

3.2 Topography

Some of the highest mountains in the world exist within the Karakoram range - 33 over 7315 m a.s.l. including four peaks over 8000 m, one of which is K2 (8611 m a.s.l.) the second highest mountain in the world. The relative relief of the main valleys is rarely less than 4000 m and even within the secondary valleys relative relief greater than 2000 m over horizontal distances of only 1 to 2 km are commonplace (Goudie *et al*, 1984). This abundance and magnitude of relief throughout the Karakoram produces a distinct vertical stratification or "altitudinal organisation" of geomorphological, hydrological and climatological process (Hewitt, 1989). Although each process has its own individual altitudinal stratification they can be synthesized into three bands of topographical features. The highest areas (mustughs) above 6000 m account for only about 2 per cent of the total area of the Karakoram. The bulk of the Karakoram lies between 3000 m and 6000 m, an area of 15,150 km^2, and is predominantly occupied by glacierised basins (von Wissemann, 1959). The area below 3000 m makes up less than a quarter of the total area of the Karakoram. It contains the major river valleys and gorges.

The highest area is that characterised by a stark landscape of snow and ice, spectacular peaks, horns, serrated ridges and knife edged interfluves with ominous avalanche slopes and snow swept rock faces. Several of these mountain and avalanche slopes descend precipitously to valley bottoms. Subdued slopes and ridges with interspersed areas of steep bare rock and massive debris slopes scarred with mud flow channels, avalanche chutes and gullies are found in abundance in the zone between 3000 m and 6000 m. In the highest region of this zone vast expanses of accumulated snow and ice feed the immense and numerous glaciers of the Karakoram (see Table 1.2). An example of such an area is *Snow Lake* in the Biafo Glacier Basin, which has been studied by the SIHP (Hewitt *et al*, 1989; Wake, 1989). Most of the runoff from the Karakoram is generated in this zone as it is the place of greatest precipitation inputs as well as containing almost all of the ablation zones of the region's glaciers. These glaciers provide a mechanism by which copious amounts of water and debris from the higher regions are transported to the lowest zone below 3000 m. Debris or *scree* slopes also transport large amounts of material from higher sections directly to the lower zone where much of it is reworked by glacial or fluvial processes.

As a result of the downward motion of materials slope angles tend to become more gentle with decreasing elevation although there remains an abundance of steep slopes forged by fluvial action and mass movement events. This lower zone is characterised by enormous debris slopes and accumulations originating from the first and second zones. Proglacial areas consisting of huge morainic deposits, glacier meltout tills and glaciofluvial outwash plains extend over vast areas. Glacier systems supply most of the enormous amount of sediment verifying their ability to erode and transport material. Most alpine streams also transport a significant quantity of sediment for the nourishment of large alluvial fans. It is not uncommon to see alluvial fans extending over several square kilometres and abruptly truncated in sheer debris faces by the main river.

All three of the zones experience a period of freeze-thaw activity which plays an important factor in making the mountain rock vulnerable to erosion (Figure 3.1). Hewitt (1968) was one of the first to study the relative importance and the spatial and temporal variations of freeze-thaw activity within the Karakoram. The zone of freeze-thaw activity migrates in altitude with the seasonal changes in temperature. There are two very important points to note here, first that a large fraction of the freeze-thaw

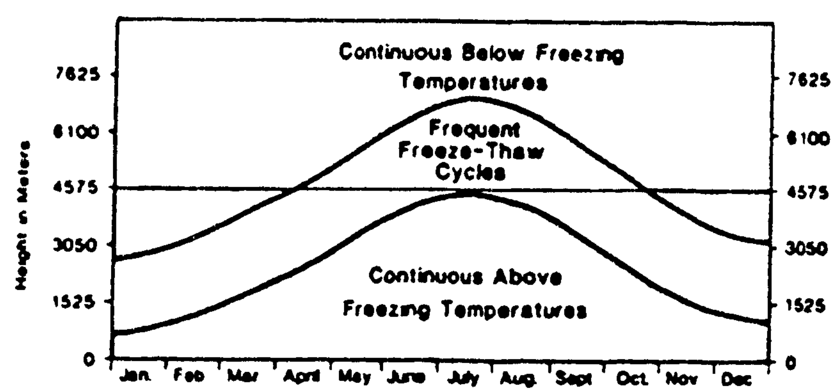

FIG. 3.1. Freeze-Thaw Cycle Within the Karakoram. (Source: Hewitt, 1989).

period occurs in the zone between 4000 m and 6000 m which correlates to the zone of highest precipitation, and secondly that all areas in the Karakoram experience below freezing temperatures.

Geomorphic activity occurs almost continuously throughout the Karakoram with extremely large events having an unusually high frequency. This is evident in the surrounding landscape and documented catastrophic historical events (Mason, 1935; Hewitt, 1982; Goudie *et al*, 1984). The remnants and scars of such events are ubiquitous. Much of the regional topography has been, and still is, greatly manipulated by the action of glacial and fluvial-glacial processes (Mayewski and Jeschke, 1979; Hewitt, 1989). Tectonic activity, extreme precipitation events and the natural instability of such steep mountain slopes play less frequent albeit highly significant roles. Human activity has a relatively insignificant effect on the environment in the Karakoram. However, irrigated terraces not only produce a suitable environment for crop cultivation but also allow for the establishment of natural vegetation. Both of these have a stabilising effect on these scattered mountain oases within the lower zone.

Such intense general and local topography has a profoundly significant influence on the climate and hydrology of the Karakoram. It is only recently that attempts to quantify these influences have been undertaken. Some influences can be inferred from other high mountainous areas which have received more scientific attention as in the French and Swiss Alps. One characteristic which is immediately obvious is the overwhelming influence that altitude has on creating temperature and precipitation gradients of globally extreme proportions.

3.3 Climate

Reliable climatic data for the Karakoram is extremely scarce. The climate record for all of Northern Pakistan is primarily based on observations from meteorological stations located outside the Karakoram mountain system or from valley bottom locations. There is very little reliable climate data for elevations greater than 3000 m although climbing exhibitions and early explorers provide some data but for short periods only. It is therefore a difficult and precarious task to classify the general Karakoram based on such data. For example, the Köppen classification scheme considers northern Pakistan to be of a dry continental mediterranean nature. Although this classification may be true for one or two small regions within the Karakoram it is most certainly inaccurate and definitely inadequate when referring to areas above 3000 m. Above 3000 m there are profound variations in the temperature and precipitation regimes imposed by altitude and local relief. Any attempt to classify climate in high mountainous areas therefore must be achieved on a basis of altitudinal zonation with consideration for local variations instead of a lateral scale.

Since about 1960, the Water And Power Development Authority (WAPDA) has maintained a number of hydrological and meteorological stations within the Karakoram in an attempt to determine the basic climatological regime of the area. The meteorological stations operated by WAPDA are all located at low elevations usually in valley bottoms. The highest meteorological station operated from 1960 to

1975 at Misgahr (3088 m a.s.l.). Several scientific expeditions have begun to augment WAPDA meteorological with data from higher altitudes but these are for short time periods only. For example, the Batura Glacier Investigation Group remained within the Batura Basin for one year (1974-75) and the International Karakoram Project for one summer in 1980. More recent and ambitious research studies by the Snow and Ice Hydrology Project (1985-1988) and the Alpine Glacier Project of the University of Manchester (1987-) both in collaboration with WAPDA have attempted to fill in this gap but with limited success. The following discussion is a description of the climate of the Karakoram region based on the above and other relevant sources.

3.3.1 Macroscale Climate

Within the mountainous regions of northern Pakistan there are two distinct climatic patterns that generally coincide with a wet and a dry season. These patterns are controlled by the thermally induced air pressure differences between the Indian subcontinent and the Indian ocean and are tied closely to the dynamics of upper air flow, including the jet stream (Ramage, 1971; Barry, 1981). During the spring and autumn the pattern is in transition from winter to summer and vice versa respectively. The winter pattern is produced as the jet stream splits into two sections as it meets the Himalayan mountains (Figure 3.2). One arm of the jet stream stays north of the Tibetan Plateau while another arm is forced southwards. For most of the winter months northern Pakistan is affected by the northern arm of the jet stream bringing cold arctic air from the north and moist mediterranean air from the west (Rao, 1981; Barry and Chorley, 1985). The moist air from the west is the principal precipitation source bringing perhaps two thirds of the annual total (Wake, 1989).

As temperatures increase with the onset of spring the southern arm of the jet stream begins to migrate northwards. Recent studies have shown that the rate of advancement of the southern arm is indirectly related to the extent of winter (Dec-Feb) snow cover (Dickson, 1984; Bhanu Kumar, 1988). The northwards advances of the southern arm causes a mixing of cold and warm air masses producing significant convection storms and the intense local dust storms of northern Pakistan (Goudie *et al*, 1984). These convection storms can increase precipitation, usually in solid form at higher elevations, such that spring is normally wetter than winter.

By the end of May the southern arm of air flow breaks up bearing the first signs of ensuing Indian summer monsoon (Figure 3.2). In many parts of India and Pakistan the monsoon delivers enormous amounts of precipitation perhaps 75-90 per cent of the annual amount whereas in the more northerly areas it may be as much as 20-40 per cent (Lockwood, 1974). Rarely, however, does the monsoon have enough energy to spill over the frontal ranges of the Himalaya into the Karakoram region where the westerly air masses are still the prime source of moisture.

When the summer monsoon does reach the inner ranges of the Karakoram the effect is a substantial increase in summer precipitation at higher elevations (Wake, 1989). Mayewski *et al* (1980) have shown that such intrusions initiated the advances of Trans-Himalayan glaciers between 1890 and 1910. At such times the availability of water within the Karakoram is greatly reduced. By October the southern arm has

A

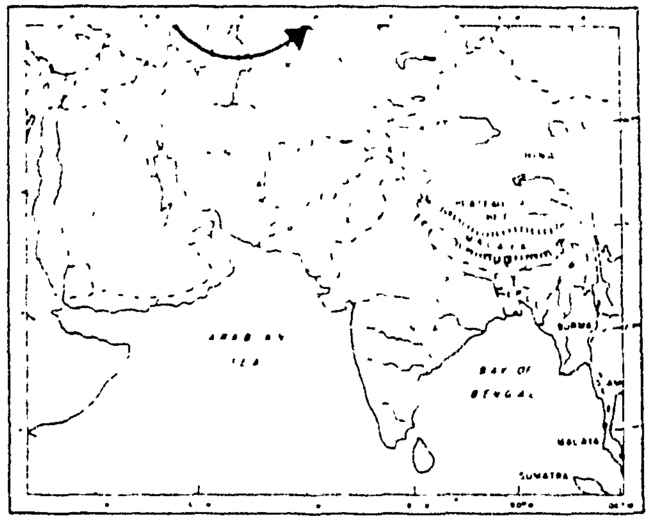

B

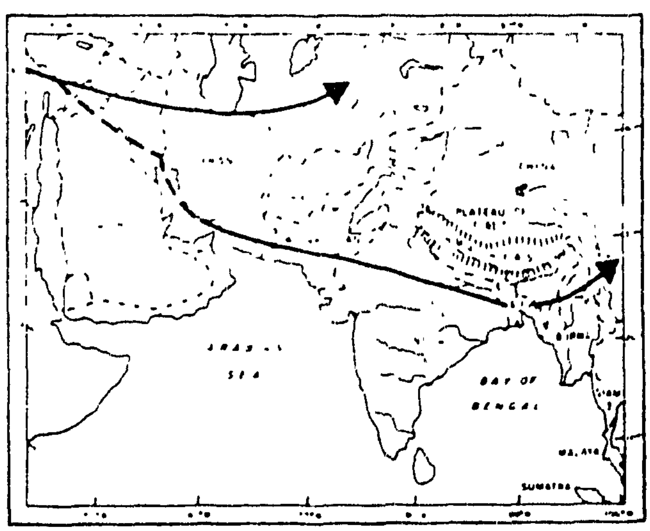

FIG. 3.2 Summer (a) and Winter (b) Positions of the Prevailing Westerly Winds (Source: Mayewski *et al*, 1988).

re-established itself and the winter climate pattern again dominates the Karakoram region. Although these large scale influences govern the broad climatic variations for the Karakoram region there is significant variation at the smaller or local scale.

3.3.2 Local Climate

The magnitude of relief and the steepness of slope found within the Karakoram exert a significant influence upon temperature, precipitation amount and form, and movement of frontal systems.

3.3.2.1 Air Temperature

There are three controlling influences on air temperature - season, altitude and local topography. Seasonal temperature variations are dependent on latitude. Altitude, while reducing the mean seasonal value, decreases the diurnal temperature range. Local topography creates variations based on aspects and relief. The Karakoram at between 35-37°N experiences cold winters and hot summers. Average monthly temperature values for Gilgit (1490 m), in the northern areas of Pakistan, show a pronounced seasonal variation (Figure 3.3). Summer maximum daily temperatures can easily reach 40 °C but minimum temperatures in winter may dip to well below the freezing mark. Valley bottoms can also exhibit extremely hot conditions - e.g. Karimabad (2409m), 1978-1984 average maximum summer temperature was 29.5 °C.

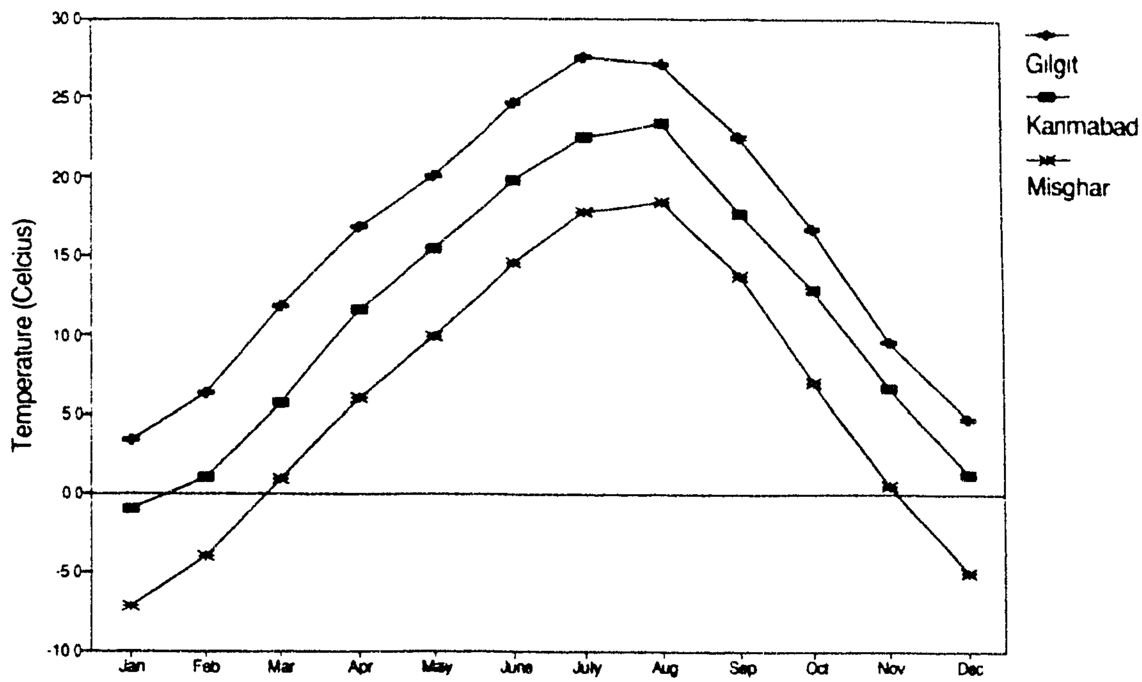

FIG 3.3 Mean Monthly Air Temperatures at Gilgit, Karimabad and Misgahr (Source: WAPDA).

For at least three months of the year the entire Karakoram range experiences temperatures below freezing. Above about 6000 m freezing temperatures are seen all year round (Hewitt, 1989). Thus, there is an extreme altitudinal range in temperature throughout the Karakoram which reaches a maximum during the summer period. Valley bottoms can be stifling with heat while at altitudes as low as 5000 m may be experiencing below freezing temperatures.

Gilgit airport (1490 m) has the only lengthy (30 years) and reliable set of data for the whole of the Karakoram region. A station at Misgahr (3088 m), now closed holds the only lengthy (15years) temperature record above 3000 m in the Karakoram

(Figure 3.3). The daily average ((Max-Min)÷2) summer temperature (May-September) was 24 °C at Gilgit and 15.0 °C at Misgahr. The average winter temperatures (October-April) were 10.0 °C and 0.0 °C for Gilgit and Misgahr respectively. Data from Karimabad falls neatly between the average monthly temperature profiles for Gilgit and Misgahr. The three stations experience similar temperature patterns with difference in the mean values attributable to the effects of altitude.

Variations in spring time temperatures have a significant influence on the timing and rate of melting snow. The coefficient of variation for mean monthly temperatures at Gilgit during the four spring months February to May from year to year and the variation in mean daily temperatures within these months is higher than any other month (Whiteman, 1985). The hydrological implications of this are enormous when considering that the greatest proportion of precipitation also occurs within the defined spring period. In years when temperatures are low there is little melting of snow and any precipitation may well fall as snow even at the lowest elevations. At higher elevations a cool wet spring would delay the glaciers contribution to streamflow well into July and will probably significantly reduce the total amount of streamflow generated from the melting of glacier ice. Cloud cover is responsible for the temperature fluctuations and reflects the size, speed, frequency and degree of occlusion of the westerly depressions during this spring period (Barry, 1981; Goudie *et al*, 1984; Whiteman, 1985).

Diurnal temperature ranges, based on monthly minimum-maximum data, for Gilgit are in the order of 10 °C to 20 °C whereas Misgahr is between 10 °C to 15 °C.

At both locations the diurnal ranges are at a minimum during winter and at a maximum in September and October. At Gilgit day time temperatures in spring increase rapidly while night time temperatures remain relatively cool. This phenomenon is not present at Misgahr because day time temperatures are still low at this time of year. During September and October, day time temperatures are still rather high while night time temperatures tend to drop significantly. There is a significant decrease in diurnal range during August at Gilgit as night time temperatures increase to "uncomfortable" levels. The spring time maximum is not present in the Misgahr record as diurnal ranges tend to gently increase throughout the spring and summer. Diurnal ranges drastically plummet after October at both locations to their minimum in December and January.

Air temperature generally decreases about 6.5 °C per 1000 m gained in elevation - the environmental lapse rate (ELR). Between Gilgit and Misgahr there is an elevation difference of just over 1600 m and an annual temperature difference of 10 °C giving a lapse rate of 6.2 °C. Using the data from the intermediate station Karimabad (2409) the ELR between Gilgit and Karimabad is 4.2 °C and from Karimabad to Misgahr is 7.8 °C thus revealing that the environmental lapse rate increases at an negatively exponential rate with altitude between stations. This increase in ELR is because of the increase of sensible heat transfers with altitude. Thus using the ELR from Gilgit, -6.2 °C/1000 m, the mean 0 °C isotherm during the summer is at about 5370 m.

Air temperature is also greatly influenced by aspect. The aspect of a mountain slope controls the effectiveness of solar radiation to heat that slope. This phenomenon is exaggerated by the very steep slopes of the Karakoram and their sub-tropical location. South facing slopes are almost perpendicular to the sun for much of the year where northerly slopes are almost explicitly excluded from receiving any insolation. This has a significant effect on the distribution of melting within a basin as air temperatures are significantly reduced on northerly slopes allowing snowlines to be as much as 1000 m lower than on southerly slopes (Goudie *et al*, 1984). This suggests that melting on northerly slopes is most likely due to air temperature rather than direct insolation as is the case for south facing slopes.

The implications are that the hydrological yield of a basin is balanced between northerly and southerly aspects and is therefore susceptible to variations in the contribution to runoff. Snow melt tends to be more much more rapid on the southerly slopes where global radiation has a high angle of incidence. On northerly slopes, which receive little direct radiation, it is temperature that appears to control the rate of melt. It seems probable that on warm cloudy days when insolation is significantly reduced water yield is similar on northerly and southerly slopes. It would also seem likely that daily maximum melting would occur at midday on southerly slopes and in mid-afternoon on northerly slopes following the diurnal cycles of insolation and temperature respectively. A combination of cooler temperatures and heavy cloud cover will obviously reduce melting on both northerly and southerly slopes.

Cloud cover would appear to be the sole governing factor in the melting of snow and ice by reducing insolation and hence air temperatures. Cloud cover is often associated with precipitation which has another interesting role to play in the hydrometeorology of the Karakoram.

3.3.2.2 Precipitation

The Karakoram has two major sources of precipitation comprising of westerly air masses and monsoonal intrusions. The westerly air masses bring most of the precipitation to the Karakoram throughout the year. During the winter period, December to March, most of the precipitation falls in solid form. However, higher elevations above 4000 m receive some snowfall during the summer months while at elevations above 4800 m all precipitation falls as snow (Hewitt, 1989). Summer snowfalls may supply a significant proportion of the annual total precipitation in most years although maximum snow accumulation almost invariably occurs during the winter period. From snow pit analysis Wake (1989) suggests that up to one third of the total annual accumulation may occur during the summer in the Biafo/Hispar Basin of the Karakoram.

The winter and spring precipitation patterns tend to be universal throughout the Karakoram region. At Gilgit, the wettest months of the year are in April and May with more than one third of the total annual precipitation. The summer months April to September bring perhaps 75 per cent of Gilgit's total precipitation. According to Whiteman (1985) summer precipitation tend to be more localised in the form of convection storms so that Gilgit is a good index station in the winter and spring but not during the summer.

The Indian summer monsoon usually do not reach the Karakoram mountains but when it does penetrate the frontal ranges there is a significant increase in annual precipitation totals. It has been estimated that as much as a third of the annual precipitation total can be attributed to monsoonal origins at these times. This has a significant effect on the hydrological regime of glacierised basins. The additional nourishment although adds mass to the glacier it also has the effect of reducing glacier melt and thus streamflow. Monsoonal storms tend to be extremely localised and fierce bringing up to 50 per cent of the annual total of precipitation in just one storm in many valley locations (Whiteman, 1985). In some of these valley locations flash floods may result producing dramatic land slides and mud slides and washing away roads crossing tributary streams and rivers.

The combined result of these two moisture sources is heavy precipitation at high altitudes. Climate stations at lower altitudes and valley bottoms indicate annual precipitation totals which are significantly reduced. For example, the average annual precipitation at Gilgit is less than 150 mm. Measurements at higher elevations of approximately 5000 m indicate precipitation totals of up to ten times this amount (BGIG, 1979; Wake, 1989). It has been estimated that precipitation totals reach a maximum of about 2000 mm at 5500 m and then decrease with increasing elevation (Hewitt and Young, 1990). This region of maximum accumulation is in the vicinity of the regional snowlines of the Karakoram glaciers which certainly must have a profound influence on regional hydrology.

The extremely warm summer temperatures cause evaporation to be greater than precipitation in the arid and semi-arid valley bottoms. Evaporation records maintained by WAPDA at Gilgit indicate evaporation levels (1120 mm) at almost ten times the amount of precipitation (136 mm) (Whiteman, 1985).

The combined characteristics of air temperatures and precipitation greatly influence the general environmental conditions within the Karakoram. Precipitation figures of between 1000 and 2000 mm at higher altitudes maintain some of the worlds largest glaciers that reside in the Karakoram. Runoff produced from the melting of glaciers provides water to the areas with considerably less precipitation. These glaciers are indeed a result of the unique and exceptional topographical and climatic factors that exist in this high mountainous region.

3.4 Glaciers of the Karakoram

The glaciers of the Karakoram cover an area of about 15000 km^2, approximately 35 per cent (Figure 1.2). Some of these glaciers fall into the realm of the longest glaciers in the world outside the polar regions (Table 1.1). The four largest glaciers account for almost a fifth of the total glacierised area of the Karakoram. There are over 100 glaciers that extend for 10 km or more in length. Most of the glaciers have deeply incised valley trunks with accumulation areas of either avalanche or direct input types. The larger glaciers, for example the Biafo and Hispar, usually have direct input type accumulation basins that expand over vast areas. Many of the glaciers are highly active or have cyclical periods of significant advancement and retreat (e.g. the Hassanabad Glacier). Several times in the recent past glaciers have surged forward blocking major river channels eventually to produce devastating outwash floods (Mason, 1935; Hewitt, 1982).

This dynamic behaviour of some of the Karakoram glaciers may be attributed to their thermal state; warm or temperate and cold or polar. Warm glaciers continue to contribute runoff during the winter season while cold based glaciers do not (Paterson, 1981). Many of the larger glaciers appear to have a combination of both warm and cold sections throughout their length, for example, the Batura Glacier (BGIG, 1979). Intermediate and smaller glaciers are probably one or the other thermal type according to their aspect as suggested by Hewitt (1985). This type of glaciological data is severely lacking and therefore the factors governing the thermal state of the regions glaciers are largely unknown.

Besides their immense size the Karakoram glaciers are known for their steepness and for having some of the lowest termini in Himalaya. They extend through a wide range of climatic environments and are therefore glaciologically complex. Their accumulation zones are often above 6000 m in areas covered in perennial snow and ice but feed glacier snouts which reach into areas of intense heat and aridity. For example, the Batura Glacier stretches for almost 60 km from an elevation over 7000 m to under 2500 m. At the snout the mean annual temperature was found to be about 10 °C with a maximum temperature of over 34 °C and a minimum of -10 °C (BGIG, 1979). From this data it was estimated that the zero degree level averages at about 4200 m. Of course during the summer this may rise to over 5000 m. The annual precipitation at the terminus is less than 100 mm but reaches over 1500 mm at 5500 m (BGIG, 1979).

Young and Schmok (1989) and Hewitt and others (1989) present some of the only glaciological data available for the Karakoram besides the Batura Glacier Investigation Group (1979). The three studies were carried out in the Barpu/Bualtar Basin, the Hispar/Biafo Basin and the Batura Basin respectively. The results indicate that the Karakoram glaciers are thick and fast moving. The flow type, most often tends to be *Blockshollen* with the glacier margins travelling down-slope at a slower rate than the rest of the glacier due to friction with the valley walls. Measurements of flow velocities are in the range of 0.50 and 0.60 m d^{-1} at the glacier centre during the summer with little reliable winter data although estimates are at about 0.20 and 0.30 m d^{-1}. Ablation rates are exceptional in the Karakoram with an average amount of roughly 8.0 m a^{-1} within the ablation area. Daily averages are about 60 mm d^{-1} with daily maximums reaching 100 mm d^{-1} (BGIG, 1979; SIHP, 1985-1988).

Ice-thickness measurements from all three basins indicate shallow snout depths of less than 200 m but reaching considerable depths near the equilibrium lines - Barpu Glacier - 560 m; Biafo Glacier - 1400 m; Batura Glacier - 500 m. The following are estimates as calculated by the authors of the relative studies of ice volumes flowing through the equilibrium line area, Barpu - 5.10 x 10^7 m^3a^{-1}; Biafo - 6.5^7 m^3a^{-1}; Batura - 10.0^7 m^3a^{-1}. The net result of all these measurements indicate a massive volume of glacier ice flows into the ablation area to be released at some later point in time as meltwater into the Indus River system. Unfortunately, discharge measurements are not yet available for the individual basins but their impact on the hydrological regime of the two main rivers draining the Karakoram can be seen by looking at their hydrological characteristics.

3.5 Hydrology

The Karakoram mountains contribute almost 25 per cent of the flow of the River Indus from almost 15 per cent of the catchment area (based on WAPDA data). The streamflow pattern is strongly seasonal with a distinct summer peak in July and August indicates the considerably large influence of the region's glaciers on river flow in the Karakoram. The short-term and year to year fluctuations of river flow also attest to the significant contribution of glacier meltwater to river flow. The average amount of glacier runoff appears to be not only a function of the degree of glacierisation of the individual basin but also with the size of the basin. For example, meltwaters from the Batura Glacier Basin (687 km^2 and 48 per cent glacierised) doubles the discharge of the Upper Hunza River (5000 km^2) which has no major glacier systems (BGIG, 1979). It is probable that up to 80 per cent of the river flow leaving the Karakoram mountains is generating by meltwaters during the summer months and between 40 per cent and 75 per cent of the total summer runoff is produced during the months July and August (Goudie *et al*, 1984; Ferguson, 1985; Hewitt and Young, 1990).

The Karakoram mountains make up almost the entire headwaters area of the Upper Indus Basin. There are four principal basins which drain the Karakoram - the Gilgit (26 000 km^2 and 27 per cent glacierised), the Hunza (13 000 km^2 and 37 per cent glacierised), the Shyok (33 000 km^2 and 9 per cent glacierised) and the Upper Indus (160 000 km^2 and 11 per cent glacierised). The Gilgit River Basin, although double the size of the Hunza but less heavily glacierised, produces about 20 per cent less streamflow. The Upper Indus including the Shyok drains more than four times the area than that of the Gilgit and Hunza Rivers combined but has only about 30 per cent more discharge because undoubtedly high runoff from the large glaciers of the Shyok and Braldu River Basins produce is offset by the low runoff from the Ladakh and Tibetan Plateau.

There can be large short term and year to year variations in streamflow. Short term fluctuations in discharge are linked directly to variations in air temperature producing the typical diurnal cycle on the hydrograph of any mountain stream (Figure 2.4). Maximum daily discharge can be more than ten times the minimum in March and up to twenty or thirty times in July and August (Goudie *et al*, 1984). Monsoonal intrusions and westerly depressions significantly reduce streamflow by reducing the amount of insolation because of increased cloud cover. Much of the precipitation associated with the intrusive event will fall as snow at higher elevations corresponding to the glacier ablation areas which will significantly reduce meltwater generation. It may then take more than two days for meltwater streams to reach their previous level of flow even after only one day of cloud.

Year to year variations in runoff are mostly determined by the dominating weather conditions that occur during the first two months of spring, April and May. It is the crucial period of time because it determines the timing and rate of snow melt.

In an average year the onset of spring in March brings warmer temperatures which generate snow melt and the tributaries lowest in elevation begin to rise. In the higher, glacierised and non-glacierised basins runoff does not begin until May. As temperatures increase throughout the summer snow melts at an increasing rate and the regional snowline increases in altitude. Soon the glacier ablation zones become exposed and massive volumes of water are released peaking river flows in July and August. If during the spring temperatures were above average and snow cover was thin, the glacier ablation zones would become exposed much sooner and for a more prolonged period of time and river levels would be higher than average. Conversely, cool spring temperatures and abundant precipitation would not expose the ablation zones until well into the summer and river levels will be significantly lower than average. Reports from local people, discharge records and records of ibex horn growth suggest a four to five year cycle of cool and warm springs (Goudie *et al*, 1984).

3.6 Summary

The chapter has presented an overview of the physiographic features of the Karakoram mountain system. It indicates a place of global extremes containing some of the world's highest mountains and some of the worlds longest alpine glaciers. The immense altitudinal range of up to 5000 m over very short distances produces severe gradients of temperature and precipitation resulting in an altitudinal organisation of vegetation, anthropogenic activities and physiographic processes. The vast areas of snow and ice store and then transfer water from zones of permanent snow and ice with annual precipitation inputs of well over 1000 mm to hot, dry valley bottoms with about 100 mm of rainfall. These glaciers exert a tremendous influence on the hydrological regime of the Upper Indus River by generating probably 80 per cent of the flow. The lack of data records makes it difficult to ascertain the relative importance of each of the hydrometeorological variables and their interrelationships. In the next chapter the study area is described, the methods chosen to foster an enhanced appreciation for the underlying physical processes governing the hydrological environment within the Karakoram are outlined and a summary of the results obtained for the 1989 field season is presented.

CHAPTER 4

MEASUREMENT RECORD

4.1 Overview

Based on experiences and results of the Snow and Ice Hydrology Project 1985-1988, reliable evaluation of hydrometeorological relationships demands a simple, practical approach. Practical difficulties and logistics for a hydrometeorological study can be immense in the rugged Karakoram Environment. One of the main goals of the Snow and Ice Hydrology Project's (SIHP) 1988 field programme was to extend its regional coverage of hydrological, meteorological and glaciological data. The programme included a reconnaissance to Pasu Glacier Basin (Figure 4.1 and Plate 4.1), where movement, ablation and ice thickness data was collected (see Figure 4.7). After this preliminary reconnaissance it was decided the Pasu Basin has a great potential in the future of the SIHP programme for hydrometeorological studies based on the following reasons:

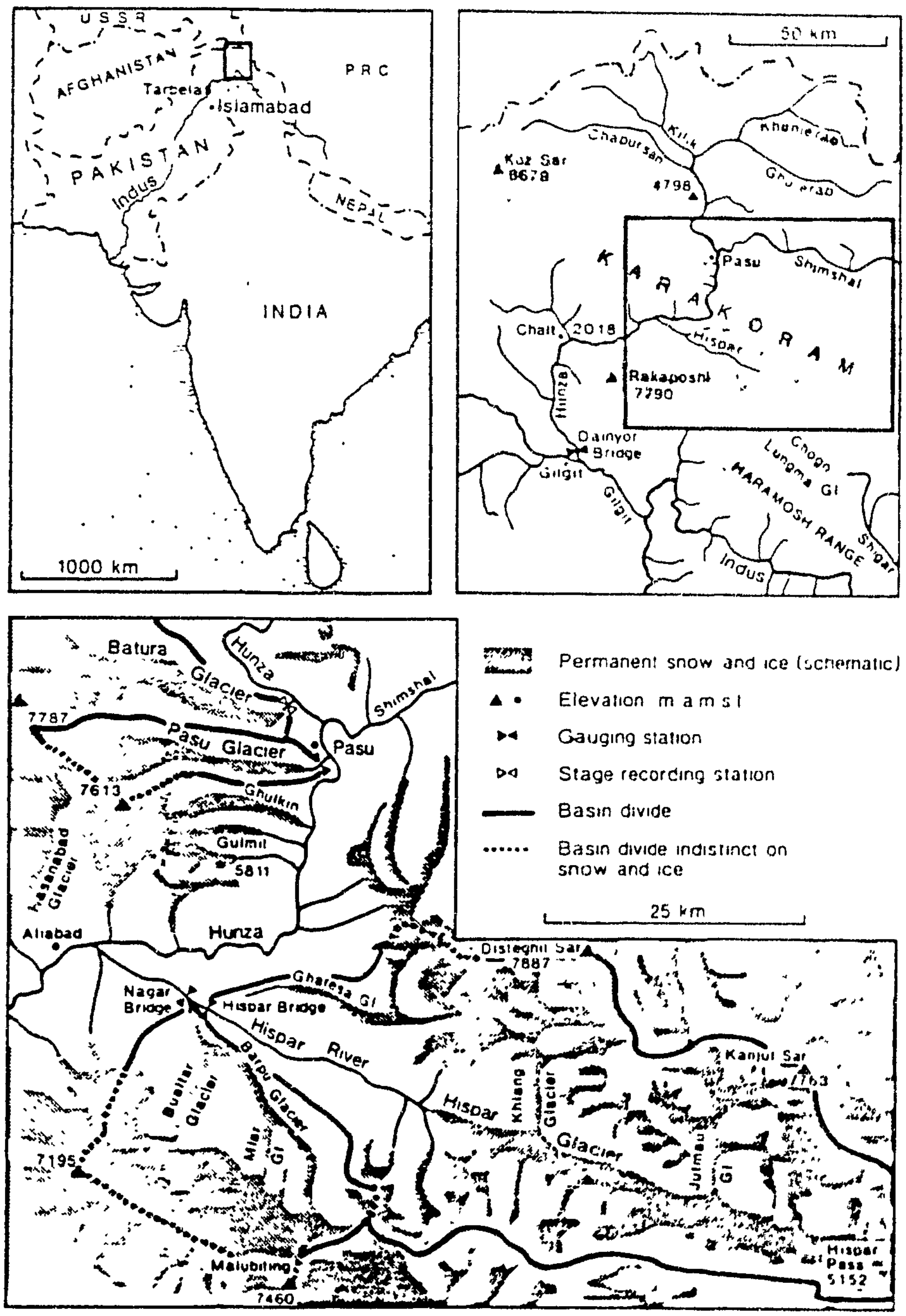

FIG. 4.1 Location of Pasu Glacier Basin, Karakoram Himalaya (Collins, 1989b).

a) Pasu Glacier is accessible from the Karakoram Highway making for simple logistics. Indeed, Pasu village, located one kilometre from the glacier snout, was used as a base camp.

b) Pasu Basin is highly glacierised (105 km^2 and 60 per cent glacierised) with more than 5000 m of relief from the stream gauge (2500 m a.s.l.) to Shispar pk. (7610 m a.s.l.). This range of elevation encompasses the major ablation zones of most other glacierised basins in the central Karakoram.

c) There are locations suitable for meteorological installations: snout area (2600-2700 m a.s.l.), Pasu Gahr (3500 m a.s.l.) and Patundas ridge (4000 m - 4600 m a.s.l.). Trails and huts established by local people provide access to these areas as well as shelter.

d) The Alpine Glacier Project (AGP) from the University of Manchester have recorded stage observations at the Pasu bridge since 1986. In 1989, the AGP started a programme of discharge measurements from the Pasu bridge. This data, however, is not yet available for this study.

e) Pasu Glacier is comparable to the Miar Glacier of the Barpu-Bualtar Basin in size, shape and morphometry, except that Pasu Glacier is heavily crevassed throughout its length, whereas the Miar Glacier is relatively free of crevasses. The Barpu-Bualtar Basin was studied by SIHP between 1986 through 1988 (Figure 4.1). No comparison with the Miar is made in the present study because 1989 is not yet available for the Barpu-Bualtar Basin in 1989 but perhaps there will be in the future. Historical data are not used as this data cannot be put into context with the 1989 data.

The above factors coupled with financial, instrumental and personnel constraints on the 1989 summer field season made the Pasu Basin a hydrologically and an economically viable research basin. Within Pasu Basin three meteorological stations were established to gather information on air temperature characteristics (Figure 4.2). Pasu Snout station also collected global radiation data. A complete set of air temperature and discharge data was collected for the period 21 May to 31 August. Incoming solar radiation data was collected from 29 May to 20 June and 10

Overleaf: Plate 4.1 View of the Pasu Glacier Basin on 28 July, 1989. Shispar Peak (7610 m) is in top left corner. The Batura Glacier is visible just right of centre.

July to 14 August. Stage was recorded from 21 May to 15 September. Pasu River was gauged twelve times during the study period. This data are summarised in Table 4.1 and daily mean temperature, discharge and solar radiation are given in Appendix A. Hourly plots of the data are given in Appendix B.

Table 4.1 Characteristics of air temperature and runoff, Pasu Basin, 1989

Station	Variable		Mean	Range
Pasu Snout (2700 m)	$T_{5\text{-}8}$	°C	15.0	5.3 — 25.4
Pasu Gahr (3500 m)	$T_{5\text{-}8}$	°C	10.7	1.2 — 21.2
Patundas (4220 m)	$T_{5\text{-}8}$	°C	5.8	-3.6 — 18.8
Pasu Bridge (2300 m)	$Q_{5\text{-}8}$	m^3s^{-1}	15.5	5.5 — 37.6

4.2 Study Site Description:

The Pasu Glacier Basin is situated on the main ridge of the Karakoram at 36°28"N 74°45"E, stretching in a west-east direction (Figure 4.2). The glacier is fed mostly by snow and rock avalanches from the extremely steep ridges of the Batura Mustagh. Pasu Glacier descends from a col at 6555m, between Shispar pk. (7610 m) and Pasu pk. (7285m) to form an impressive icefall between 5500 m and 4300 m a.s.l (Plate 4.2). After the icefall the glacier flows eastward through a deeply incised tract to its snout at 2650 m a.s.l. with a mean slope of 18 per cent, over a distance of about 22 km. The drainage area of the glacier totals 104 km^2, while the glacier covered

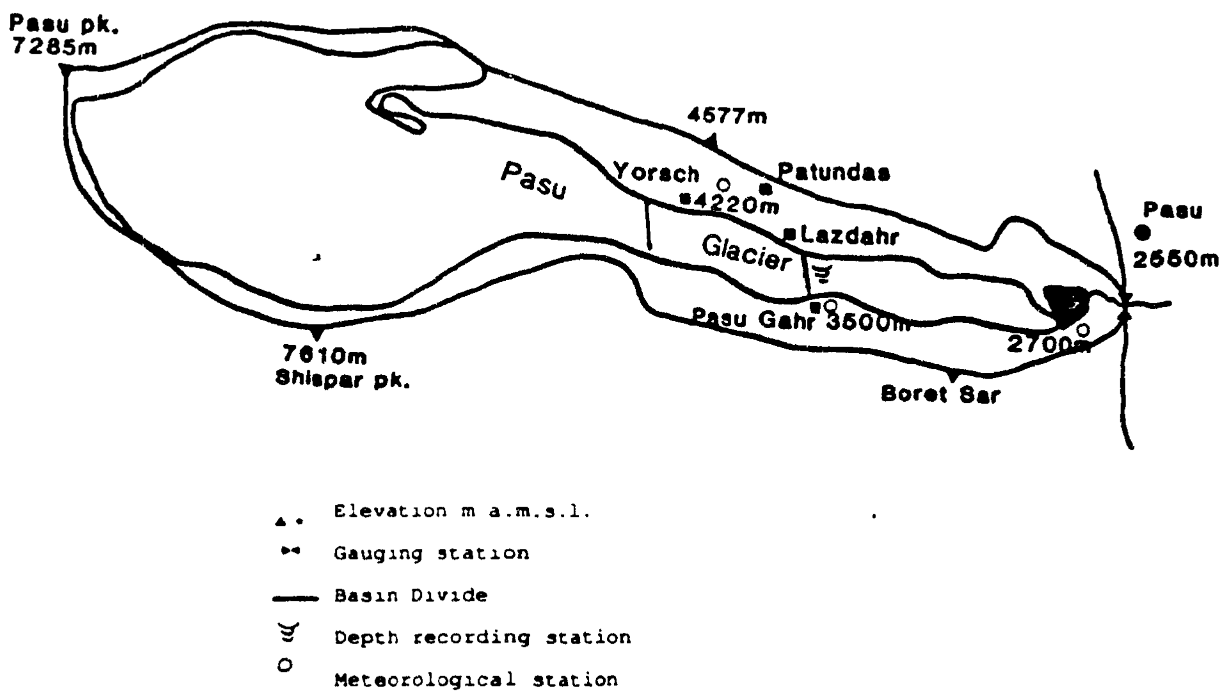

FIG. 4.2 Schematic Diagram of the Pasu Glacier and Measurement Stations.

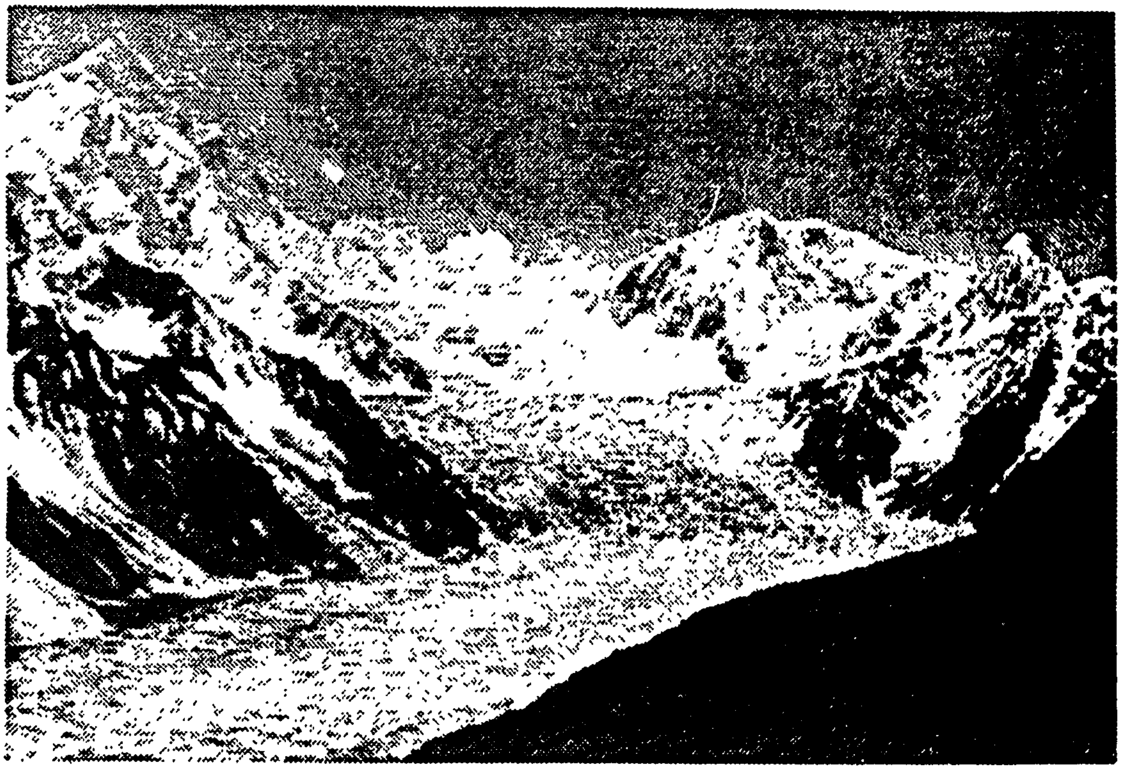

Plate 4.2 View of Pasu Glacier Icefall on 8 August, 1989. Note the position of the transient snowline within the Icefall. (Photo. B. Boyce)

area, 62 km^2, occupies 60 per cent of the drainage area. The equilibrium line is at approximately 4300-5500 m a.s.l., at the region just above the ice fall (see Figure 4.3). The accumulation area above this is 29 km^2, not including the area (18 km^2) covered by rock. The ablation area is 33 km^2. The accumulation/ablation (Ac/Ab) ratio of the Pasu Glacier is therefore about one. This is the same value for the Batura Glacier (BGIG, 1979) but is less than that for the Biafo Glacier which is about 1.25 (Hewitt *et al*, 1989). It is uncertain how Pasu Glacier compares with other glaciers within the Karakoram because of the lack of glaciological data. The Ac/Ab ratio for Pasu Glacier is, however, comparable to some Rocky Mountains glaciers such as Peyto (Young, 1977a). The accumulation area of the Pasu Glacier is approximately 5 km wide at its maximum while the trunk of the glacier narrows from the ice fall at 2.5 km to less than 0.5 km at the snout. The hypsometric curve for Pasu Basin (Figure 4.2) illustrates the altitudinal organization of the basin and glacier.

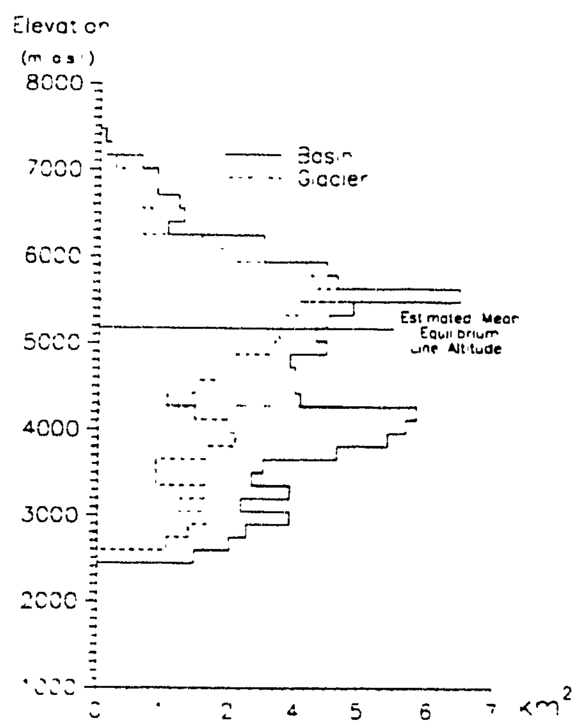

FIG. 4.3 Hypsometric Curves of the Pasu Glacier and Pasu Basin.

Vegetation is scarce throughout most of the basin except for small bands between 3200 m and 4000 m on the north and south facing slopes as well as on the flat surface of Patundas. Both the north and south facing slopes are vegetated by clumps of juniper and mesic pine. The flat surface of Patundas accommodates low growing mats of Cobresia and Polygonum spp. with abundant bare ground. At the lowest reaches of the basin thickets of sea buckthorn (Hippophae rhamnoides) and other thorny bushes line meltwater and irrigation streams.

The Pasu Glacier is separated from its northern neighbour, the Batura Glacier (59 km in length), by a relatively smooth ridge slightly less than one kilometre in width (Plate 4.3). The ridge starts from an outcrop of dolomite, near the Hunza river, at 3500 m stretching over 25 km to Pasu Pk. (7285 m). A 5 km section, between 4100 m and 4600 m a.s.l., is exceedingly flat compared with its surroundings and is called Patundas by the local people. Glacial erratics found on Patundas, composed of granodiorite found only in the upper most region of the basin, suggest the surface was formed as a result of Pleistocene glaciation (Derbyshire *et al*, 1984). From 4600 m to Pasu pk. (7285 m), Patundas is a jagged granodiorite ridge permanently covered in snow and ice. To the south, the Pasu Glacier watershed is distinguished from its southern neighbour, the Ghuilkin Glacier (19 km in length), by a ridge sharply contrasting Patundas (Plate 4.4). While covering a similar elevation range, ascending from Beret Sar (4100 m) to Shispar pk. (7610 m) over a comparable distance, the southern ridge is dominated by jagged peaks of great vertical relief. The face of the southern ridge has several small glaciers. The high steep ridges defining Pasu Basin, are an ideal environment for the enhancing and trapping of precipitation.

Plate 4.3 The flat surface of Patundas as viewed from the South ridge. At the bottom centre in Pasu Gahr (3500 m), location of meteorological station number two.

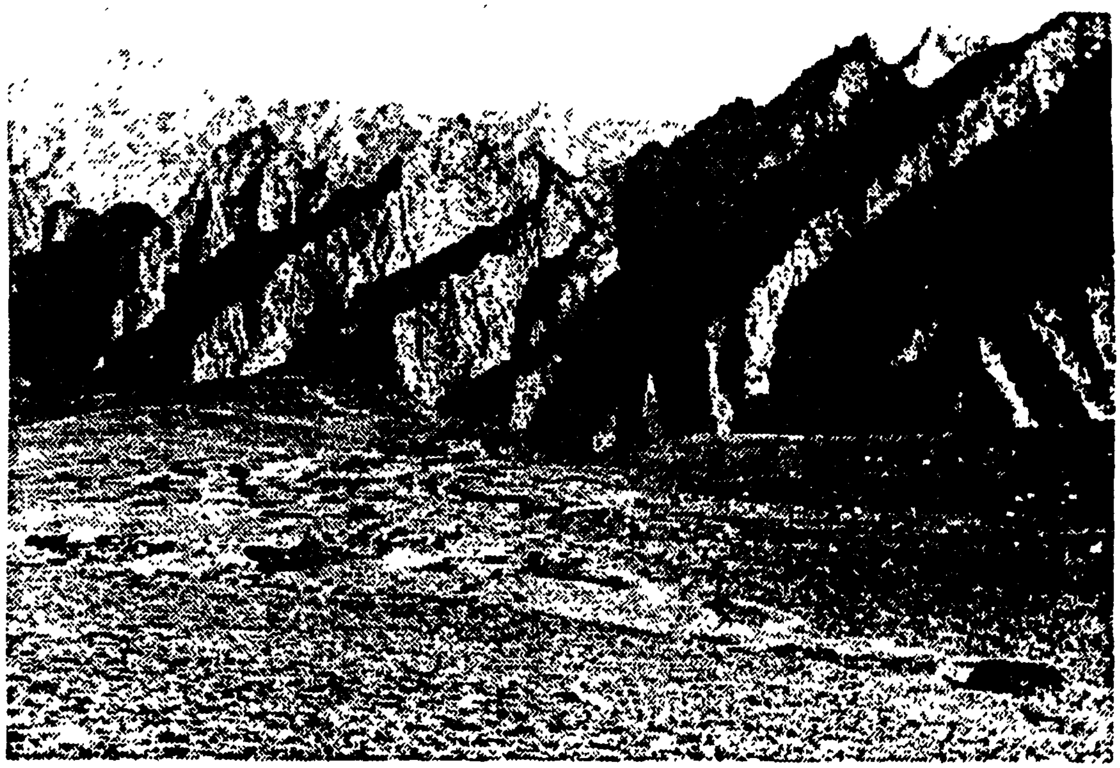

Plate 4.4 Comparision of the south ridge of Pasu Basin with the north ridge (Patundas 4200 m)

4.3 Pasu Glacier

Most of the surface of Pasu Glacier is free of debris with exception of the glacier margins and the snout region (Plate 4.1). A narrow stripe of debris covers the glacier margins and extends onto the glacier for at most 50 m. The debris consists of rock materials avalanching from talus slopes. Debris covers an area of around 1 km^2 of the glacier snout region. Although ablation on the middle and lower glacier tongue is very intense, there is no surface drainage system. Besides the main ice fall near the head of the glacier there are a series of minor ice falls and areas of constriction creating a surface dominated by large crevasses and seracs throughout most of its length. Surface meltwater therefore penetrates the ice body at many points to become part of the englacial and subglacial drainage system. The snout is sharply pointed and lies mostly on the southern side of the valley. There is only one meltwater outlet now, in 1980 there were two (Goudie *et al*, 1984), emerging from between the rock step and the glacier where it enters a lake not present in 1980 (Figure 4.4 and Plate 4.1). The lake empties into Pasu River which meanders for about 900 m through a broad outwash valley before entering the Hunza River (Plate 4.5). Estimates of electrical conductivity during the 1989 field season, taken above and below the lake, suggest water flows quickly through the lake. It is not known if another stream emerges underneath the snout where it is immersed in the lake. Polish lines, semi-debris clad roche-moutonnées and an ancient series of lateral moraines reveal the glaciers former extent.

Intermittent records of snout positions are available from observations and

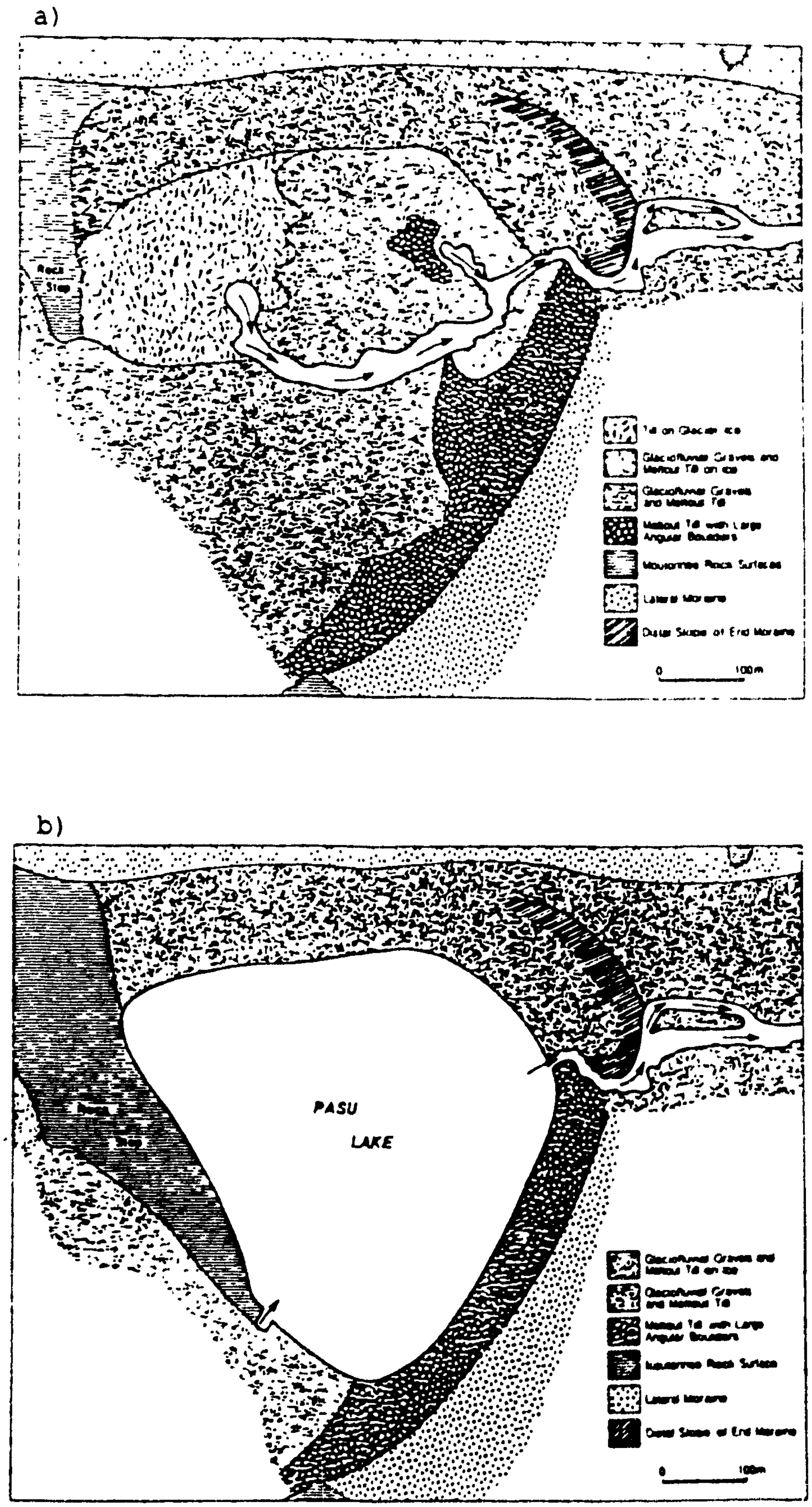

FIG. 4.4 Pasu Lake 1980 (a), 1989 (b) (Source for (a): Goudie *et al*, 1984).

Plate 4.5 The Pasu River and Pasu Bridge from the north lateral moraine. The bridge is location of the gauging station and stage recoding device.

measurements of different scientific and climbing expeditions visiting the region between 1885 and 1980. The position of the Pasu Glacier snout has fluctuated in a similar periodic pattern with other Hunza Valley glaciers (Mayewski and Jeschke, 1979; Goudie *et al*, 1984) (Figure 4.5). A rapid advance between 1907 and 1913 of 500 m was followed by a period of recession until 1966 near its pre-1907 position. The emergence of Pasu Lake in 1984 caused the snout to retreat by 200 m although the snout remained at the same elevation. The slow and intermittent retreat of the snout is probably due an increase in global temperatures since the little ice age in the mid 1800's.

During the 1988 field season two stake profiles were maintained and monitored over a three week period from 16 July to 12 August by members of WAPDA and the SIHP (Figure 4.6). The profiles were located at Pasu Gahr and Yorsch, the two relatively smooth sections on the glacier surface (Figure 4.2). Average surface velocity through the Pasu Gahr profile was 0.75 m d^{-1} or 272.14 m a^{-1} (assuming constant flow rate) and the average ablation rate was 0.103 m d^{-1}. The Yorsch profile average surface velocity was 0.58 m d^{-1} or 210.49 m a^{-1} (assuming constant flow rate) with an ablation rate of 0.065 m d^{-1} (Figure 4.6). An estimated ablation gradient of 0.5 m/100 m between the two profiles is similar to the ablation gradient of 0.63 m/100 m for the Batura Glacier (BGIG, 1979). Depth soundings revealed a maximum ice depth of approximately 300 m for the Pasu Gahr profile. Unfortunately, depth soundings are not available for the Yorsch profile due to equipment malfunction.

The glacier flow pattern at the Pasu Gahr profile was similar to Blockshollen

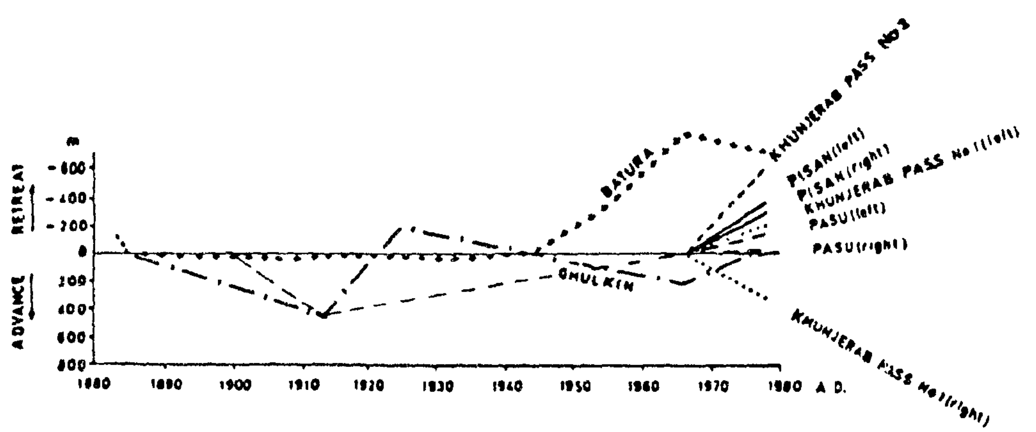

FIG. 4.5 Fluctuations of the Pasu Glacier and Selected Glaciers of the Karakoram (Source: Goudie *et al*, 1984).

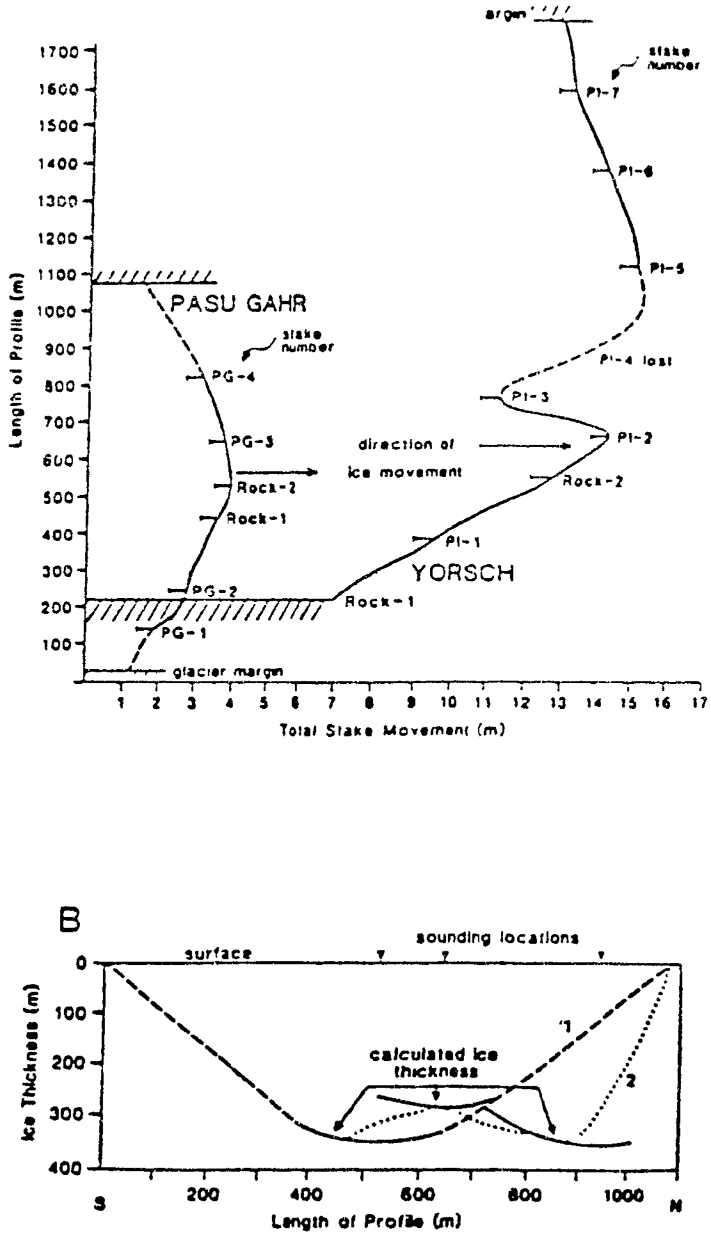

FIG. 4.6 Glaciological Measurements of the Pasu Glacier, 1988. Pasu Gahr and Yorsch profiles were monitored from 16 July to 12 August, 1989.

flow. At the Yorsch profile a much more complex flow pattern was observed, the ice flow pattern was separated into five streams. This may be a result of the centre of the glacier being slowed down by the compressional forces exerted on the glacier as the valley narrows below the ice fall. Comparing the two profiles, Pasu Gahr has a greater velocity than Yorsch by 0.22 m d^{-1} . This is due to the Yorsch profile being wider than the Pasu Gahr profile by more than 0.5 km. Pilleweizer (1957) measured the velocity of Pasu Glacier to be 430 mm d^{-1} or 157 m a^{-1} (assuming constant flow velocity) (Figure 4.6). Pilleweizer's 1957 profile was down-glacier from Pasu Gahr near the snout where velocities are slower.

4.4 Meteorological Records

Effective representation of hydrometeorological relationships within high mountain areas can be accomplished with a small network of meteorological stations. Within the Pasu Glacier Basin three meteorological stations covered a large altitudinal range (1500 m) and general differences in basin morphology (Figure 4.3). The lowest station near Pasu Snout is at an similar altitude to that of the glacier snout (2700 m a.s.l.). The highest station was established on the flat section of the Patundas ridge at an elevation of 4220 m a.s.l. A medial station, Pasu Gahr (3500 m a.s.l.), operated as another data source in the case of mechanical failure or "drift" in measurement in either the high or low altitude stations. Daily mean discharge at Pasu River and temperatures at the three meteorological stations are given in Appendix A (see Figure 5.1).

Each meteorological station consisted of a Carleton Instruments, model T9420 thermohygrograph, recording air temperature and relative humidity, and a Min/Max Thermometer as a check against the thermohygrograph. The thermohygrographs were placed inside standard wooden Stevenson Screen (0.40 m x 0.20 m x 0.25 m) at approximately 1.5 m above the ground surface. The thermohygrographs and Min/Max thermometers were calibrated against two high precision thermometers and laboratory calibrated Grant thermistor probes before being placed in the field. The thermistor probes were connected to a Grant series 1200 Squirrel data logger. The two precision thermometers and the data logger thermistors were in strict agreement with each other. Thermohygrograph and Min/Max thermometer readings were checked against a precision thermometer after placement in the field and throughout the field season.

Due to the distance and terrain involved in reaching Pasu Gahr and Patundas meteorological stations, weekly charts were used for recording data. The relatively close proximity of the Pasu Snout station to base camp enabled daily charts to be employed. The charts were digitized into computer form at hourly intervals, on the hour, for Pasu Gahr and Patundas. Charts from the Pasu Snout station were digitized at 15 minute intervals on the quarter hour. An example of each meteorological station chart can be found in Appendix C. The data logger recorded average temperature and incoming solar radiation at fifteen minute intervals on the quarter hour. Data stored in the logger was down-loaded into a laptop computer.

4.4.1 Pasu Snout Meteorological Station

The Pasu Snout meteorological station was established at an altitude comparable to that of the glacier snout on a flat area of an end moraine 250 m down-valley from the glacier (Plate 4.1). The general surroundings consist primarily of meltout tills, glaciofluvial gravels, a series of lateral moraines, an outcrop of dolomite, a lake and the glacier tongue. The station is slightly protected from direct katabatic winds by a mound of till.

Pasu Snout thermohygrograph began operation on 21 May and recorded data until 31 August. The mean summer daily air temperature recorded at the snout was 15 °C (Table 4.1). Maximum and minimum temperatures were 25 °C on 12 July and 5 °C on 21 June respectively. Three thermistor probes and a Texas Instruments radiometer, all connected to a squirrel logger, were set up along side the snout station. The incoming solar radiometer was attached to the top of the Stevenson screen. One of the thermistor probes was placed inside the Stevenson screen, juxtaposed to the thermohygrograph temperature sensor, for a comparative study between temperature recording devices. The remaining two thermistor probes were placed within a custom made screen set up nearby and at the same elevation as the Stevenson screen. This set up was used for an auxiliary study on comparing the effect of screen types on air temperature readings. The custom made screen consists of two 10 mm thick white plastic tubes the smaller tube (0.4 m x 0.1 m) being mounted inside the larger tube (0.45 m x 0.13 m).

4.4.1.1 Comparison of Thermohygrograph and Data Logger Temperature Records

Throughout the study period a Grant Squirrel Data Logger with three thermistor probes recorded temperatures at fifteen minute intervals at the Pasu Snout meteorological station (Table 4.1). The data logger temperatures are an average of temperatures recorded every second for that fifteen minute period. One thermistor probe (Probe One) was placed along side the thermohygrograph temperature sensor inside the Stevenson Screen. The remaining two thermistors were placed within a home-made screen at a distance of 10 meters from and at the same height as the Stevenson Screen (Probes Two and Three). Probe one acted as a check against the thermohygrograph while probes Two and Three acted as a test between screen type.

The hypothesis for this study is that there is no significant difference (o=0.05) in the average recorded temperature for a given period of time between sensor type and screen type. It is assumed that any difference in recorded temperature between the thermohygrograph and probe One is attributable to the recording device type and method. Based on the data from the study period there is no significant difference at the 95 per cent confidence level between the average summer air temperatures recorded by the thermohygrograph and probe One. Also based on the same data, there is no significant at the 95 per cent confidence level between average air temperature recorded in the Stevenson screen by probe One and average air temperature recorded in the home-made screen by probes Two and Three. It follows that there was no significant difference between average air temperatures recorded by probes Two and Three.

The results of this experiment illustrate the reliability and integrity of the summer air temperature data recorded by the thermohygrograph at the Pasu Snout meterological station. From the experimenters point of view the fundamental difference between the two air temperature recording instruments is the transformation of the "raw" data into digital form for analysis purposes. The data logger down-loads into a Personal Computer directly, however, this set up costs several times more than for the thermohygrograph.

4.4.2 Pasu Gahr Meteorological Station

Pasu Gahr meteorological station (3500 m a.s.l.) was placed on the south side of the basin on top of a lateral moraine in an area sparsely covered by juniper bushes (Plate 4.4). The station is sufficiently protected from glacier winds by another lateral moraine. Data collection commenced on 24 May until 31 August and is summarised in Table 4.1. The mean daily summer air temperature recorded at Pasu Gahr was 10 °C with maximum and minimum temperatures of 21 °C on 28 July and 1 °C on 21 June respectively. To the south of the station is a large talus slope partially covered by <u>Artemisia</u> steppe and terminating in an abrupt jagged ridge. The station is 100 m from the glacier edge at 25 m higher in elevation than the glacier surface.

4.4.3 Patundas

On 6 June the Patundas meteorological station was placed on the flat section of Patundas ridge at 4220 m a.s.l. and recorded air temperatures until 31 August (Table

4.1). The area is dominated by spurs of slate breaking the flat superficial ground cover (Plate 4.6). Mean daily summer air temperature over this period was 6.0 °C with a maximum and minimum daily temperature of 19.0 °C on 28 July and -4.0 °C on 14 June respectively.

4.5 Discharge Records

The velocity-area method was used for the determination of discharge measurements consisting of stream velocity, depth measurements and distance across the stream between verticals. Unfortunately, the dilution method, standard for fast, turbulent river flow, could not be used at Pasu. The distance between the meltwater outlet stream and the gauging sight was too short to allow a complete mixing of the dilute solution so an alternative technique was employed. All discharge measurements were carried out by members of the Alpine Glacier Project (AGP) and WAPDA. Discharge measurements were taken from Pasu Bridge using a Valeport propeller-type current metre and a 40 Kg weight. The current metre and weight were lowered into the river from the bridge by an automated crane mounted on top of a vehicle. Velocity measurements were taken at the rise, peak and set of the daily stream flow patterns throughout the season. Velocity measurements were made velocity readings at 0.2 0.4 0.6 0.8 of the depth below the water surface at 0.5 m verticals across the width of the stream. An average velocity was derived for each vertical. Total discharge for the river cross-section is obtained by summation of the width (b_i), depth (d_i) and mean velocity (v_i) of water in the i^{th} vertical of m verticals into which the cross-section was divided:

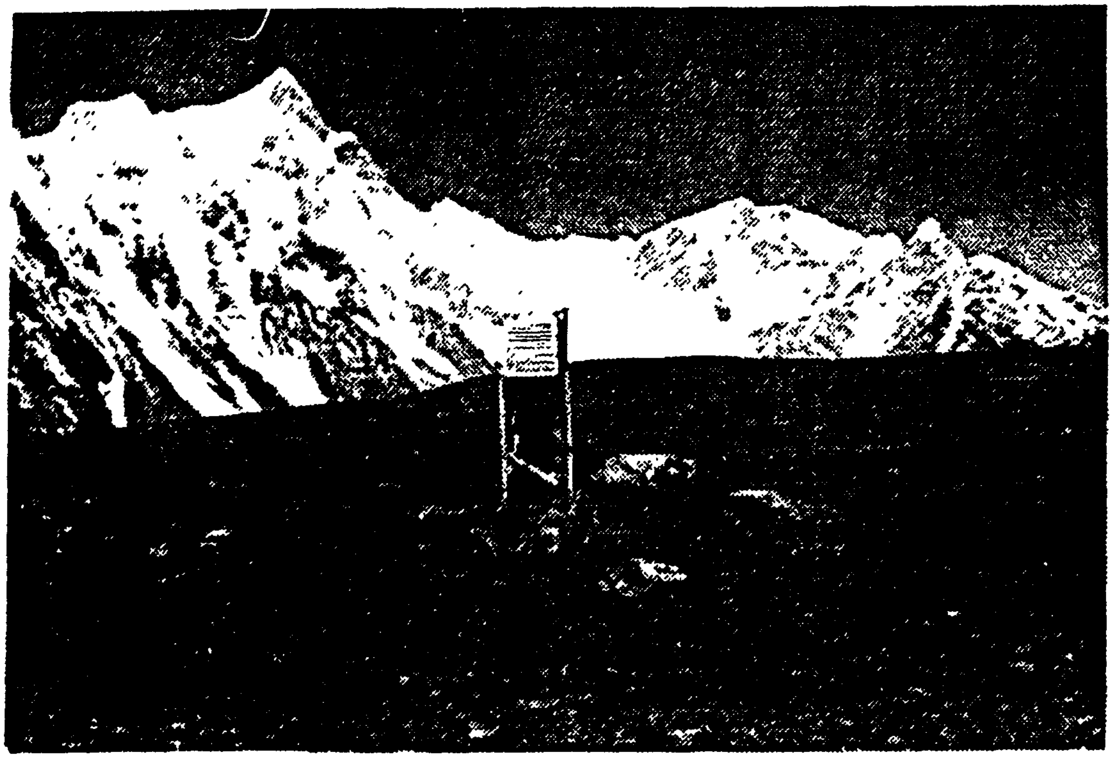

Plate 4.6 The Patundas meteorological station with Shispar Peak (7610 m) in the background.

$$Q = \Sigma(b_i \cdot d_i \cdot \overline{v_i}) \qquad (4.1)$$

Twelve discharge measurements were taken throughout this period at different times of the day giving a complete coverage of the characteristics of the flow regime throughout the ablation season. Discharge readings were used to establish a relation between stage (water level) and streamflow. The method used in developing a rating curve to illustrate the stage-discharge relation, is to draw a median curve through a scatter of points of plotted discharge versus stage measurements. The stage-discharge rating equation for any river is given in equation 4.2:

$$Q = \mathbf{k}\mathrm{h}^{\mathrm{n}} \qquad (4.2)$$

where **k** is the coefficient of the relation, **h** is the stage and **n** is an exponent of **h**. The stage measurements, recorded at 15 minute intervals on the quarter hour using a Tiny data logger, were collected at the gauging site between 21 May and 31 August. Using this data the stage-discharge rating for the Pasu River is:

$$Q = 28.18 * \mathrm{h}^{1.78} \qquad (4.3)$$

From equation 4.3 the Pasu hourly discharge record was calculated and is shown in Figure 4.2. The mean daily summer flow was 16 m^3s^{-1} with a maximum of 38 m^3s^{-1} and a minimum of 6 m^3s^{-1}. Gaps in flow data are related to adjustments in the glacier drainage system or sediment clogging the stage recording instrument.

4.6 Nature of errors in this study

Errors of observation are usually grouped as random, systematic and spurious. *Random* errors are referred to as experimental errors and observations deviated from the mean in accordance with the laws of chance, such that the distribution usually approaches a normal distribution (Norcliffe, 1984). These errors are statistical in nature and can normally be reduced by using a sample of greater than thirty observations. In the context of this study, these variations around the mean value are not errors in the true sense of the word but, natural variations associated with meteorological and hydrological phenomena. *Systematic* errors are those errors which can not be reduced by increasing the number of observations. These errors are inherent in the instruments and equipment used in the measurement programme. *Spurious* errors are human errors, instrument malfunctions and inadequate observation sites which can not be statistically or otherwise be analyzed (Stoddard, 1982).

A comparison of the temperature record from each station indicates an almost perfect synchronisity between the three thermohygrographs (see Figure 5.1 and Appendix B). Air temperatures, at all three altitudes, fluctuate in unison reflecting general weather conditions within the basin. Differences in air temperature values between stations are attributable to the differences in altitude of the stations. Air temperature naturally decreases with increasing altitude. Therefore, it can be assumed that each weather station is representative of the general climate of the basin and not by peculiarities in the local environments.

Systematic errors are usually supplied with the instrument by the manufacturer. The thermohygrographs used in this study have a systematic error of ±0.1 degree celsius. The high precision thermometers and the Max/Min thermometers, used to check the thermohygrographs precision, each have a systematic error of ±0.1 degree celsius. The Grant thermistor probes, used at the Pasu Snout station, also have systemic errors of ±0.1 degree celsius. The conversion of thermohygrograph charts into digital form adds another ±0.1 degree celsius. Since the error associated with the thermometers encompass the error range of the thermohygrographs, the air temperature values recorded by the thermohygrographs are within ±0.2 degrees celsius.

The radiometer is guaranteed, by the manufacturer, to be within ±0.01 cal cm^{-2} min^{-1} with the error occurring during low solar incidence.

The error associated with measurements of discharge from glacial streams are difficult to quantify accurately. A glacial meltwater stream is very dynamic. Flash floods, fluctuating discharge, extreme suspended sediment and bedload movement hinder velocity measurement by current metre. Even during periods of low flow, the Pasu River is extremely turbid. Modification of the stream bed between measurement periods will attach some degree of error to the discharge calculations, however, there were no drastic changes to the bed profile. The foundation of the Pasu bridge provides support against the erosive force of the river as well as providing a secure location from which velocity measurements can be made. Velocity measurements were taken as to procure a large number of observations throughout the range of river flow fluctuation. In this respect greater confidence can be placed in determining the stage-discharge relation.

4.7 Summary

Despite financial, instrumental and environmental restraints the 1989 field study accomplished its major objective, the collection of temperature, incoming solar radiation and discharge data. Three meteorological stations at different altitudes were established within the boundaries of the Pasu Basin to measure the characteristics of air temperature through the ablation season. One meteorological station, Pasu Snout (2700 m a.s.l.), recorded incoming solar radiation data for a large fraction of the ablation season. Continuous monitoring of stage levels on the Pasu River coupled with twelve gaugings of the Pasu River supply a record of runoff over the same period as the temperature record. Based on the synchronous plots of meteorological variables and discharge, confidence is high with respect to the representativeness of the data within the study basin. The following chapter examines the relationships between and within meteorological stations and with discharge. Comparisons with results from similar glacierised basins around the world are also made.

Chapter 5

Relationships Between Air Temperature and Runoff

5.1 Overview

Solar radiation is the main source of energy for snow and ice melt in highly glacierised basins. However, it is often difficult to employ a complete energy balance approach to determine melt on the surface of snow and ice. Financial and practical limitations on the 1989 field season demanded a simpler approach of using air temperature as an index of available energy for melt. Air temperature data is often used as a surrogate for radiation since snow and ice melt follow the pattern of air temperature much better than radiation and data are liberally available. Air temperature represents the heat balance processes and the advection of air masses of different thermal conditions Lang and Braun (1988) and therefore is a physically based variable. Lang (1968), Lang and Braun (1988) and Braun and Aellen (1990) determined that air temperature represents variations in global radiation and that daily air temperature range represents global radiation better than daily mean temperature and hence is a good indicator of melt. Based on their results for glacierised basins

2 of/de 2

PM-1 3½"x4" PHOTOGRAPHIC MICROCOPY TARGET
NBS 1010a ANSI/ISO #2 EQUIVALENT

1.0 4.5 2.8 2.5 5.0 3.2 2.2 5.6 3.6 4.0 2.0 1.1 1.8 1.25 1.4 1.6

PRECISION[SM] RESOLUTION TARGETS

in the Swiss Alps this study will examine the hypothesis of which characteristic of air temperature measured with the Pasu Basin, daily mean or range, is better related to runoff from the Pasu Glacier Basin. Total incoming solar radiation was collected during the study period although it is not the best indicator of snow and ice melt in glacierised basins as it peaks on 21 June of every year and then decreases through the ablation season whereas melt usually reaches a peak in late-July to early-August. Incoming radiation will also be compared to temperature variables and to discharge. Summary characteristics of air temperature, incoming radiation and discharge for the 1989 season are given in Table 4.1. A listing of daily mean temperature, discharge, radiation and daily temperature range is given in Appendix A. Plots of hourly data are provided in Appendix B.

Hydrometeorological conditions in the Pasu region for 1989 were greatly influenced by frequent intrusions of westerly air masses. Cool cloudy conditions persisted throughout most of the season at all elevations although much wetter conditions clearly prevailed above 3500 m often associated with summer snow falls above 4000 m. Some storm events may be the result of monsoonal invasions particularly in August. It is difficult to put the 1989 season at Pasu Basin into a spatial and temporal context within the Karakoram and indeed in Pasu Basin because of the lack of available data. No reliable temperature data are known to have been collected anywhere in the Karakoram except for Gilgit which is unavailable at this time and no historical temperature data exists for Pasu. In order to attempt to put the 1989 field season into a historical perspective, the environmental lapse rate computed within the Pasu Basin can be used to estimate the summer temperature at Gilgit for the months June, July and August. Data for May are not used since the field season did not begin until in late-May. The environmental lapse rate of -6.1 °C/1000 m as measured in Pasu Basin is comparable to the ELR derived from the WAPDA data for Gilgit, -6.2 °C/1000 m (see page 53). The historical 30 year mean average temperature for the months June through August at Gilgit was 26.4 °C. Using the environmental lapse rate from Pasu Snout with a mean summer temperature for the three month period of 15.6 °C the mean temperature at Gilgit is calculated to have been 23.0 °C. The actual 30 year mean for Gilgit for the months June to August was 26.4 °C which is 3.4 °C greater than the estimated mean air temperature. A difference of 3 °C is a significant difference in temperature which suggests that the 1989 summer temperatures were well below average.

From high water marks along the Indus, Hunza, Batura and Pasu Rivers it was obvious that river levels were well below those from last year and previous years. Runoff data are not yet available for the 1989 season from discharge stations located throughout the Karakoram so there is no data to substantiate this evidence. However, based on this information and discussions with many villagers and from the results of the 1989 ELR computations it is probable that the summer of 1989 was well below the normal values for both temperature and discharge.

5.2 Patterns of Runoff and Air Temperature

The curve of discharge is in phase with that of daily mean temperature recorded at three meteorological stations varying in altitude within Pasu Basin (Figure 5.1).

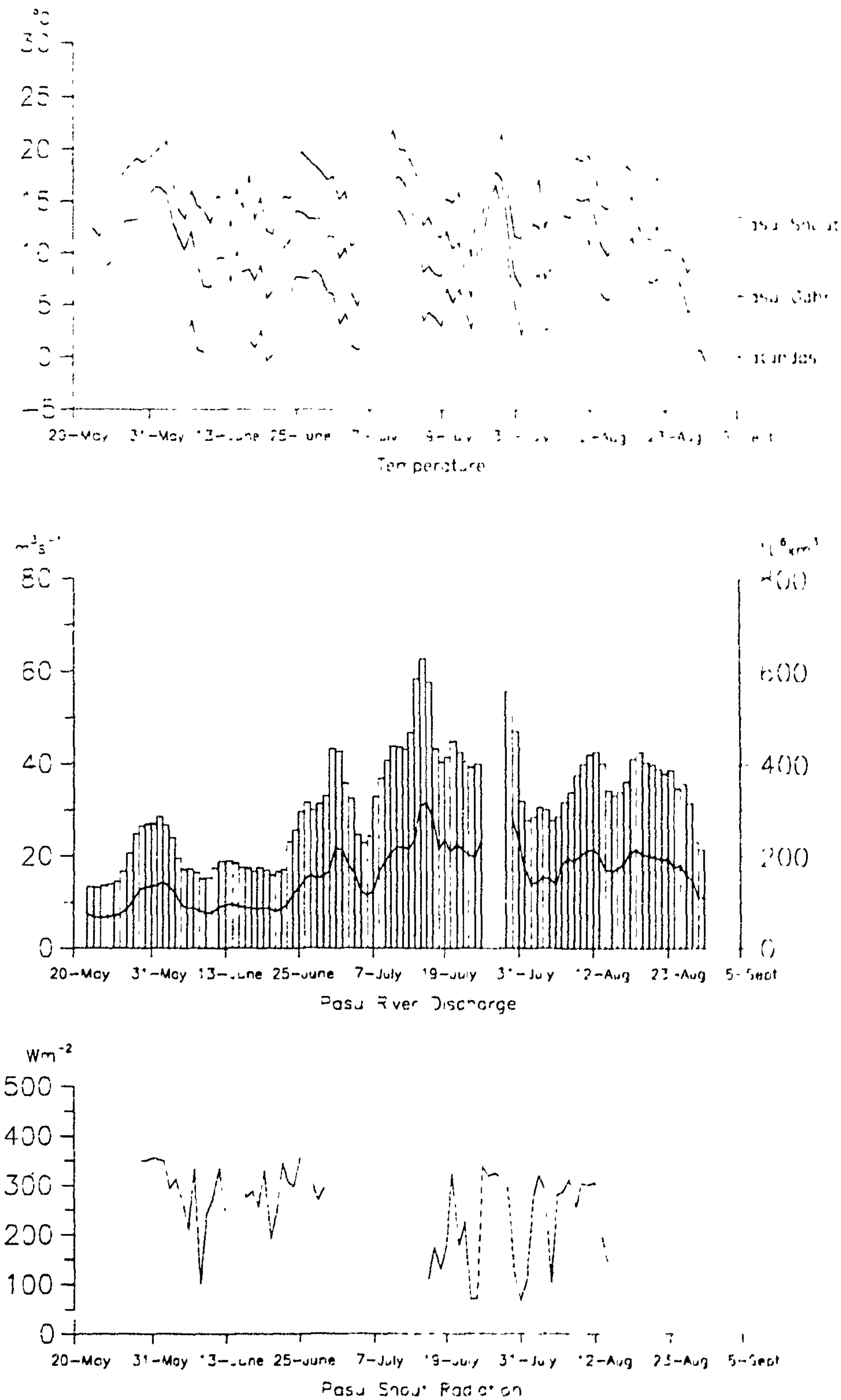

FIG. 5.1 Curves of mean daily and total discharge, daily mean tempeature at Pasu Snout, Pasu Gahr and Patundas and daily mean incoming solar radiation.

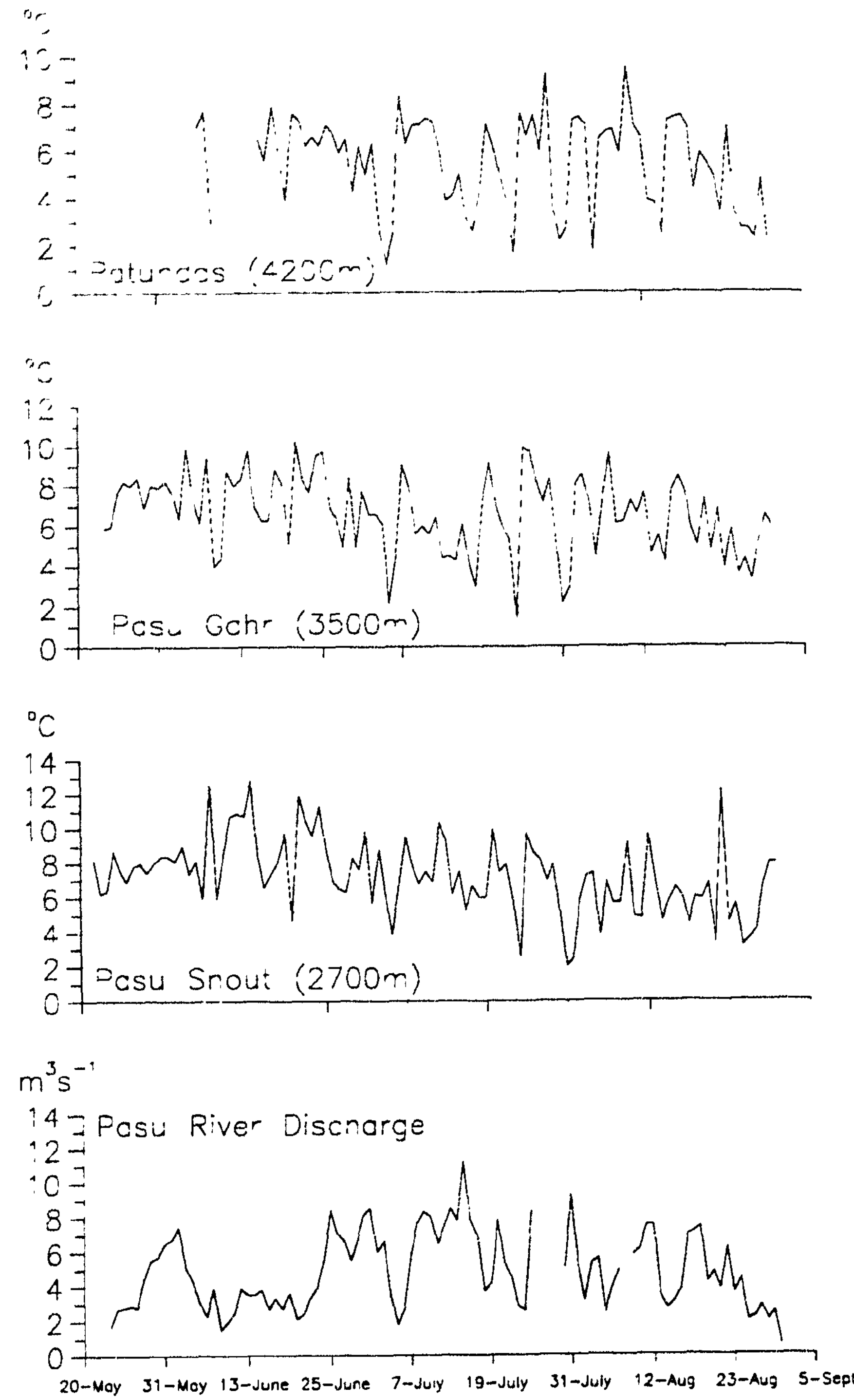

FIG. 5.2 Curves of daily range of discharge and tempeature at Pasu Snout, Pasu Gahr and Patundas.

Three major runoff events on 1-2 July, 14-16 July and 26-29 July are assumed to be related to major adjustments in the glacier drainage system. Temperatures at all meteorological stations show a general increasing seasonal trend to mid-August after which temperatures decreased rapidly. The seasonal trend is greater with increasing altitude although it is masked by the major periodic variations. Variations in daily temperature range (Figure 5.2) do not appear to follow either daily mean temperature or daily mean discharge. There is an underlying downward trend in daily temperature range at all three stations although there is great fluctuations around the mean values through the summer. Daily range in temperature appears to be better associated with daily mean incoming solar radiation than daily mean temperature in Figures 5.1 and 5.2 although the pattern of mean temperature is similar.

Two cyclical patterns dominate the data record, firstly the characteristic diurnal variation in temperature and flow (Figure 5.3) and secondly a more secular cycle of roughly ten to fourteen days where daily mean flow and temperature generally increase and then are subdued by prevailing cloudy conditions (Figure 5.1).

5.2.1 Diurnal variations in Runoff and Temperature

Monthly plots of diurnal variation for each hydrometric variable in Figure 5.3 reveal the characteristic daily variation in mean hourly temperature and discharge. Minimum air temperature for all three meteorological stations were recorded an hour or two after sunrise in each month at between 0500 - 0700 hrs. The lag between sunrise and increasing air temperature is a result of the time taken in transferring heat

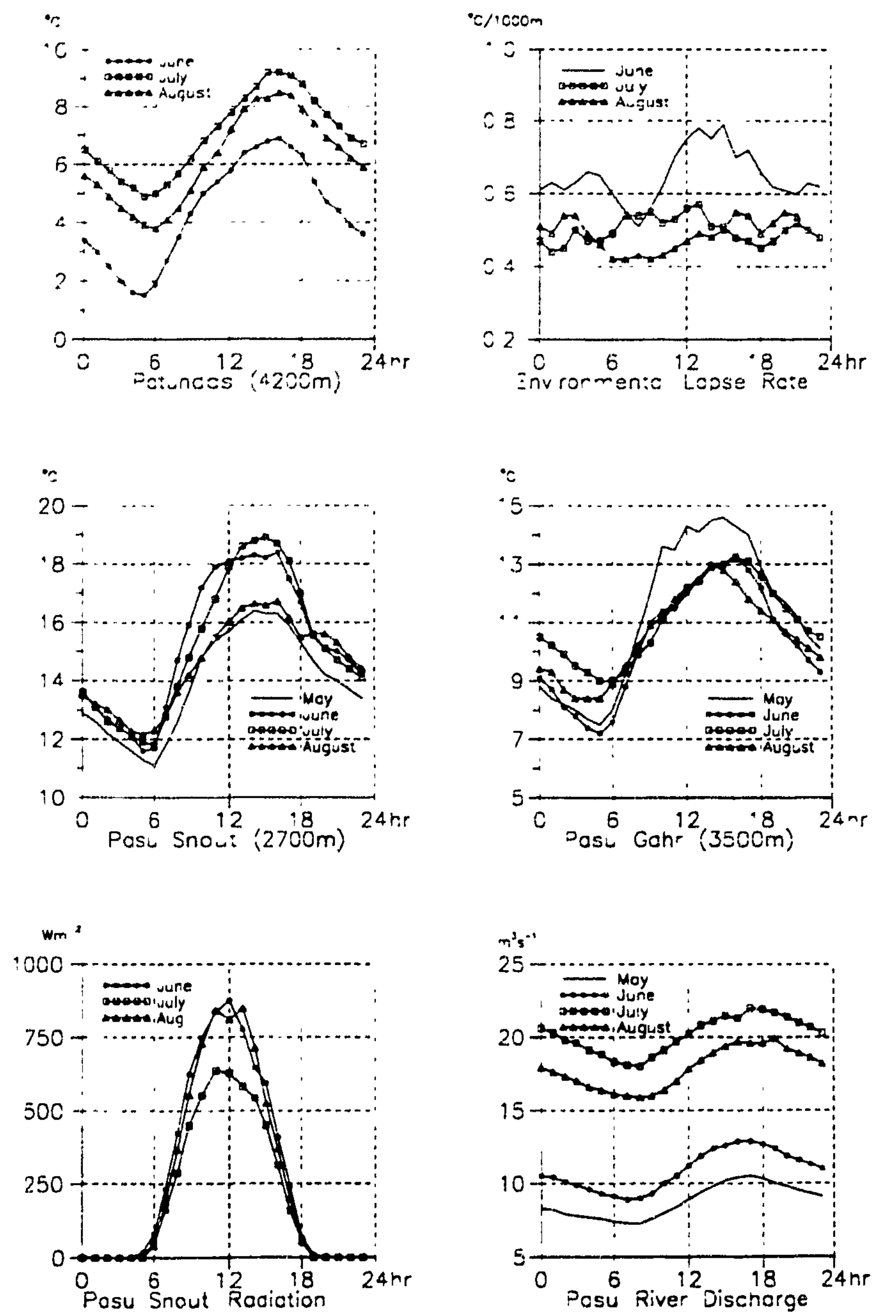

FIG 5.3 Diurnal variations in discharge, incoming solar radiation air temperature, and the Environmental Lapse Rate between Pasu Snout and Patundas within the Pasu Basin.

from the ground surface up to the temperature recording apparatus. There is also a lag between stations as the sun rises over a mountain ridge striking the Patundas station an hour earlier than the Pasu Snout station. Pasu Gahr is the only exception as minimum temperature occurs before sunrise in August. The phenomenon is related to the induction of warm air from higher altitudes producing a temperature inversion at Pasu Gahr. Minimum daily discharge occurs at 0700hrs in May and June and 0800hrs in July and August.

In most cases temperature and discharge increase at a steady rate from minimum temperature towards the daily maximum. The rate of increase differs from month to month and between stations. Pasu Snout has the greatest rate of increase in all months while Patundas has the lowest reflecting the decreasing daily temperature range with increasing altitude. Monthly variations are primarily a result of the changing energy inputs of solar radiation. Maximum and minimum daily temperatures were not consistent between months and between altitudes. Maximum daily temperature are more horizontal for the months May, June and August than in July because of the higher degree of cloudiness during these months. At Patundas daily maximum temperatures were usually at 1600 hrs with the exception of May. Pasu Gahr maximum temperatures occurred at 1500 hrs in May, 1600hrs in June and July and 1400 hrs in August. Maximum temperature at Pasu Snout in May occur at 1400 hrs, June maximum temperatures at 1600 hrs and July and August at 1500 hrs. Sun set at Pasu Snout was at 2000 hrs in the months May and June and at 1900 hrs in July and August. The sun set behind a mountain ridge giving Patundas a longer period of daylight than at the snout. There is a marked dip in temperature near 1800 hrs in

August at Pasu Snout caused by strong katabatic winds which also cause the occurrence of earlier maximum air temperatures at the snout as compared to Patundas. The glacier winds do not reach the Patundas plateau but remain within the confines of the glacier valley. Discharge reaches a daily maximum at 1700 hrs in May, June and July and at 1900 hrs in the month of August giving an estimated lag time from maximum daily temperature of between three to four hours on average for the season.

Daily ranges are generally large during periods of warm weather and small during cloudy periods. There is a weak positive relationship between daily mean temperature and daily range in temperature as represented by the correlation coefficients in Table 5.1. Daily temperature range at Pasu Snout generally decreases through the season because of the influence of katabatic winds in reducing daily maxima temperatures in late-July and early-August. Daily minimum temperatures are at times relatively high in July at Pasu Snout, for example 18 °C on 11 July, because of increased longwave incoming radiation during the night hours under the warm humid conditions. Daily maximum at Pasu Snout are reduced by katabatic winds. Pasu Snout had the six greatest daily ranges of which five were in the month of June and the sixth, the greatest of the season of almost 13 °C, was on 14 June. Diurnal temperature range at Pasu Gahr and Patundas are greatest in July corresponding to periods of high mean temperature. The minimum range for the season was recorded at Patundas, 1.2 °C, on 5 July.

Diurnal ranges in discharge are smallest during the month of May and early-June and greatest in late-July and early-August as is the characteristic nature of

Table 5.1. Correlation Coefficients showing the relationship between daily mean temperature and daily temperature range.

Pasu Snout	Pasu Gahr	Patundas
0.23	0.28	0.37

glacier-fed streams (see Figure 5.6). Like temperature, discharge is greatly affected by the degree of cloud cover and fluctuations in the diurnal range of discharge are more pronounced than daily mean discharge. The plots of daily mean and range suggest a strong positive relation which is confirmed by the strong positive correlation coefficient of 0.66. There is a positive relation between daily range in discharge and daily range at Patundas (r=0.39) with only very weak positive relation for temperature range at Pasu Snout and Pasu Gahr (r=0.12 and r=0.14 respectively).

The diurnal variation in the environmental lapse rate (ELR) between Pasu Snout and Patundas is effectively an index of the different meteorological conditions between the two stations accounts for the difference in altitude (Figure 5.2). The ELR is high during the month of June because of low temperatures associated with a snow covered surfaced at Patundas while Pasu Snout is experiencing very warm temperatures. The almost reversed diurnal variations in July and August are explained somewhat by the dampening affect on maximum daily temperatures at Pasu Snout by katabatic winds but may also be related to the fact that August was an extremely cloudy month. The large increase and decrease in the ELR between 1600 and 1800 hrs in July is a result of the different timing of maximum daily temperatures between the two stations.

5.2.1.1 Cloud Cover

Cloud co·er has a great effect on daily mean and range in temperature and discharge as shown in Figure 5.4. The storm event of 22 to 24 July (Days 3-5) drastically reduced daily mean temperature by 6 °C, 5 °C and 3°C at Pasu Snout, Pasu Gahr and Patundas respectively. Daily mean discharge decreasing slightly during the event although the range has been reduced considerably. There was a 100 per cent cloud cover on 23 and 24 July (Days 4-5) with a ceiling at about 3500 m producing heavy showers in the morning between 0400 and 1000 hrs at Pasu Snout. On 25 July (Day 6) there was a fresh shallow snowcover on Patundas. On 20 July (Day 1) there was little cloud cover and the difference between minimum and maximum temperature is about 10 °C, 9 °C and 7 °C respectively. Daily range of discharge for the same day is 9 m^3s^{-1}.

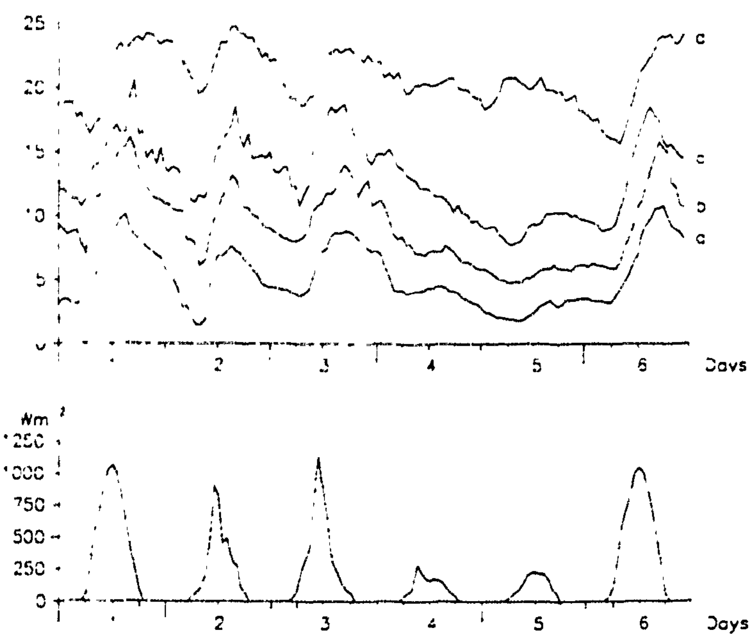

FIG. 5.4 The effect of cloud cover (represented by global radiation in bottom graph) on daily mean temperature (a-c in °C representing Pasu Snout (a), Pasu Gahr (b) and Patundas (c)) and discharge (d in m^3s^{-1}) from 20 July (Day 1), a day with little cloud cover to 25 July (Day 6). On July 24 (Day 5) a 100 per cent cloud cover was observed with a trace of precipitation at Pasu Snout.

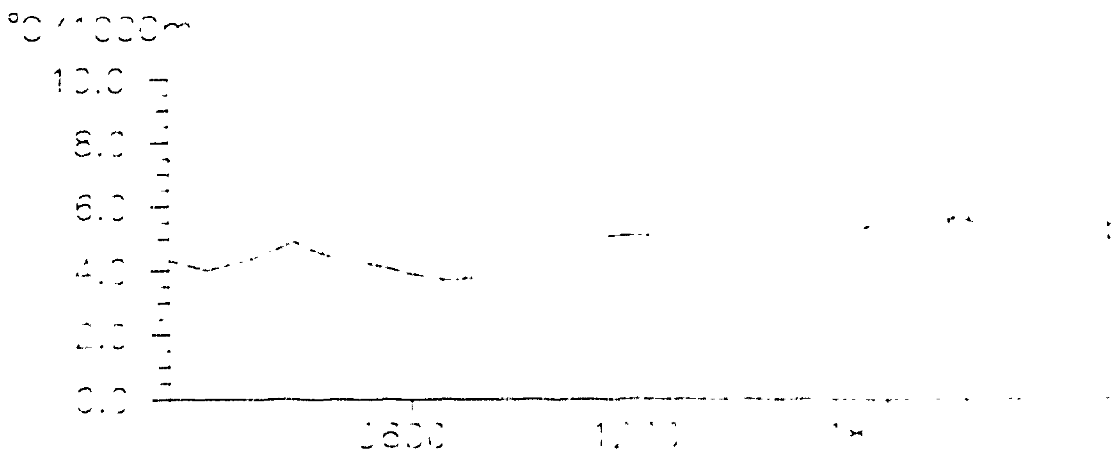

FIG. 5.5 Lapse Rates during a mostly clear day (solid line) and a mostly cloudy day (dashed line).

Figure 5.5 illustrates the environmental lapse rates between meteorological stations within the Pasu Basin on a cloudless day and a day with 100 per cent cloud (Day 5) the daily temperatures range for each meteorological station was about 2 °C while daily range of discharge was 3 m^3s^{-1}. Discharge appears to follow the pattern of temperature at the two higher stations to a greater degree than Pasu Snout. The ELR for the cloud-free day is very similar to the diurnal variation for the month of July as seen in Figure 5.2. Cloud cover has the effect of decreasing ELR because of its more pronounced effect on Patundas temperatures than Pasu Snout temperatures. This confirms the notion that cloud cover is responsible for reversed effect in ELR between July and August in Figure 5.3.

5.2.2 Temporal Variations in Runoff and Temperature

A general secular cycle of ten to fourteen days in atmospheric conditions dominates the data record for the summer of 1989 (Figure 5.1). From 23 May to 7 June flow and temperature at Pasu Snout and Pasu Gahr increased to levels not observed again until mid-July and then deteriorated to levels comparable with the beginning of the period. A period of subdued and generally decreasing daily flow and temperature followed for about twelve days until another period of increasing and then decreasing flow and temperature between 22 June and 6 July. This is immediately followed by another period between 6 July and 19 July and another between 20 July and 2 August. Although not as pronounced this pattern starts again from 3 August to 14 August after which there is another increase in flow and temperature then both drop steadily as cold cloudy and wet weather persisted to at least the end of August.

5.2.2.1 Pasu Snout Meteorological Station

Daily temperature at Pasu Snout displays a very slight increasing seasonal trend until mid-August after which temperature declines (Figure 5.1). Maximum daily mean rises from 20.7 °C to 21.4 °C on 4 June and 28 July respectively. Daily mean air temperature at Pasu Snout decreased from the start of the record on 21 May until 25 May after which the temperature rose steadily to 20.7 °C on 4 June and was not exceeded until 11 July. From 5 June to 21 June temperature fluctuated around the seasonal mean of 15 °C as a result of frequent precipitation events and generally overcast conditions. Temperature was affected by strong mountain winds, warm up-valley winds in the afternoon and cool down-valley winds at night. Indeed, this period produced some of the greatest daily temperature ranges, averaging nearly 11 °C, and also the greatest fluctuations in daily temperature range, for example, from 6 °C to 13 °C from 7 to 8 June.

A short period of the highest radiation inputs between 21 and 26 June increased daily mean temperature from 11.8 °C to 19.7 °C. Daily temperature range averaged 7 °C over this very warm period. Temperature remained high until 4 July when one of the most intense storms of the season reduced mean temperature to 10.6 °C and the diurnal range was limited to only 4 °C. From 6 to 11 July temperature increased to its summer maximum hourly value of 25.4 °C and daily mean of 21.8 °C. Daily range was 7 °C on the hottest day of the summer. Between 12 and 16 July daily mean temperature decreased to 12.6 °C as a storm system inundated the Pasu region until 25 July. Near seasonal maximum temperatures were reached on 29 July with a daily mean of 21.4 °C after the storm cleared. Another major storm reduced mean daily air temperature to 11.4 °C on 1 August with a temperature range of only 2 °C, the minimum value for the summer.

Katabatic winds in the afternoon affect Pasu Snout meteorological station during late-July to mid-August subduing daily maximum temperature. Temperature increased to more than 17 °C on 4 August only to be reduced again to 12.4 °C by another storm event on 5 August. From 6 to 12 August temperature increased to 19 °C with a daily range of almost 10 °C. Although not reducing daily temperature values, several precipitation events occurred between 12 and 22 August. The most extreme of these events, from 14 to 16 August, precipitation was continuous although the mean temperature remained above 14 °C and the daily range was greater than 6 °C. These events are assumed to be monsoonal in origin because of the relatively warm daily temperatures coupled with the fact that these storms approached from the south. Cooler wet conditions dominated over the remainder of August decreasing temperature to well below the seasonal average by 26 August and reaching the seasons minimum daily mean temperature of 8.2 °C on 28 August.

5.2.2.2 Pasu Gahr Meteorological Station

Pasu Gahr daily mean temperature has a very similar seasonal trend to that at Pasu Snout although the rate of increase is slightly greater. The maximum daily mean increased from 14 °C on 25 June to 17.8 °C on 28 July while Pasu Snout rose by only 0.7 °C over the same period. The pattern of daily mean temperature and daily range is parallel to Pasu Snout with most deviations attributable to altitude and local site characteristics. Conditions at Pasu Gahr, however, were generally wetter than at Pasu Snout on account of its higher elevation. Maximum daily mean temperature occurred on 28 July with a value of 17.8 °C. Maximum daily mean temperatures generally occur later than Pasu Snout especially from mid-July because of the effect of katabatic winds on the Pasu Snout station. Katabatic winds did not have the same impact on Pasu Gahr because it was shielded from direct force by a lateral moraine up-valley of the station.

5.2.2.3 Patundas Meteorological Station

Patundas temperature remained relatively low until late-June while the winter snow cover remained on Patundas. This may be significant in that the pattern of discharge essentially parallels that of temperature at Patundas. During the month of July Patundas temperatures increased at a much greater rate than at Pasu Snout and Pasu Gahr. Mean daily temperatures at Patundas for the month of August generally increase until the middle of the month then decline sharply. The daily mean temperature of 7.6 °C on 25 June rose to 16.5 °C on 28 July. During the storm event between 20-22 June Daily mean temperature remained near 0 °C producing the summer's coldest instantaneous hourly temperature of -3.4 °C and daily mean temperature of -0.4 °C on 20 June. On 20 June daily temperature range was nearly 4 °C and snowfall was abundant. Daily temperatures at Patundas rose to above 7 °C for several days between 23 to 29 June melting a large fraction of the remaining winter snow cover. Daily temperature range decreased through this period and up to 3 July as minimum daily temperatures began to increase because of warmer nighttime temperatures. From 30 June to 5 July daily mean temperature dropped from 7.5 °C to as low as 0.7 °C and the daily range was reduced to 1.2 °C the lowest of the season. Fresh snow covered Patundas from 3 July until 8 July. The season high temperature to date occurred on 12 July when the daily mean temperature rose to 13.6 °C and when the maximum temperature of the season was recorded at Pasu Snout. From 15 to 25 July daily mean temperature remained below 7 °C at Patundas accompanied on several occasions with early morning snowfalls. The lowest temperature during this period was 3 °C and the daily range was 4.2 °C. The maximum daily mean temperature recorded at Patundas of 15.8 °C occurred on 28 July and the maximum instantaneous hourly temperature was 18.8 °C. The major storm event between 30 July and 1 August reduced mean temperature to 2.1 °C. Maximum temperatures at Patundas increased from 8 °C on 4 August to 11.8 °C on 19 August even though the weather was very unstable. Indeed, the temperature dropped to 2.6 °C and the daily range was reduced to 1.7 °C the following day. Cool wet conditions at Patundas from 20 August to 31 August decreased the daily mean from 8.8 °C to -0.4 °C and with an appreciable amount of snowfall on Patundas.

The general trend in the difference in air temperature between stations is inverse to the trend of daily mean temperature such that the smallest difference occurs during peak temperatures on 28 July and the largest difference occurs during the coldest period on 21 June (Figure 5.4). Maximum daily mean temperatures between 25 June and 29 August increased by 0.7 °C, 3.8 °C and 8.9 °C at Pasu Snout, Pasu Gahr and Patundas respectively. This is significant as it reveals the magnitude of increases in temperature is greater with increasing altitude. For example, in Figure 5.1, the increase in temperature from 5 to 12 July is 10 °C, 12 °C and 14 °C at Pasu Snout, Pasu Gahr and Patundas. Figure 5.5 also further illustrates this phenomenon as lapse rates are 2 °C/1000 m greater on a cloudless day as compared to a cloudy day.

5.2.2.4 Pasu River Discharge

The seasonal pattern of runoff for the Pasu River is typical of a glacier fed river (Figure 5.1). Peak daily mean flows occur in July and August and are almost double the flow in May and June. The magnitude of the difference is as about expected based on longer records of discharge from other glacierised basins (Young, 1982; Collins, 1989a). Daily ranges in discharge show a generally increasing trend from May to July (Figure 5.6). The difference between minimum and maximum daily discharge increases dramatically from May to late-July and decreases through August (Figure 5.6) which is characteristic of glacier-fed streams (see Figure 2.4).

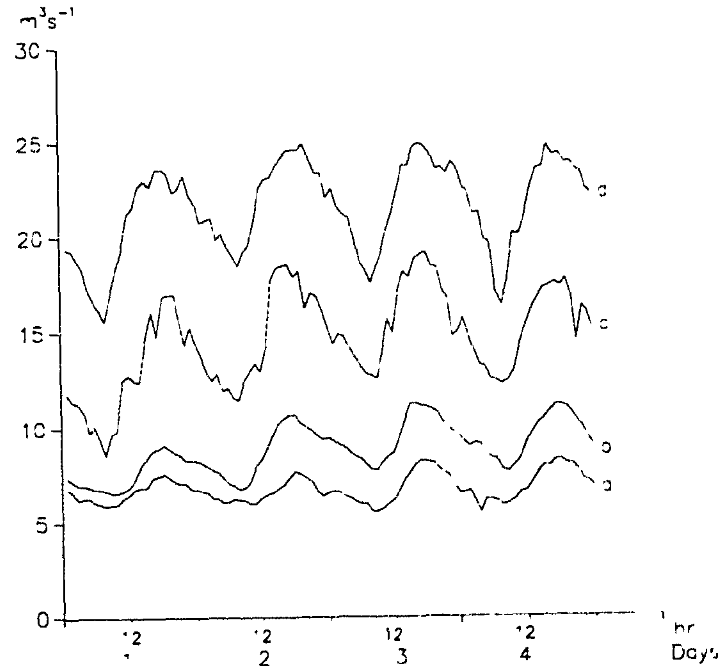

FIG. 5.6 Discharge of the Pasu River over selected four day periods in 1989: (a) 23-26 May; (b) 11-14 June; (c) 25-28 June; (d) 10-13 July.

Between 22 May and 3 June daily mean discharge doubles from 7.4 m^3s^{-1} to 14.4 m^3s^{-1} and the daily ranges increases by nearly ten fold from 0.8 m^3s^{-1} to 7.4 m^3s^{-1}. Intermittent snowfalls and cold temperatures at elevations above 3500m restricted runoff between 4 and 21 June from 13.5 m^3s^{-1} to as low as 7.6 m^3s^{-1} on 10 June and 8 m^3s^{-1} on 21 June. The range in daily flow was reduced to as low as 1.5 m^3s^{-1} on 9 June. During the period from May to late-June the drainage system appears to have remained stable producing a relatively smooth daily flow pattern superimposed by natural diurnal variations (see Appendix B). During the night of 23 June an adjustment to the glacier drainage system took place after which the diurnal pattern becomes irregular with many smaller peaks superimposed on both rising and recession limbs. The glacier drainage system must have undergone a massive hydraulic re-organisation as snow and ice melt increased with increasing temperature. The irregular diurnal pattern continued for the remainder of the study period. Discharge slowly increases from 22 June to 30 June and then rises sharply which maybe the result of an emptying of a large reservoir within the glacier drainage system. From 1 to 6 July daily discharge was halved from 21.9 m^3s^{-1} to 11.5 m^3s^{-1} in reaction to snowfall at elevations as low as 3900 m. By 4 July flow had diminished to levels before the glaciological event and continued to decline until 6 July at a mean of 11.5 m^3s^{-1}. Daily range reaches its maximum by 4 m^3s^{-1} of 11.2 m^3s^{-1} on 15 July and daily mean flow reaches its recorded seasonal maximum on 16 July of 31.6 m^3s^{-1} five days after daily mean temperature at Pasu Snout reached its summer maximum. The abrupt rise in flow from 23.7 m^3s^{-1} on 14 July to 30.8 m^3s^{-1} on 15 July is considered to result from the release of water from the breaching of a blocked conduit in the glacier drainage system. This is evidenced by the slightly reduced flow in 12 and 13 July.

On 15 July the instantaneous fifteen minute maximum discharge was measured at 39.4 m^3s^{-1}. On 18 July flow had returned to values recorded before the event and slowly decreased until 25 July when an extreme quantity of water was released from the glacier destroying the recording equipment. It is not known whether flow increased as a result of very warm temperatures or if it was the result of a glacier drainage event. It is probable, however, that daily mean flow for the event was greater than the recorded mean flow of 16 July as evidenced by the rapid decrease in flow from the instantaneous fifteen minute value of 42.2 m^3s^{-1} on 30 July to the daily mean of 14 m^3s^{-1} on 2 August. The maximum daily mean discharge for the month of August does not exceed the level recorded on 1 July. Storm events reduced the daily range to 2.6 m^3s^{-1} on 14 August remaining below 3 m^3s^{-1} from 26 August to the end of the month when mean discharge was reduced to levels last recorded on 23 June.

Figure 5.6 reveals the evolution of the glacier drainage system as increased volumes of meltwater are forced through conduits with increasing summer temperatures. The daily range of discharge increased from 2 m^3s^{-1} in (a) to more than 7 m^3s^{-1} in (d) reflecting the retreat of the snowline and a growing area of the glacier ablation zone exposed to solar radiation. Frequent storms and mostly cloudy conditions which prevailed in August reduced flow below levels in July allowing conduits in the glacier drainage system to contract with the effect of delaying meltwater runoff and the dampening daily range of flow.

The three very distinct peak flow periods observed on the Pasu River during the study season appear to be the result of major disruptions within the glacier drainage system. The first two events occur near the end of a cycle when temperatures are decreasing from cycle maximum and significant increases in daily flows (Figure 5.1). The event of 1-2 July appears to be the result of an under-developed conduit system responding to stresses of water build-up from increased meltwater generation. This phenomenon is seen in glacierised basins in the Swiss Alps as temperatures warm in spring, for example, Collins (1989b) and Iken *and others* (1983). Sustained cool cloudy conditions throughout May and June kept snow and ice melt runoff to a level which may have permitted the conduit system to remain in a state of infancy. The relatively minor incident of 22 June indicates that the drainage system was experiencing a certain degree of stress.

The second and more pronounced event of 15 July behaves in a very similar manner as the first event, however, this event probably resulted from a blocked conduit as evident in the reduced flow prior to peak flow. The third event of 28-30 July may not be associated with a glacial drainage system event. It is entirely possible that large quantities of meltwater were generated during four days of clear skies which produced the highest recorded temperatures of the season. The conduit system may have been capable of coping with the increased flow since the recessive limb corresponds very well with the pattern of decreasing temperatures at Patundas. This indicates there was minimal retention of water within the system, however, some adjustments to the drainage system may have taken place during the event while the conduits were completely saturated.

5.3 Relations Between Temperature Characteristics and Incoming Solar Radiation

The effectiveness of daily temperature range and daily mean temperature as a surrogate for summer energy inputs is assessed by examining their degree of association with incoming solar radiation by means of correlation coefficients as presented in Table 5.2 (Figure 5.1 and Figure 5.2). It must be assumed that incoming radiation measured at Pasu Snout is not representative of the distribution of incoming radiation over the entire catchment because of the degree of cloud cover in any high mountain basin is highly variable (Barry, 1981). It should also be noted that the meteorological variables are not independent of one another and therefore no significance levels can be applied to the values in Table 5.2. It is valid, however, to use the correlation coefficients as a measure of the degree of association between

Table 5.2: Matrix of correlation coefficients showing relationships between air temperature characteristics and incoming solar radiation within Pasu Basin during the two periods of global radiation data. Period I is between 4 and 29 June, Period II is between 16 July and 14 August (see Figure 5.1).

	Daily Mean Temperature			Daily Temperature Range		
	Pasu Snout	Pasu Gahr	Patundas	Pasu Snout	Pasu Gahr	Patundas
Period I	0.68	0.59	0.62	0.34	0.52	0.53
Period II	0.77	0.79	0.68	0.70	0.83	0.88

these variables for analysis of interrelationships. Characteristics of air temperature show a strong degree of association with daily mean incoming solar radiation over altitudinal and temporal scales. Period II has much stronger degrees of association than Period I because natural heat balance variations reaching a maximum in July and August. Results from Period I suggest early-summer mean temperature is better related to incoming radiation than temperature range at all three meteorological stations. During Period II mean temperature at the lowest meteorological station, Pasu Snout, is better related to incoming radiation whereas at the highest altitude, Patundas, temperature range is much better related to incoming radiation than mean temperature. Temperature range and mean temperature at Pasu Gahr both have strong relations with incoming radiation. Daily temperature range at Patundas during period II has the greatest degree of association with incoming radiation of all values.

Based on the results in Table 5.2, there is little evidence that the daily range in air temperature is better associated with daily mean incoming radiation than the daily mean temperature. It appears the characteristic of temperature contributing the most information about the available energy for melt is dependent on season and altitude for the Pasu Basin. These results confirm the tendency of weather conditions to change the degree of association between air temperature characteristic and incoming radiation. These results indicate that the much greater range in altitude in the Karakoram provides greater meteorological variations from arid valley bottoms to perennial snow and ice covered mountain peaks as opposed to the Swiss Alps. Indeed, Patundas is at an altitude greater than most peaks in the Swiss Alps. The altitudinal position of Patundas and Pasu Gahr therefore better represent variations in summer energy inputs responsible for snow and ice melt in the Karakoram much better than stations in the valley bottom as indicated by the strength of correlation coefficients in Table 5.2. In this case, variations in runoff within the Pasu Basin are best estimated by using daily range data from altitudes corresponding to the major runoff zones between 3500 and 5500 m and not from the valley station as suggested by Lang and Braun (1988).

5.4 Relations Between Meteorological Characteristics and Runoff

The extent to which variations in meteorological conditions affect runoff from Pasu Glacier can be assessed by an examination of the correlation coefficients between the relevant variables. Curves of mean air temperature are in phase with that of discharge as shown in Figure 5.1 which suggests that summer energy inputs are exerting a strong influence in the Pasu Basin. There are two distinct exceptions which are related to peak flow events induced by major adjustments in the glacier drainage system on 1-2 July and 16-18 July. These events are glaciological in origin not hydrometeorological so the discharge values for these events are not included in this analysis. Curves of daily temperature range shown in Figure 5.2 appear to have a slight inverse relationship with daily mean discharge (Figure 5.1).

5.4.1 Relations between Incoming Radiation and Runoff

Correlation coefficients computed between daily mean discharge and daily incoming solar radiation during individual months and over the entire summer season are given in Table 5.3. Relationships tend to vary with altitude within the Pasu basin,

Table 5.3: Correlation coefficients showing relationships between incoming solar radiation and runoff within Pasu Basin.

June	July	August	May-August
0.31	0.42	-0.14	-0.29

air temperature characteristic and season. Relations between discharge and incoming radiation are naturally weak during the summer season since discharge increases until late-July and early-August while incoming radiation slowly decreases from its peak in late-June. The relationship is positive in June since discharge and radiation are both increasing although the rate of increase for each variable is rather different as indicated by the low value. The data values for radiation in July are only available from the second half of the month when weather conditions are poor and radiation is already naturally decreasing. Discharge is reduced by cloudy conditions with the affect of lowering amounts of available energy for melt and therefore a good positive relationship occurs as indicated by the strength of July's correlation coefficient. An inverse relationship between discharge and radiation develops in August as radiation is slowly decreasing whereas discharge is generally steady although it begins to decrease late in the month. The weak negative value for the summer period emphasises the naturally inverse relationship between discharge and radiation for this length of time.

5.4.2 Relations between Air temperature Characteristics and Runoff

Correlation coefficients representing the strength of relationship between air temperature and discharge variables are given in Table 5.4. Relations between daily mean temperature and discharge are much greater than relations between discharge and daily temperature range. The negative coefficients for the May-August period at all three meteorological stations indicate flow tends to increase as daily temperature range is decreasing and vice versa. Daily mean temperatures are all strongly positive revealing that mean temperature is a much better indicator of melt from the Pasu Basin than daily range. The highest meteorological station, Patundas 4200m,

Table 5.4: Matrix of correlation coefficients showing relationships between air temperature characteristics and runoff within Pasu Basin.

	Daily Mean Temperature			Daily Temperature Range		
	Pasu Snout	Pasu Gahr	Patundas	Pasu Snout	Pasu Gahr	Patundas
June	0.79	0.79	0.84	0.01	0.15	0.31
July	0.28	0.41	0.50	0.16	0.15	0.28
August	0.71	0.77	0.83	0.14	-0.16	0.13
May-August	0.32	0.45	0.66	-0.31	-0.30	-0.13

consistently produces the strongest degree of association with discharge. The prevailing meteorological conditions at Patundas may therefore provide a very reasonable indication of the quantity of ice melt in the form of runoff. It is essential to determine the extent of exposed glacier ice and the prevailing meteorological conditions governing the area of exposed ice. Patundas temperatures should therefore provide a good indication as to the rate at which the transient snowline rises through the summer and perhaps the final altitude reached. Mass balance studies in high mountain regions should be used to prove the reliability of air temperature as an indicator of relations with discharge (Hino *et al*, 1987, Braun and Aellen, 1990). It would therefore be necessary to establish the critical temperatures at which the snowline reached the foot of the icefall and the top of the icefall. Based on the data collected during the 1989 field season it would appear that the snowline reached the icefall when temperatures reached about 10 °C and must be greater than 17 °C to reach the top of the ice fall. Mountain glaciers of the Alps and the Rockies are greatly influenced by summer snowfall which may cover a large proportion of the ablation area and perhaps even all of it (Young, 1978, Collins, 1989b). In the Karakoram this event is highly unlikely as the ablation zones reach well below the limit of summer snow fall to areas that receive little solid precipitation in winter.

5.4.3 Evolution of the Transient Snowline

Monitoring the movement of the transient snowline was difficult because of the highly crevassed nature of the glacier surface. The snowline appeared more as a discontinuous area of snow cover rather than a distinct "line" although the term line will be used for the rest of this study. Observations of the snowline were carried out weekly from 25 May to 31 August. On 25 May the snowline was just below Yorsch at an altitude between 3800 and 4000 m (Figure 4.2). During the month of June, which was dominated by cool temperatures and several precipitation events at all altitudes, the snowline slowly retreated to the main ice fall at 4300 m. The area of glacier below 4300m is about 20.5 km^2 which represents about 33 per cent of the glacier. The transient snowline remained stranded in the ice fall between about 4500 and 5000 m from early-July through to mid-August. Observations on 25 and 31 August were obstructed by cloud cover and snow fall, however, it is likely the snowline reached the bottom of the ice fall or perhaps even further down-glacier. At Patundas on 31 August it was snowing heavily with at least 150 mm of snow covering the ground.

Observations of the Pasu glacier transient snowline revealed that the snowline fluctuated within the confines of the main ice fall between 4500m and 5500mm for most of the summer season. The ice fall covers a large range in elevation over an extremely short distance. Within the ice fall the snowline may lower several hundred metres in elevation while not significantly reducing the area of exposed glacier ice. Of course, the opposite is also true. The snowline may not advance above the ice fall unless summer temperatures are above the seasonal average. This has broader implications as many of the Karakoram glacier also contain a major icefall around this elevations, for example, the Barpu glacier in the Barpu-Bualter Basin (Figure 4.1) and the neighbouring Batura glacier (BGIG, 1979).

It is most likely the effect of cloud cover and associated storm events which have the greatest influence on runoff rather than the precipitation under these conditions. Precipitation would increase runoff from a nival basin but in a highly glacierised catchment the effect of precipitation is a reduction in meltwater because of the inverse effect of cloud cover on melt.

Meteorological condition w 'hin the Pasu Basin during 1989 may have been well below long-term season normals. Analysis of this data suggests that either of the two air temperature characteristics, daily mean or daily range, could be employed to provide an effective index of the available energy for melt. However, the results in Table 5.4 indicate that mean daily air temperature is much better related to runoff than daily temperature range. The high degree of cloudiness prevalent during the study season may have distorted the results. It may be that daily range temperature is better related to discharge during a year when air temperatures are average or above average as indicated by the results in Table 5.2. Daily mean air temperature measured at 4200 m consistently gave the best results although mean temperature from Pasu Snout and Pasu Gahr were highly correlated with discharge in June and August. The strengths of the relationships are also affected by adjustments and delays within the glacier drainage system caused by great variations in meteorological conditions most prominent during the month of July.

Chapter 6

CONCLUSIONS

The data record collected from the Pasu Basin during the summer field season of 1989 permitted a basic but very useful examination of relations between air temperature and runoff within a highly glacierised basin in the Karakoram mountains. Based on the data record of 102 days of air temperatures at three different altitudes and discharge at the Pasu bridge a strong relationship definitely exists between these variables. This study has also shown that the strength of the relationship between temperature and runoff is as should be expected in a highly glacierised alpine basin. The physical basis of the relationship is the intimate link between solar energy raising the temperature of the air by means of heat balance mechanisms and hence the melting of snow and ice. Air temperatures have been used by many researchers as a surrogate for this energy variable and it has been shown that this assumption is also relevant to the Pasu Basin.

Based on the results of the analysis applied to the data collected in the Pasu Basin both daily temperature range and daily mean temperature provide a good index of the energy available for the melting of snow and ice. Daily mean temperature is a much better index of snow and ice melt represented by runoff from the Pasu Basin. Indeed, the relationships show a very strong physically based relationship exists between daily mean runoff and daily mean temperature during all weather conditions. The degree of strength of the relationship increases with the altitude for the three meteorological stations. The highest meteorological station, Patundas (4200 m) provides large amounts of explanation of the variations in summer runoff. At this altitude the prevailing meteorological condition governing the evolution of the snow line and hence the amount of glacier ablation are best monitored.

It is therefore recommended that any further meteorological stations to be set up in the Karakoram region should be located within the major runoff zones between 3500 m and 5500 m as this provides the best representation of the prevailing meteorological conditions effecting ice melt. Records of minimum and maximum temperature should also be kept along with mean temperatures. Such a station could be set up with a data logger so that it had to be visited only a minimal number a times or indeed only once during a summer season.

The predominance of cloudy conditions is assumed to have subdued the strength of the relationships investigated in this study. Indeed, cloudy conditions clearly played a major role in controlling the interrelationships between hydrometeorlogical variables with the Pasu Basin. It is suggested that the 1989 summer field season experienced mean summer temperature values below the normal average temperature for this area by three degree celsius. This was particularly noticeable in the rather low river levels throughout the Karakoram.

It is also suggested that the evolution of the snowline be closely observed and used in the analysis as a control to determine if the air temperature characters can produce reliable estimations of the location of the snowline. It is not recommended that air temperature alone be used as a predictive variable for runoff from a glacierised basin in the Karakoram. Although a large fraction of the variance of runoff can be expressed by records of air temperatures, there are other factors which are essential and should definitely be taken into account. Firstly, the amount of winter precipitation is of major importance to the quantity and timing of the glacier contribution to river flow. A rather large amount of attention has recently been given in this direction by means of satellite imagery analysis. Secondly, and intimately linked with the first, the meteorological conditions of the spring months April and May will have a profound effect on the timing of the beginning of the glacier contribution to river flow. And thirdly, the impact of summer monsoonal intrusions on the hydrological regime of the Karakoram region appears to be that of reducing flows for that year. However, the quantity of monsoonal precipitation is suspected to be about one third of the total annual precipitation and therefore may provide for increased flows in following years. In any event, monsoonal intrusions are as yet still unpredictable and therefore will probably have a great effect on any hydrological model that does not take this effect into account.

REFERENCES

Ageta, Y., 1976. Characteristics of the precipitation during the monsoon season in Khumbu Himalaya, *SEPPYO, Journal of the Japanese Society of Snow and Ice*, **38**, *special issue: Glaciers and Climates of Nepal Himalaya*, 84-88.

Ambach, W., and Kuhn, M., 1987. Altitudinal shift of the equilibrium line in Greenland calculated from heat balance characteristics, in J. Oerlemans (ed.) Glacier Fluctuations and Climatic Change, Kluwer Academic Publishers, 281-288.

Anderson, E.A., 1973. Techniques for predicting snow cover runoff, in *The Role of Snow and Ice in Hydrology (Proceedings of the Banff symposium September, 1972), International Association of Hydrologic Sciences Publication* **107**, 840-867.

Andrews, John, T., 1975. *Glacial systems: an approach to glaciers and their environments*, Duxberg Press, Mass.

Barry, R.G., 1981. Mountain weather and climate, Methuen, New York.

Barry, R.G., and Chorley, R.J., 1985. *Atmosphere, weather and climate*, Methuen and Co. Inc., London.

Barry, R.G., and Claudia, C.V.W., 1974. Topo and Microclimatology in Alpine Areas, in Ives, J., and Barry R. (eds.), Arctic and Alpine Environments, Methuen, London, 73-84.

Batura Glacier Investigation Group (BGIG), 1979. The Batura Glacier in the Karakoram Mountains and its variation, *Scientia Sinica*, **22**, 958-974.

Behrens, H., Bergman, H., Moser, H., Ambach, W., and Jochum, O., 1975. On the water channels of the internal drainage system of the Hintereisferner, Ötztal Alps, Austria, *Journal of Glaciology*, **14**(72), 375-382.

Bishop, B.C., Angstrom, A.K., Drummond, A.J., and Roche, J.J., 1966. Solar Radiation Measurements in the High Himalayas (Everest Region), *Journal of Applied Meteorology*, **5**, 94-104.

Braithwaite, R.J., 1981. On glacier energy balance, ablation, and air temperature, *Journal of Glaciology*, **27**(97), 381-391.

Braithwaite, R.J., and Olesen, O.B., 1988. Effect of glaciers on annual runoff, John Dahl Land, South Greenland, *Journal of Glaciology*, **34**(117), 200-207.

Braun, L. and Aellen, M., 1990. Modelling discharge of glacierised basins assisted by direct measurements of glacier mass balance. *I-Hydrological Measurements; the water cycle (Proceedings of two Lausanne Symposia, August, 1990). IAHS Publication*, **193**, 99-106.

Brugman, M.M., unpublished. Water flow at the base of a surging glacier, (Ph.D. thesis, California Institute of Technology, Pasadena, 1986.)

Burkimsher, M., 1983. Investigations of glacier hydrological systems using dye tracer techniques: observations at Pasterzengletscher, Austria, *Journal of Glaciology*, **29**(103), 403-416.

Butz, D., 1989. The agricultural use of melt water in Hopar settlement, Pakistan, *Annals of Glaciology*, **13**, 35-39.

Collier, E.P., 1955. Glacier variations and trends in runoff in the Canadian Cordillera, *International Association of Hydrological Sciences Publication* **46**, 344-357.

Collins, D.N., 1982a. Temporal variations of meltwater runoff from an alpine glacier, in *Hydrological Research Basins (Proceedings of the symposium on Bern, Hydrological Research Basins, 1982), International Association of Hydrological Sciences Publication* **107**, 761-789.

Collins, D.N., 1982b. Flow-routing of meltwater in an alpine glacier as indicated by dye tracer tests, *Beiträge zur Geologie der Schweiz - Hydrologie*, **28**(II), 523-534.

Collins, D.N., 1984. Climatic variation and run off from alpine glaciers, *Zeitschrift für Gletscherkunde und Glazialgeologie*, **20**, 127-145.

Collins, D.N., 1989a. Hydrometeorological conditions, mass balance and runoff from an alpine glacier, in J. Oerlemans (ed.) Glacier Fluctuations and Climatic Change, Kluwer Academic Publishers, 235-260.

Collins, D.N., 1989b. Seasonal development of subglacial drainage and suspended sediment delivery to melt waters beneath an alpine glacier, *Annals of Glaciology*, **13**, 45-50.

Derbyshire, E., Jijun, L., Perrott, F.A., Shuying, X., and Waters, R.S., 1984. Quaternary glacial history of the Hunza Valley, Karakoram Mountains, Pakistan, in K. Miller (ed.), *The International Karakoram Project*, **2**, Cambridge University Press, New York, 456-495.

Dey, B., Goswami, D.C., and Rango, A., 1983. Utilization of satellite snow-cover observations for seasonal streamflow estimates in the Western Himalayas, *Nordic Hydrology*, **14**, 257-265.

Elliston, G.R., 1973. Water movement through the Gornergletscher, in *the Hydrology of Glaciers (Proceedings of the Cambridge, symposium, 1969), International Association of Hydrological Sciences Publication* **95**, 79-84.

Ferguson, R.I., 1985. Runoff from glacierised mountains: a model for annual variation and its forecasting, *Water Resources Research*, **21**, 702-708.

Finster W.R., 1960. German Glaciological and Geological Expedition to the Batura Mustagh and Rakaposhi Range, *Journal of Glaciology*, 3(28), 787-788.

Flohn, H., 1974. A Comparative Meteorology of Mountain Areas, in J.P. Ives and R.G. Barry (eds.) Arctic and Alpine Environments, Methuen: London, 55-71.

Fountain, A.G., 1989, The storage of water in, and hydraulic characteristics of, the firn of South cascade Glacier, Washington State, U.S.A., *Annals of Glaciology*, **13**, 69-75.

Garnier, B.J., 1970. The evaluation of surface variations in solar radiation income, *Solar Energy*, **13**, 21-34.

Geiger, R., 1965. The climate near the ground, Harvard University Press, Cambridge Mass.

Gilbert, O., Jamieson, D., Lister, H., and Pendlington, A., 1969. Regime of an Afghan Glacier, *Journal of Glaciology*, *8*(52), 51-65.

Gleeson, T.A., 1953. Effects of various factors on valley winds, *Journal of Meteorology*, **10**, 262-269.

Goodison, B., 1972a. An analysis of climate and runoff events for Peyto Glacier, Alberta, *Environment Canada, Inland Waters Directorate Scientific Series* No. 21.

Goodison, B., 1972b. The distribution of global radiation over Peyto Glacier, Alberta, *Environment Canada, Inland Waters Directorate Scientific Series* No. 22.

Goudie, A.S., Brunsden, D., Collins, D.N., Derbyshire, E., Ferguson, R.I., Hashmet, Z., Jones, D.K.C., Perrott, F.A., Said, M., Waters, R.S., and Whalley, W.B., 1984. The Geomorphology of the Hunza valley, Karakoram Mountains, Pakistan, in K. Miller (ed.), The International Karakoram Project, **2**, Cambridge University Press, New York, 359-410.

Graf, W.L., 1976. Cirques as glacier locations, *Arctic and Alpine Research*, **8**(1), 79-90.

Gregory, K.S. and Walling, D.E., 1973. Drainage basin form and process: A geomorphological approach. Ed. Arnold Publishers Ltd. 41 Bedford Square, London, 189-191.

Greuell, W., and Oerlemans, J., 1987. Energy balance calculations on and near Hintereisferner (Austria) and an estimate of the effect of greenhouse warming on ablation, in J. Oerlemans (ed.) Glacier Fluctuations and Climatic Change, Kluwer Academic Publishers, 305-324.

Gudmundsson, G., 1975. Short term variations of a glacier fed river, *Tollus*, **12**(3), 341-353.

Gupta, R.P., Duggal, A.J., Rao, S.N., Sankar, G., and Singhal, B.B.S., 1982. Snow cover area vs. snow melt runoff relation and its dependence on geomorphology - A study from the Beas Catchment (Himalayas, India), *Journal of Hydrology*, **58**, 325-339.

Harding, R.J., 1978. The variation of the altitudinal gradient of temperature within the British Isles, *Geografiska Annaler*, **60**A, 43-49.

Harding, R.J., 1979. Altitudinal gradients of temperature in the Northern Penniner, *Weather*, **34**, 190-201.

Haserodt, K., 1984. Abflußverhalten der Flüsse mit Bezügen zur Sonnenscheindaur und zum Niederschlag zwischen Hindukusch (Chitral) und Hunza-Karakorum (Gilgit, Nordpakistan), *Mitteilungen der Geographischen Gasellschaft un Müchen*, November, 1984, 129-161.

Henderson-Sellers, A., and Robinson, P.J., 1986. Contemporary climatology, John Wiley & Sons Inc., New York.

Hewitt, The freeze-thaw envirnment of Karakoram Himalaya, *Canadian Geographer*, **12**, 85-98.

Hewitt, K., 1985. Snow and ice hydrology in a remote, high mountain region: the Himalayan Sources of the Indus, *Snow and Ice Hydrology Project Working Paper* **1**.

Hewitt, K., 1982. Natural Dams and Outburst Floods of the Karakoram Himalaya, *International Association of Hydrological Sciences Publication* **138**, 259-269, (Proceedings of the Exeter Symposium, Hydrological Aspects of Alpine and High Mountain Areas).

Hewitt, K., 1986. The Upper Indus Snow Belts: Snowfall and Sources of Water Yield in K. Hewitt (ed.) Snow and Ice Hydrology Project - Annual Report and Scientific Papers 1985, Wilfrid Laurier University, Waterloo, 58-63.

Hewitt, K., 1989. The altitudinal organisation of Karakoram geomorphic processes and depositional environments, *Zeitschrift für Geomorphologie*, **76**, 9-32.

Hewitt, K., Wake, C.P., Young, G.J. and David, C., 1989. Hydrological investigation at Biafo Glacier, Karakoram Range Himalaya: An important source of water for the Indus River. *Annals of Glaciology*, **13**, 103-108.

Hino, M., Hasebe, M., and Noda, K., 1987. Estimation of volume of snow melt from temperature of snowline and residual snow amount, *Journal of Hydrology*, **93**(3), 25-39.

Hodge, S.M., 1974. Variations in the sliding of a temperate glacier, *Journal of Glaciology*, **13**(69), 349-369.

Hooke, R.L., Gould, J.E., and Bronge, G., 1983. Seasonal variations in surface velocity, Storglaciaren, Sweden, *Geografiska Annalar*, **65**A(3-4), 263-277.

Hooke, R.L., Wold, B., and Hagen, J.O., 1985. Subglacial hydrology and sediment transport at Bondhusbreen, south

Humphrey, N., Raymond, C., and Harrison. W., 1986. Discharges in turbid water during mini-surges of Variegated Glacier, Alaska, U.S.A., Journal of Glaciology, **32**(111), 195-207.

Iken, A., Röthlisberger, H., Flotron, A., and Haeberli, W., 1983. The uplift of Unteraargletscher at the beginning of the melt season - A consequence of water storage at the bed of the glacier, *Journal of Glaciology*, **29**(101), 29-46.

Kang, X., and Xie, Y., 1989. The character of the weather and climate in the West Kunlun Mountain area in summer, 1987, *Bulletin of Glacier Research (Japanese Society of Snow and Ice)*, **7**(1989), 77-81.

Kasser, P., 1959. Der Einfluss von Gletscherrückgang und Gletschervorstoss auf den Wasserhaushalt, *Wasser-und Energiewirtschaft*, **51**(6), 155-168.

Klige, R.K., 1985. The influence of climate on the water balance of glaciers, *Polar Vestnik Moskovskogo Universitea,* Seriya **5** Geografiya (1), 21-25.

Krimmel, R.M., and Tangborn, W.V., 1974. South Cascade: the moderating effect of glaciers on runoff, in *Proceedings of the Western Snow Conference, 42nd Annual Meeting,* Fort Collins, 9-13.

Krimmel, R.M., Tangborn, W.V., and Meier, M.F., 1973. Waterflow through a temperate glacier, in *The Role of in Hydrology (Proceedings of the Banff symposium September, 1972), International Association of Hydrologic Sciences Publication* **107**, 401-416.

Kuhn, M., Markl, G., Kaser, G., Nickus, U., Obleitner, F., and Schneider, H., 1985. Fluctuations of climate and mass balance: different responses of two adjacent glaciers, *Zeitschrift für Gletscherkunde und Glazialgeologie*, **21**, 409-416.

Lang, H., 1968. Relations between glacier runoff and meteorological factors on and off the glacier, in *IUGG General Assembly, Berne, International Association of Hydrological Sciences, Publication* **79**, 429-439.

Lang, H., 1973. Variations in the relation between glacier discharge and meteorological elements, in *the Hydrology of Glaciers (Proceedings of the Cambridge, symposium, 1969) International Association of Hydrological Sciences, Publication* **95**, 85-94.

Lang, H., Leibundgut, C., and Festel, E., 1981 Results from tracer experiments on the water flow through the Aletschgletchser, *Zeitschrift für Gletscherkunde und Glazialgeologie*, **15**(2), 1979, 209-218.

Lang, H. and Braun, L., 1988. On the information content of air temperature in the context of snow melt estimation, *Hydrology of Mountainous Areas, (Proceedings of the Strbske Pleso Workshop, Czechoslovakia, June 1988), International Association of Hydrological Sciences Publication* **190**, 347-354.

Lauscher, F., 1976, Weltweite Typen der Höhenabhängigkeit des Niederschlags, *Wetter u. Leben*, **28**, 80-90.

Lockwood, J.G., 1974. The monsoon climate of southern Asia, World Climatology, London Edward Arnold, 147-175.

Loewe, F., 1959. Some Observations of Radiation Budget and of the Ablation of Glacier Ice in the Nanga Parbat Region, Pakistan, *Science*, **11**(5) 229-236.

Makhdoom, M.T.A., and Solomon, S.I., 1986. Attempting flow forecasts of the Indus River, Pakistan using remotely sensed snow cover data, *Nordic hydrology*, **17**, 171-184.

Mason, K., 1935. The study of threating glaciers. *Geographical Journal*, **85**, 24-35.

Mayewski, P.A., and Jeschke, P.A., 1979. Himalayan and Trans-Himalayan glacier fluctuations since AD 1812, *Arctic and Alpine Research*, **11**(3), 267-287.

Mayewski, P.A., Pregent, G.P., Jeschke P.A., and Naseeruddin, A., 1980. Himalayan and Trans-Himalayan Glacier fluctuations and the South Asia monsoon record, *Arctic and Alpine Research*, **12**(2), 171-182.

Meier, M.F., 1973. Hydraulics and hydrology of glaciers, in *The Role of Snow and Ice in Hydrology (Proceedings of the Banff symposium September, 1972), International Association of Hydrologic Sciences Publication* **107**, 353-369.

Meier, M.F. and Roots, E.F, 1982. Glaciers as a water resource. *Nature and Resources*, UNESCO **18**, 7-14.

Mercer, J.H., 1975., *Glaciers of the northern-hemisphere*, **2**, CRREL, Hanover, N.H., 371-409.

Nakawa, M., and Young, G.J., 1982. Estimate of glacier ablation under a debris cover from surface temperature and meteorological variables. *Journal of Glaciology*, **28**(98), 29-34.

Norcliffe, G.B., 1984. *Inferential Statistics for geographers: an introduction*, 2 ed., London, Hutchinson.

Obled, C., and Harder H., 1979. A review of snow melt in the mountainous environment, in Colbeck, S.C., and Ray, M. (eds.) *Proceedings Modelling of Snow Cover Runoff*, U.S. Corps of Engineers CRREL Hanover, New Hampshire, 179-204.

Oerlemans, J., 1986. Glaciers as indicators of a carbon dioxide warming, *Nature*, **320**(17), 607-609.

Östrem, G., 1973. Funoff forecasts for highly glacierised basins, in *The Role of Snow and Ice in Hydrology (Proceedings of the Banff symposium September, 1972), International Association of Hydrologic Sciences Publication* **107**, 1111-1132.

Östrem, G., and Stanley, A.D., 1969. Glacier mass balance measurements, a manual for field and office work, Canadian Department of Energy, Mines and Resources, and the Norwegian Water Resources and Electricity Board, Inland Water Branch Series No. 66, Department of the Environment, Ottawa, Canada.

Paterson, W.S.B., 1981. *The physics of glaciers*, 2nd. edn., Pergamon Press, Oxford, New York, Toronto, Sydney, Paris, Frankfürt.

Pillewizer, W., 1957, Bewegungsstudien an Karakorum gletscher, *Geomorph. Studien Machatscheck, Festscher*, Eng. Petermanns M.H., **262**, 53-60.

Raina, V.K., Kaul, M.K., and Singh, S., 1977. Mass-balance studies of Gara Glacier, *Journal of Glaciology*, **18**(80), 415-423.

Rango, A., Solomonson, V.V., and Foster, J.L., 1977. Seasonal streamflow estimation in the Himalayan region employing meteorological satellite snow cover observations, *Water Resources Research*, **13**(1), 109-112.

Rango, A., Feldman, A., George, T.S., and Ragan, R.M., 1983. Effective use of LANDSAT data in hydrologic models, *Water Resources Bulletin*, **19**, 165-174.

Rao, Y.P., 1981. The Climate of the Indian Subcontinent, in Takahashi, K., and Arakawa, H. (eds.) Climates of Southern and Western Asia, World Survey of Climatology, **9**, Elsevier Scientific Publishing Co. Netherland, 67-119.

Rasmussen, L.A. and Tangborn, W.V., 1976. Hydrology of the North Cascades region, Washington. I Runoff, precipitation and storage characteristics, *Water Resour. Res.*, **12**, 187-202

Reiter, E.R., 1963. Jet Stream Meteorology, University of Chicago Press.

Röthlisberger, H., 1972. Water pressure in intra- and subglacial channels, *Journal of Glaciology*, **11**(62), 177-203.

Röthlisberger, H., and Lang, H., 1987. Glacial hydrology, in *Glacio-Fluvial Sediment Transfer,* A.M. Gurnell and M.J. Clark (eds.), John Wiley & Sons Ltd., 207-232.

Schytt, V., 1967. A study of 'ablation gradient', *Geografiska Annaler*, **49**A, 327-332.

Shaw, E.M., 1984. *Hydrology in Practice*, Van Nostrand Rienhold (UK) Co. Ltd.

Shreve, R.L., 1972. Movement of water in glaciers, *Journal of Glaciology*, **11**(62), 205-214.

Snow and Ice Hydrology Project, 1985. Annual Report 1985, Canadian Centre; Wilfrid Laurier University, Waterloo, Ontario, Canada.

Snow and Ice Hydrology Project, 1986. Annual Report 1986, Canadian Centre; Wilfrid Laurier University, Waterloo, Ontario, Canada.

Snow and Ice Hydrology Project, 1987. Annual Report 1987, Canadian Centre; Wilfrid Laurier University, Waterloo, Ontario, Canada.

Snow and Ice Hydrology Project, 1988. Annual Report 1988, Canadian Centre; Wilfrid Laurier University, Waterloo, Ontario, Canada.

Snow and Ice Hydrology Project, 1989. Annual Report 1989, Canadian Centre; Wilfrid Laurier University, Waterloo, Ontario, Canada.

Stenborg, T., 1970. Delay of run-off from a glacier basin, *Geografiska Annaler*, **52**(A), 1-30.

Stenning, A.J., Banfield, C.E., and Young G.J., 1981. Synoptic controls over katabatic layer characteristics above a melting glacier, *Journal of Climatology*, **1**, 309-324.

Stoddard, R.H., 1982. Field techniques and research methods in geography, Dubuque, Iowa, Kendal Publ. Co.

Sudgen, D.E., and John, B.J., 1984. Glaciers and landscape, Edward Arnold, London.

Tangborn, W.V., Krimmel, R.M., and Meier, M.F., 1971. A comparison of glacier mass balance by glaciological, hydrological and mapping methods, South Cascade Glacier, in *(Proceedings of the Moscow Symposium August, 1971), International Association of Hydrological Sciences Publication* **104**, 197-201.

Tarar, R.N., 1982. Water resources investigation in Pakistan with the help of Landsat Imagery - snow surveys 1975-1978, in *Hydrological Aspects of Alpine and High Mountain Areas (Proceedings of the Exeter Symposium, July, 1982), International Association of Hydrological Sciences Publication* **138**, 177-198.

von Wissman, H., 1959. Die Heutige Vergletscherung und Schneegrenze in Hoch Asien. Abh. Math - Naturwissen. Kl. **14**, Akademie der Wissenschaften und der Literatur in Mainz, Steiner Verlag, Weisbaden, 307p.

Wake, C.P., 1989, Glaciochemical Investigations as a tool for determining the spatial and seasonal variation of snow accumulation in the Central Karakoram, Northern Pakistan, *Annals of Glaciology*, **13**, 279-284

Whiteman, P.T.S., 1985. Mountain Oases: a technical report of agriculture studies (1982-1984) in the Gilgit District, Northern Areas, Pakistan, U.N. Food and Agriculture Organisation / U.N. Development Programme Islamabad, PAK/80/009, Gilgit.

Xie, Y., Kang, X., and Takahashi, S., 1989. Radiation balance in the Gozha Glacier region, in the West Kunlun Mountains, *Bulletin of Glacier Research (Japanese Society of Snow and Ice)*, **7**(1989), 83-87.

Yafeng, S., and Xiangsong, Z., 1984. Some studies of the Batura Glacier in the Karakoram Mountains, in K. Miller (ed.), The International Karakoram Project, **1**, Cambridge University Press, New York 51-63.

Yafeng, S., and Wenying, W., 1980. Research on snow cover in China and the avalanche phenomena of Batura Glacier in Pakistan, *Journal of Glaciology*, **26**(94), 25-30.

Young, G.J., 1977a. Relations between mass-balance and meteorological variables on Peyto Glacier, Alberta, 1967-1974, in *Proceedings of the Symposium on the Dynamics of Temperate Glaciers, 6-9 September 1977, Munich, Germany*, Zeitschrift für Gletscherkunde und Glazialgeologie, **13**, 111-125.

Young, G.J., 1977b. The seasonal and diurnal regime of a glacier-fed stream, in R.H. Swanson and P.A. Logan (Compilers), *Alberta Watershed Research Program Symposium Proceedings, 31 August - September 1977, Northern Forest Research Centre),* Information Report NOR-X-176, Forestry Service, Fisheries Environment Canada, 111-126.

Young, G.J., 1980. Streamflow formation in a glacierised watershed in the Rocky Mountains, Canada, in *the and Prediction on Runoff from Glaciers and Glacierised (Proceedings of the Tbilisi Symposium, September, 1978),* Materialy Gliatsiologicheskii Issledovanii, Khronika, Obsuzhdeniia, Mezhduvedomstvennyi Geofizicheskii Komitet, Sektsiia Glatsiologii, Institut Geografii, Academy Nauk SSSR/*Data of Glaciological Studies, Chronicle, Discussion, Section of Glaciology of the Soviet Geophysical Committee* and Institute of Geography, Academy of Sciences of the U.S.S.R., **39**, Moscow, in Russian 55-62, in English 134-139.

Young, G.J., 1982. Hydrological relationships in a glacierised mountain basin, in Glen,J.W. (ed.), *Hydrological Aspects of Alpine and High Mountain Areas, (Proceedings of the Exeter Symposium, 19-30 July 1982), International Association of Hydrological Sciences Publication* **138**, 51-59.

Young, G.J. and Hewitt, K., 1990. *Hydrology of Mountainous Areas, (Proceedings of the Strbske Pleso Workshop, Czechoslovakia, June 1988), International Association of Hydrological Sciences Publication* **190**, 139-151.

Young, G.J., and Schmok, J.P, 1989, Ice loss in the ablation area of a Himalayan glacier: studies on Miar Glacier, Karakoram, Pakistan, *Annals of Glaciology,* **13**, 289-293.

Zuzel, J.F., and Cox, L.M., 1975. Relative importance of meteorological variables in snow melt, *Water Resources Research,* **11**(1), 174-176.

APPENDIX A

Table of Daily Mean Temperature for Pasu Snout, Pasu Gahr and Patundas and Daily Mean Discharge of the Pasu river and Daily Mean Values of Solar Radiation

Date	Pasu Snout (°C)	Pasu Gahr (°C)	Patundas (°C)	Discharge (m^3s^{-1})
21/5/89	17.0	99.9	99.9	99.9
22/5/89	14.2	99.9	99.9	7.4
23/5/89	12.3	99.9	99.9	6.7
24/5/89	11.5	8.1	99.9	6.6
25/5/89	14.2	8.7	99.9	6.8
26/5/89	15.9	9.3	99.9	7.0
27/5/89	16.9	10.9	99.9	7.3
28/5/89	18.0	13.0	99.9	8.4
29/5/89	18.5	13.1	99.9	10.4
30/5/89	19.1	13.2	99.9	12.6
31/5/89	18.6	14.0	99.9	13.3
1/6/89	19.0	15.4	99.9	13.5
2/6/89	19.6	16.3	99.9	13.6
3/6/89	20.1	16.3	99.9	14.4
4/6/89	20.7	15.7	99.9	13.5
5/6/89	16.7	12.8	99.9	12.1
6/6/89	14.1	11.5	99.9	9.8
7/6/89	13.2	10.2	1.5	8.6
8/6/89	15.9	12.0	3.5	8.6
9/6/89	14.6	9.0	0.7	8.2
10/6/89	14.1	6.8	0.5	7.6
11/6/89	12.8	6.7	99.9	7.7
12/6/89	15.5	9.5	99.9	8.8
13/6/89	15.0	9.4	99.9	9.5
14/6/89	12.3	7.2	99.9	9.5
15/6/89	16.2	10.1	99.9	9.3
16/6/89	14.3	8.2	2.9	8.8
17/6/89	17.5	8.5	1.6	8.7
18/6/89	13.1	7.3	0.9	8.4
19/6/89	15.3	8.8	2.5	8.8
20/6/89	12.0	5.6	-0.4	8.5
21/6/89	11.8	6.5	0.3	8.0
22/6/89	14.4	8.9	3.2	8.4
23/6/89	15.4	10.5	4.9	9.6
24/6/89	15.2	11.2	6.0	11.7
25/6/89	18.5	14.0	7.6	13.0
26/6/89	19.7	13.8	7.6	14.9
27/6/89	19.0	13.2	7.5	15.9

28/6/89	18.4	13.3	8.4	15.1
29/6/89	17.8	13.3	7.8	15.8
30/6/89	17.0	11.6	6.2	16.7
01/7/89	17.3	11.6	6.1	21.9
02/7/89	15.1	9.4	3.1	21.3
03/7/89	15.9	10.5	4.2	18.1
04/7/89	10.6	6.2	1.1	16.2
05/7/89	11.0	4.9	0.7	12.4
06/7/89	13.1	7.0	1.1	11.5
07/7/89	15.3	10.4	4.7	12.4
08/7/89	17.1	13.5	8.5	16.7
09/7/89	19.1	14.3	10.1	18.6
10/7/89	20.2	16.3	11.9	20.5
11/7/89	21.8	17.0	13.4	22.1
12/7/89	20.0	17.3	14.1	22.0
13/7/89	19.9	16.6	13.0	21.7
14/7/89	18.9	14.5	10.2	23.7
15/7/89	17.4	12.0	6.6	30.8
16/7/89	12.6	8.1	3.5	31.6
17/7/89	13.4	8.8	4.4	28.8
18/7/89	11.8	8.0	3.8	21.7
19/7/89	11.5	7.8	3.0	23.7
20/7/89	15.2	12.1	6.6	21.0
21/7/89	14.8	10.4	5.2	22.6
22/7/89	15.8	11.0	6.5	21.3
23/7/89	12.8	8.1	4.6	20.3
24/7/89	9.7	5.8	2.7	19.7
25/7/89	13.9	10.2	6.9	23.5
26/7/89	17.1	14.1	11.5	99.9
27/7/89	19.1	16.5	14.8	99.9
28/7/89	20.3	17.8	16.5	99.9
29/7/89	21.4	17.0	14.0	99.9
30/7/89	15.5	11.9	9.2	28.0
31/7/89	11.7	7.9	5.0	23.5
01/8/89	11.4	6.8	2.1	17.4
02/8/89	15.0	10.5	4.4	14.0
03/8/89	15.5	12.8	7.5	14.4
04/8/89	17.1	12.5	7.9	15.4
05/8/89	12.4	7.5	2.6	15.1
06/8/89	14.3	8.7	3.2	14.0
07/8/89	16.9	12.9	7.2	18.0
08/8/89	17.1	13.8	9.3	19.5
09/8/89	17.3	13.4	9.3	19.0
10/8/89	19.2	15.3	9.2	20.1
11/8/89	18.8	15.0	10.9	21.1
12/8/89	19.5	15.3	11.3	21.5
13/8/89	17.8	13.2	8.5	20.1
14/8/89	14.7	10.9	6.1	17.2

15/8/89	14.2	9.8	5.5	16.7
16/8/89	15.1	10.8	6.3	17.1
17/8/89	16.7	13.8	9.7	18.3
18/8/89	18.5	15.1	10.6	20.7
19/8/89	17.9	15.5	11.7	21.5
20/8/89	16.9	12.7	8.8	20.3
21/8/89	14.6	11.5	7.9	20.1
22/8/89	14.7	11.4	7.1	19.6
23/8/89	17.4	12.7	7.7	19.2
24/8/89	14.7	10.4	5.9	19.4
25/8/89	14.6	10.5	5.7	17.5
26/8/89	13.0	8.5	4.3	18.0
27/8/89	9.8	6.8	2.0	15.8
28/8/89	8.2	4.4	1.0	14.7
29/8/89	9.8	5.0	0.2	11.2
30/8/89	12.0	6.2	0.9	10.9
31/8/89	12.4	6.0	-0.4	99.9

Note: 99.9 represents missing data.

APPENDIX B

Plots of Daily Mean Temperature at Pasu Snout, Pasu Gahr and Patundas and Daily Mean Discharge of the Pasu River

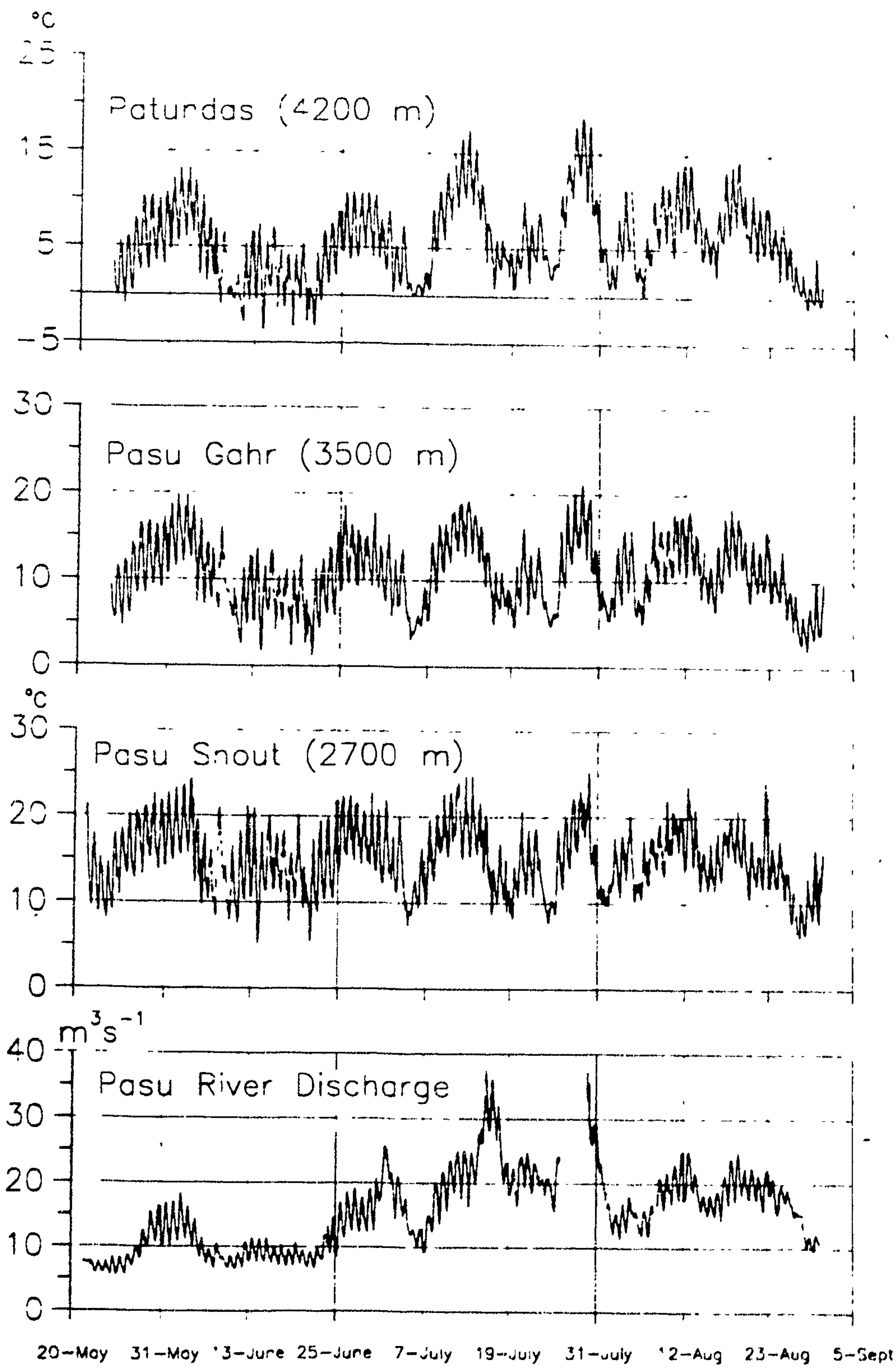

APPENDIX C

Selected Charts from 20-27 July, 1989 from Pasu Snout, Pasu Gahr and Patundas.

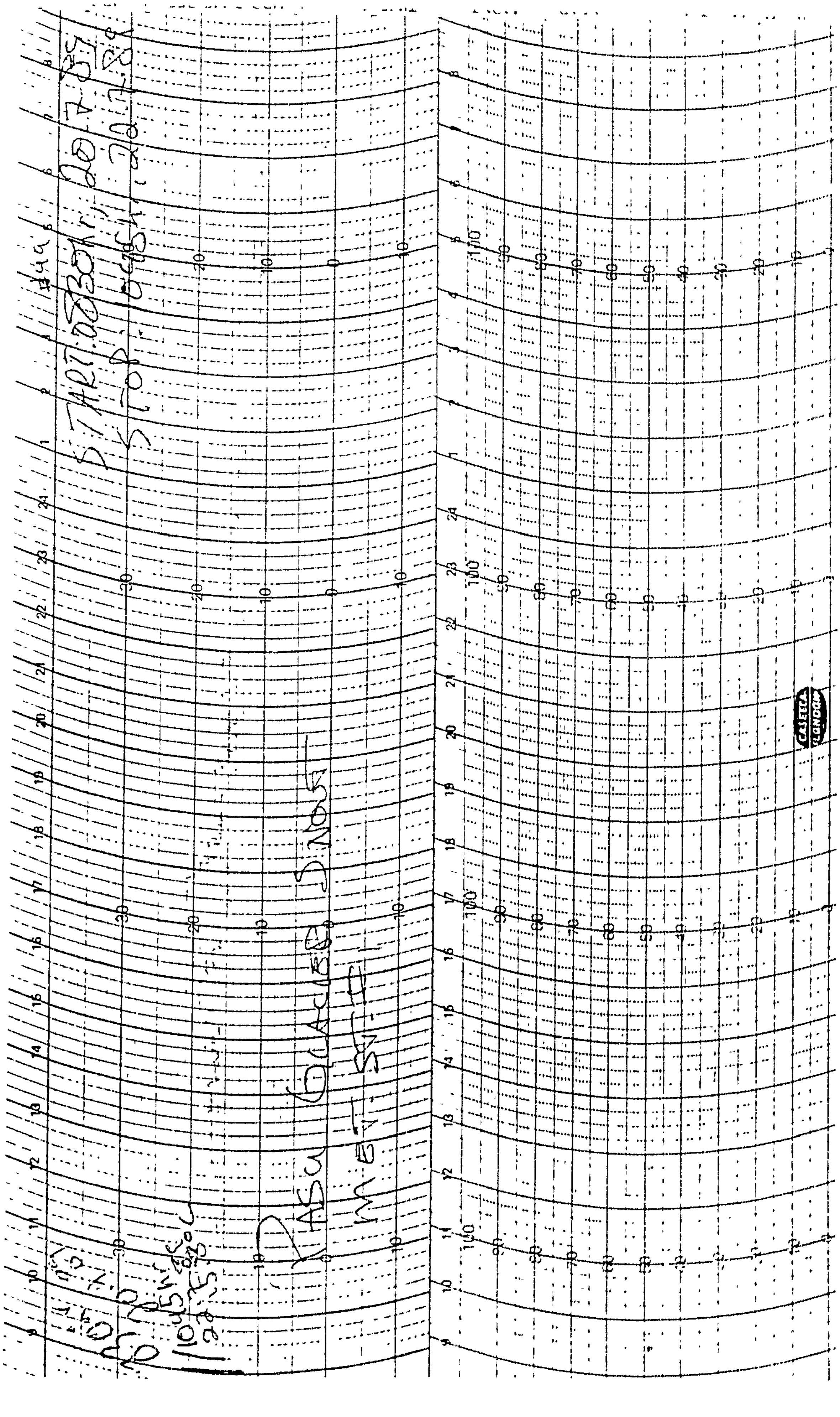
START: 0830hr, 20.7.89
STOP: 0845hr, 22.7.89
RASU GLACIER SNOUT
MET. ST-I
CASELLA LONDON

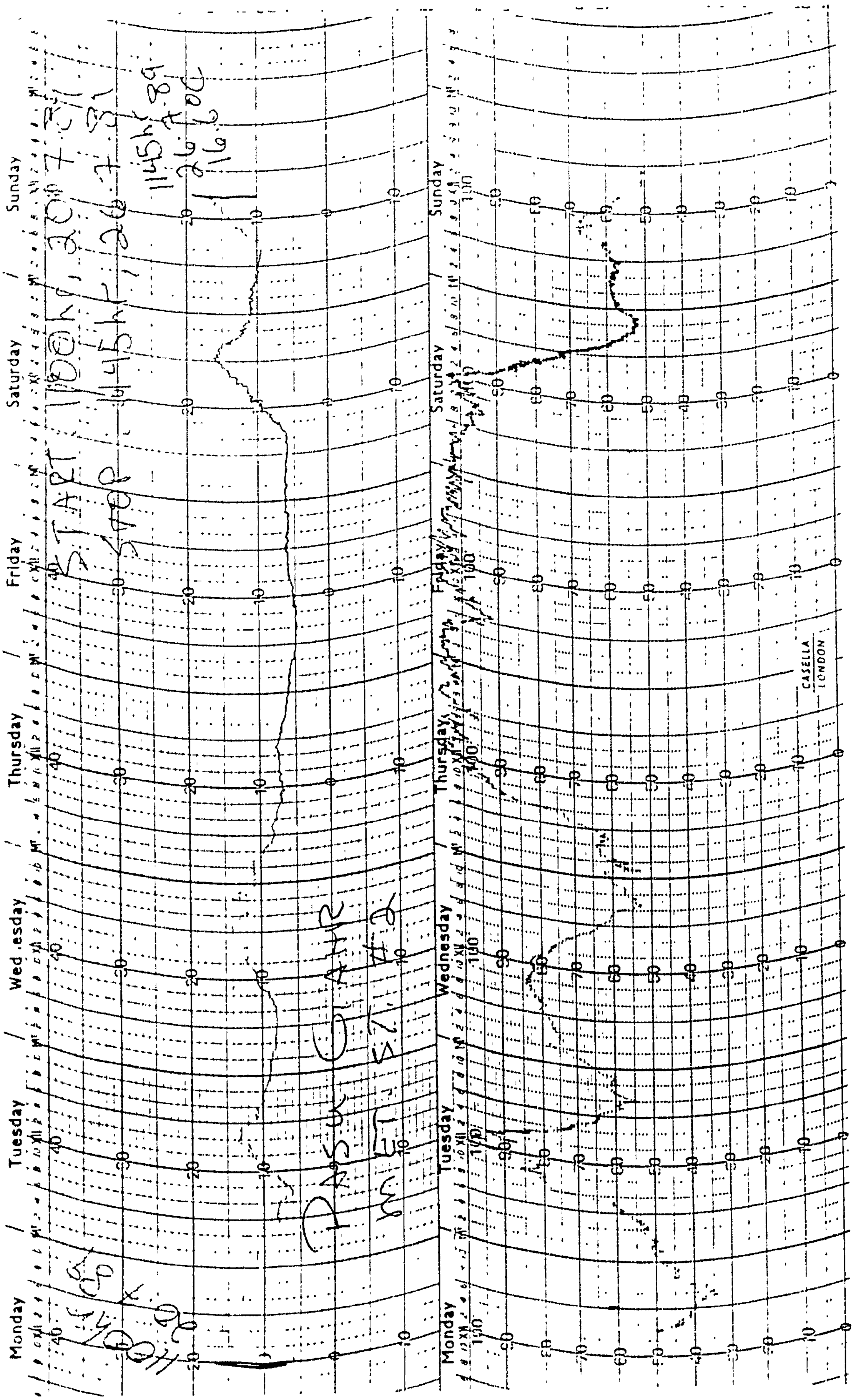
Monday
Tuesday
Wednesday
Thursday
Friday
Saturday
Sunday
CASELLA
LONDON

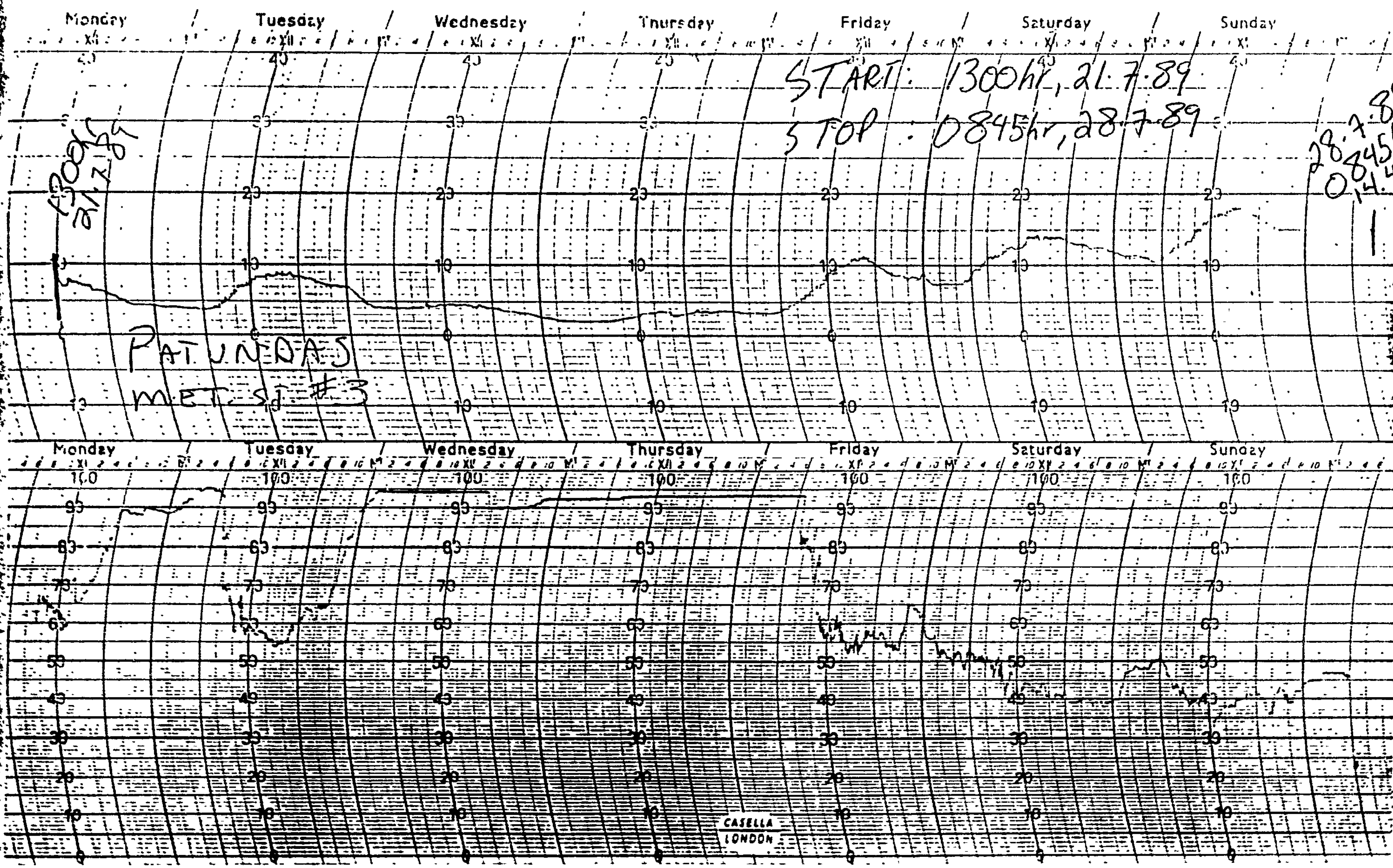
Monday
Tuesday
Wednesday
Thursday
Friday
Saturday
Sunday
START: 1300hr, 21.7.89
STOP: 0845hr, 28.7.89
1300hr
21.7.89
PATUNDAS
MET. st #3
CASELLA
LONDON